

*Cy 1*



3 4456 0049953 8

# An Evaluation of HTGR Primary Burning

J. W. Snider    D. C. Watkin

OAK RIDGE NATIONAL LABORATORY  
CENTRAL RESEARCH LIBRARY  
DOCUMENT COLLECTION  
**LIBRARY LOAN COPY**  
DO NOT TRANSFER TO ANOTHER PERSON  
If you wish someone else to see this  
document, send in name with document  
and the library will arrange a loan.  
UCN-7969  
(3 3-67)



## OAK RIDGE NATIONAL LABORATORY

OPERATED BY UNION CARBIDE CORPORATION • FOR THE U.S. ATOMIC ENERGY COMMISSION

Printed in the United States of America. Available from  
National Technical Information Service  
U.S. Department of Commerce  
5285 Port Royal Road, Springfield, Virginia 22151  
Price: Printed Copy \$7.60; Microfiche \$1.45

This report was prepared as an account of work sponsored by the United States Government. Neither the United States nor the United States Atomic Energy Commission, nor any of their employees, nor any of their contractors, subcontractors, or their employees, makes any warranty, express or implied, or assumes any legal liability or responsibility for the accuracy, completeness or usefulness of any information, apparatus, product or process disclosed, or represents that its use would not infringe privately owned rights.

# OAK RIDGE NATIONAL LABORATORY

OPERATED BY  
UNION CARBIDE CORPORATION  
NUCLEAR DIVISION



POST OFFICE BOX X  
OAK RIDGE, TENNESSEE 37830

December 9, 1974

Report No.: ORNL-TM-4520 Classification: Unclassified

Author(s): J. W. Snider and D. C. Watkin

Subject: An Evaluation of HTGR Primary Burning

Request compliance with indicated action:

Heidrun Barnert-Wiemer was not properly given credit for her contribution of Appendix A to the subject report. Attached you will find a corrected title page printed on gummed stock. Please moisten and affix to your copy(ies) of ORNL-TM-4520.

A handwritten signature in cursive script that reads "J. L. Langford".

J. L. Langford  
Laboratory Records Department  
Information Division

*Handwritten:* JLM  
1/27/75

ORNL-TM-4520  
UC-77 - Gas-Cooled Reactor Technology

Contract No. W-7405-eng-26

CHEMICAL TECHNOLOGY DIVISION

AN EVALUATION OF HTGR PRIMARY BURNING

J. W. Snider

D. C. Watkin

With an Appendix by Heidrun Barnert-Wiemer,  
Guest Scientist from KFA-Jülich, West Germany

NOVEMBER 1974

OAK RIDGE NATIONAL LABORATORY  
Oak Ridge, Tennessee 37830  
operated by  
UNION CARBIDE CORPORATION  
for the  
U. S. ATOMIC ENERGY COMMISSION



3 4456 0049953 8

.

.

.

.

.

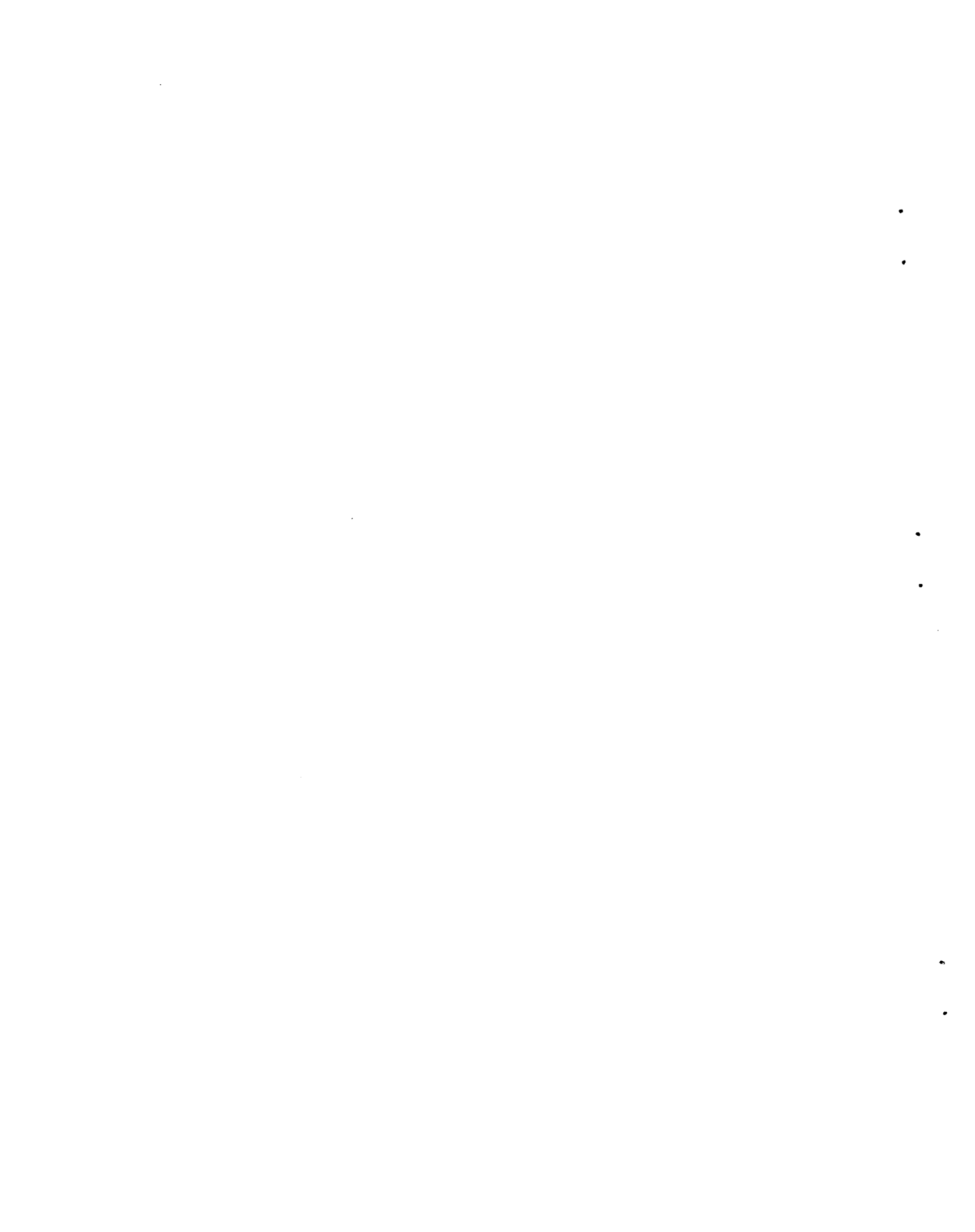
.

## CONTENTS

	<u>Page</u>
Abstract .....	1
1. Introduction and Summary .....	2
2. Description of the Primary Burner Modules .....	4
2.1 Whole-Block Burner Module .....	7
2.1.1 Feed Handling Equipment .....	7
2.1.2 Whole-Block Burner .....	11
2.1.3 Whole-Block Product Burner .....	15
2.1.4 Classifiers .....	15
2.1.5 Particle Crusher .....	16
2.1.6 Auxiliary Process Equipment .....	16
2.1.7 Remote Handling and Maintenance Equipment .....	18
2.2 Fluidized-Bed Burner Module .....	19
2.2.1 Feed Preparation .....	19
2.2.2 Fluidized-Bed Burner .....	22
2.2.3 Primary-Burner Product Hoppers .....	30
2.2.4 Auxiliary Process Equipment .....	31
2.2.5 Remote Handling and Maintenance Equipment .....	34
3. Space Requirements for Primary Burning .....	34
3.1 Whole-Block Burning .....	35
3.2 Fluidized-Bed Burning .....	44
4. Cost Estimates .....	53
4.1 Equipment Costs .....	55
4.1.1 Whole-Block Burning .....	55
4.1.2 Fluidized-Bed Burning .....	55
4.2 Cost of Heat Removal System .....	55
4.3 Building Cost .....	60
4.3.1 Whole-Block Burning .....	66
4.3.2 Fluidized-Bed Burning .....	66

	<u>Page</u>
4.4 Other Direct Construction Costs .....	67
4.5 Total Direct Construction Cost .....	67
4.6 Estimates of Indirect Construction Costs .....	67
4.7 Owner's Cost Estimates .....	67
4.8 Total Estimated Cost .....	69
4.9 Cost Sensitivities .....	69
4.9.1 Sensitivity to Module Costs .....	69
4.9.2 Sensitivity to Building Cost .....	70
5. Conclusions and Recommendations .....	70
6. References .....	76
Appendix A: Preliminary Experimental Studies of a One-Sixth- Scale Whole-Block Burner .....	79
A.1 Introduction .....	79
A.2 Literature Survey .....	80
A.3 Description of the Equipment .....	83
A.3.1 The HTGR Fuel Block .....	85
A.3.2 Burner and Off-Gas System .....	93
A.3.3 Instrumentation .....	97
A.4 Experimental Procedures and Results .....	98
A.4.1 Procedure of a Typical Run .....	98
A.4.2 Burning Rate and Burning Behavior .....	99
A.4.3 Heat Removal and Temperature Control .....	104
A.4.4 Particle Breakage .....	113
A.4.5 Off-Gas Composition .....	118
A.4.6 Formation of Graphite Fines .....	119

	<u>Page</u>
A.5 Whole-Block Burner Calculations .....	120
A.5.1 Burning Rates and Temperatures for Radiation- Controlled Heat Transfer .....	120
A.6 Recommendations .....	123
Appendix B: A Summary of Technical Considerations for the Whole-Block and Fluidized-Bed Burners .....	129
B.1 Burner Feed Preparation .....	129
B.2 Feeding the Burners .....	135
B.3 Burning the Graphite .....	138
B.4 Heat Removal .....	145
B.5 Burner Product Withdrawal .....	148
B.6 Off-Gas Handling .....	149
Appendix C: HTGR Fuel Element and Fuel Particle Nomenclature at the Reprocessing Plant .....	153



AN EVALUATION OF HTGR PRIMARY BURNING

J. W. Snider

D. C. Watkin

## ABSTRACT

An economic and technical comparative study was made of the reference method, fluidized-bed burning, and an alternative method, whole-block burning, for performing the primary burning step in HTGR fuel reprocessing. For each method, considerations were made of the ancillary equipment for heat removal and the fuel and ash handling; crushing was also included in the case of fluidized-bed burning. The scale of primary burning was that of a reprocessing plant handling the spent fuel from ~50,000-MW(e) HTGR generating capacity. Preliminary designs were prepared for the major equipment components and/or modules in canyons equipped with the necessary remote maintenance features. Cost estimates were prepared for the equipment items using a fractional cost factor for multiple modules. The cost of the building associated with the primary burning step was estimated using the volume of concrete in the heavily shielded canyons and the area of the operating corridors adjacent to or above the canyons. The cost of primary burning is guesstimated to be about \$100 million, with no significant difference between fluidized-bed and whole-block burning. The layout of the various canyons suggests that a modular head-end plant with add-on capability is more easily obtainable with the whole-block burner than with the fluidized-bed burner. The development of a fluidized-bed burner with a low length/diameter ratio should be a developmental goal.

A report of studies made by Dr. H. Barnert-Wiemer with a one-sixth whole-block burner is included as an appendix.

## 1. INTRODUCTION AND SUMMARY

The High Temperature Gas-Cooled Reactors (HTGRs) currently being marketed by the General Atomic Company utilize the thorium fuel cycle. Economic as well as resource conservation incentives exist to utilize the  $^{233}\text{U}$  produced from the relatively inexpensive  $^{232}\text{Th}$ . The use of  $^{233}\text{U}$  in one HTGR reduces the  $^{235}\text{U}$  fuel requirements from about 140 MT SWU/1000 MW(e) for no  $^{233}\text{U}$  recycle to about 80 MT SWU/1000 MW(e) with  $^{233}\text{U}$  recycle. A fuel recycle development program<sup>1</sup> (AEC-supported) is currently under way at the General Atomic Company\* (GAC), at the Allied Chemical Company\*\* (ACC), and at the Oak Ridge National Laboratory (ORNL) to demonstrate the recovery and recycle of  $^{233}\text{U}$  in the HTGR fuel cycle.

The HTGR utilizes graphite as a moderator and is helium cooled. The uranium and thorium fuels are in the form of spherical carbide and oxide compounds present in large graphite fuel blocks containing holes through which the coolant helium flows. Fuel recycle consists, in part, of recovering the fuel from the blocks and re-forming it into spheres which are coated with pyrolytically deposited carbon and SiC. The recovery flowsheet is a burn-leach process.<sup>2</sup> The first step in the burn-leach process is the combustion of the irradiated graphite fuel blocks to form carbon dioxide, which is subsequently decontaminated and discharged to the atmosphere. The combustion process is accomplished in three steps: (1) primary burning, (2) primary burner product separation and treatment, and (3) secondary burning.

The HTGR fuel reprocessing plant must reprocess about one spent fuel element annually for each megawatt of HTGR installed electrical generating capacity. Thus, about 50,000 spent HTGR fuel elements will be processed annually from a 50,000-MW(e) HTGR economy. Approximately 50 large HTGR reactors will supply fuel to such a HTGR fuel reprocessing plant. Further, each reactor may have as many as three types of fissile fuels, each of which requires a separate reprocessing flowsheet. For the

---

\*San Diego, Calif.

\*\*Idaho Falls, Idaho.

purpose of this study, it has been assumed that no fuel element will contain more than two of the three fissile fuels at reprocessing time, and that each spent HTGR fuel element will contain a single fertile material, thorium. Implicit in this is the fact that all  $^{233}\text{U}$  streams, irrespective of reactor cycle number and  $^{233}\text{U}$  enrichment or  $^{232}\text{U}$  contamination, are considered equivalent for purposes of reprocessing and refabrication.

The minimum amount of separation required for the fissile materials is achieved by designing a reprocessing-refabrication system that is independent of specific reactors. While this method may be attractive from an economic viewpoint, it may be inconsistent with accountability and safeguards requirements. The maximum amount of separation required for the fissile materials is achieved by designing a reprocessing-refabrication system that not only separates by type of fissile particle but also maintains reactor identity, at least through dissolution. This latter case is the one considered here.

At HTGR fuel cycle equilibrium, approximately 575 "25R", 31 "25W", and 394 "23R" fuel elements are received annually at the HTGR reprocessing plant from one reactor (see Appendix C for a description of the fuel elements). Thus, if one could receive and hold for reprocessing the entire annual reactor discharge, only three primary burn batches would be handled per reactor. Considering the probable earliest startup date of an HTGR reprocessing plant and a reasonable HTGR growth rate, it is conceivable that an amount of spent-fuel storage space sufficient for six months of plant operation, (i.e., space for ~24,000 elements) will exist by the time the reprocessing plant is operational.

This study consists of an evaluation of two systems for accomplishing the primary burning: whole-block burning (WBB), and fluidized-bed burning (FBB). The latter is presently the reference process for the HTGR Reprocessing Prototype Facility. The systems, one of which has undergone only preliminary studies (WBB) and one of which has undergone considerable developmental studies (FBB), are examined. Thus, the amount of technical information on which the evaluation is based is unequal for the two systems, a fact which must be recognized at each step in the evaluation.

From this study it is concluded: that the estimated cost (building and equipment) for primary burning is about \$100 million (no significant difference between the WBB and the FBB); that ease of operation and reliability should be used as the bases for choosing between the WBB and the FBB; that the crusher and handling system required for the FBB system represents about 30% of the module FBB equipment cost; that a FBB with a low length/diameter ratio is less costly than a FBB with a high length/diameter ratio; that a reliable pneumatic transport system should be developed; and that, in comparing alternative processing, one must consider both the equipment and the facility requirements.

The experimental WBB studies, which were made by Dr. H. Barnert-Wiemer, are described in detail in Appendix A. A summary of WBB and FBB technical considerations as related to scale-up is included in Appendix B.

## 2. DESCRIPTION OF THE PRIMARY BURNER MODULES

A large-scale HTGR fuel reprocessing plant will require the simultaneous operation of several primary burners. It is envisioned that these burners will be installed and operated as modular systems. Further, it is assumed that the modules will be located within a canyon which interfaces with a fuel element identification and sorting canyon (I & S canyon) and a secondary burning and dissolution canyon (SB & D canyon). An assumed requirement for remote operation is that each canyon be connected to a decontamination and maintenance cell. Figure 1, which is a plan view of the WBB canyon as related to the I & S canyon and the SB & D canyon, and Fig. 2, which is the counterpart for the FBB canyon, are shown for the purpose of modular orientation. The canyon structures are described in Sect. 3. The equipment comprising singular modules is discussed in this section.

Primary burner modules for one WBB and two FBB systems [one system in which the feed material and the recycled soot are burned in a single burner (1-FBB), and one system in which the feed material and the recycled soot are burned in separate burners (2-FBB)] are considered. The necessary auxiliary, remote handling, and maintenance equipment is discussed.

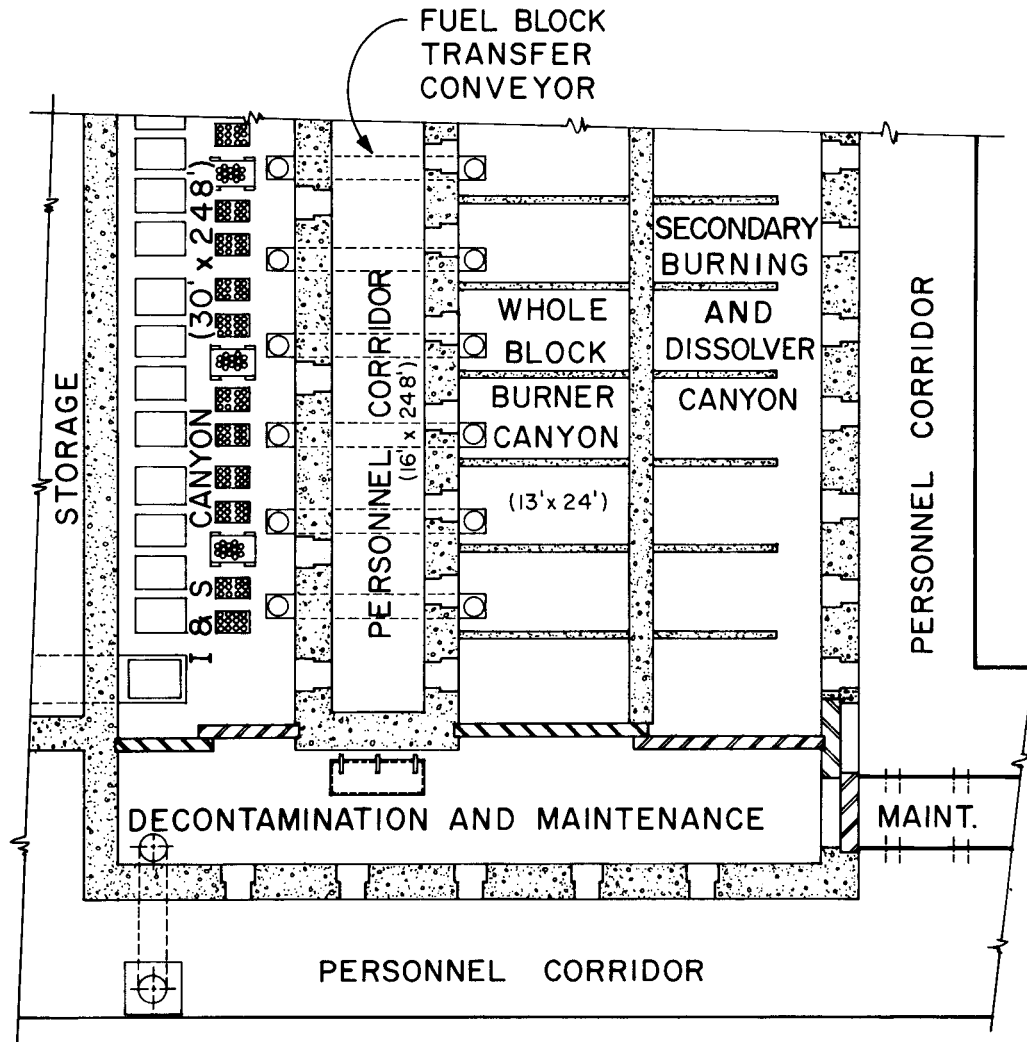


Fig. 1. Orientation of the WBB canyon as related to the I & S and SB & D canyons.

ORNL DWG 73-11891R1

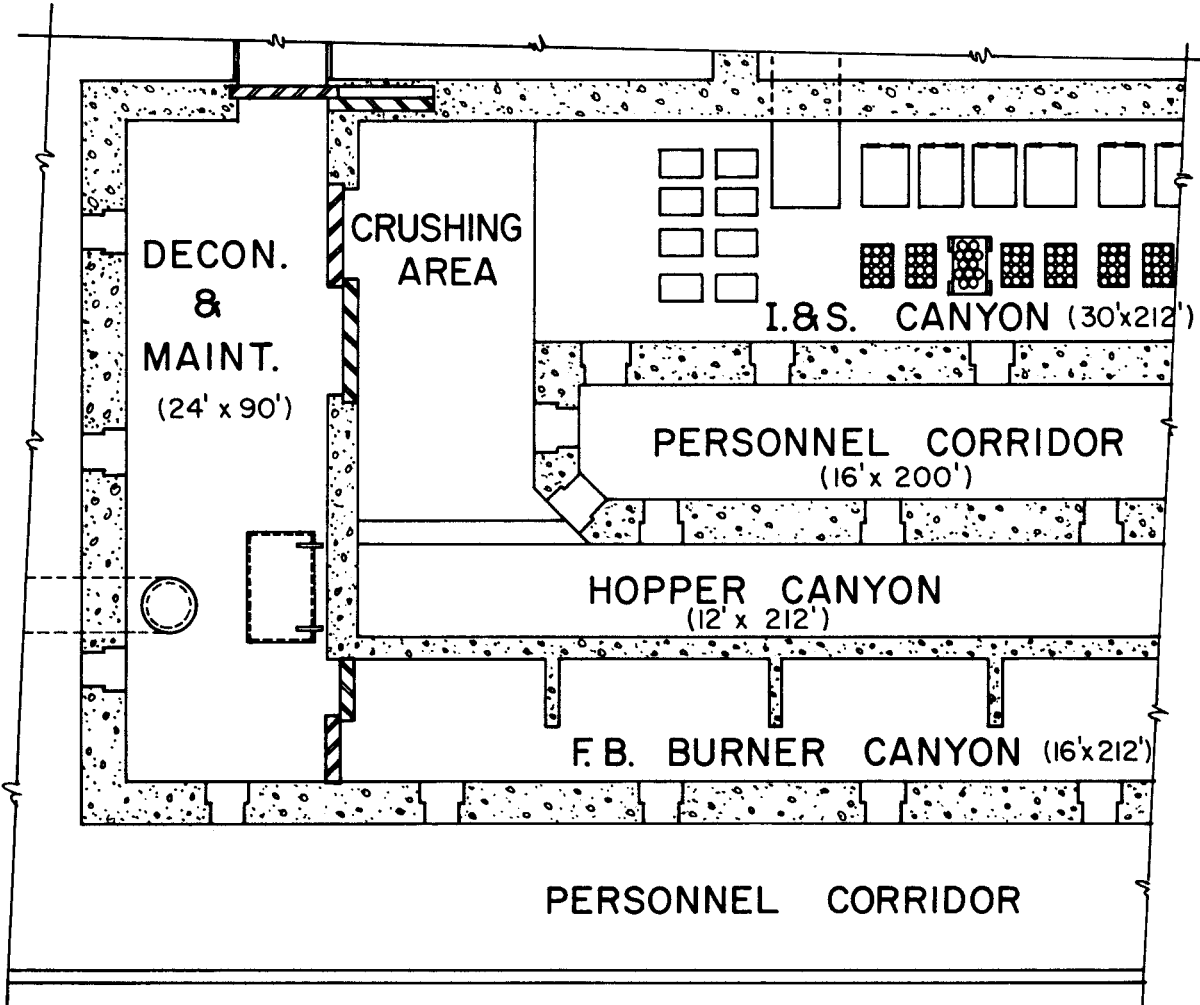


Fig. 2. Orientation of the FBB canyon as related to the I & S and hopper canyons.

## 2.1 Whole-Block Burner Module

The whole-block burning of spent HTGR fuel elements refers to the burning of the elements in the as-received condition (Fig. 3). In this report, fuel element and fuel block are considered to be synonymous. The WBB module described in this section is designed to accomplish the burning of 16 spent HTGR fuel elements per day.

### 2.1.1 Feed handling equipment

After being sorted, the spent fuel blocks will be transferred from the storage, sorting, and identification area through gas locks, via special fuel block transfer conveyors (see Fig. 4), into a particular burner cubicle located within the WBB canyon. The spent fuel block is removed from the transfer conveyor by a special manipulator and loaded into the WBB via a rotatable fuel block cradle located so as to align the block with the floor of the purgeable gas lock. This fuel block cradle is used to turn the fuel element from a vertical to a horizontal position for charging into the purgeable gas lock (Fig. 5).

The fuel block charging chamber, which is located at the opposite end from the combustion zone, consists basically of a gas lock with inner and outer closures and a series of rams for conveying the fuel block into the burner. To charge the burner, one fuel block at a time is placed in the positioning cradle by a special fuel block handling tool. The positioning cradle is then rotated 90°, thus aligning the fuel block (axis now horizontal) with the gas lock outer closure. A ram pushes the fuel block through the outer closure, which has been opened, and into the gas lock. After the ram has been withdrawn, the outer closure has been shut, and the air lock purged, the inner closure is opened and the fuel block is shoved into position for feeding the burner by another ram. Subsequently, the inner closure is shut, and the gas lock is again purged. The fuel block is now in position to be slowly pushed into the combustion zone by the feed ram that automatically advances the fuel blocks, keeping the burning face always within the prescribed burning zone of the burner. This is accomplished via a thermocouple control circuit which signals the motor operating the feed ram. The loading procedure is repeated about every 1.5 hr during burner operation.

PHOTO 1667-71

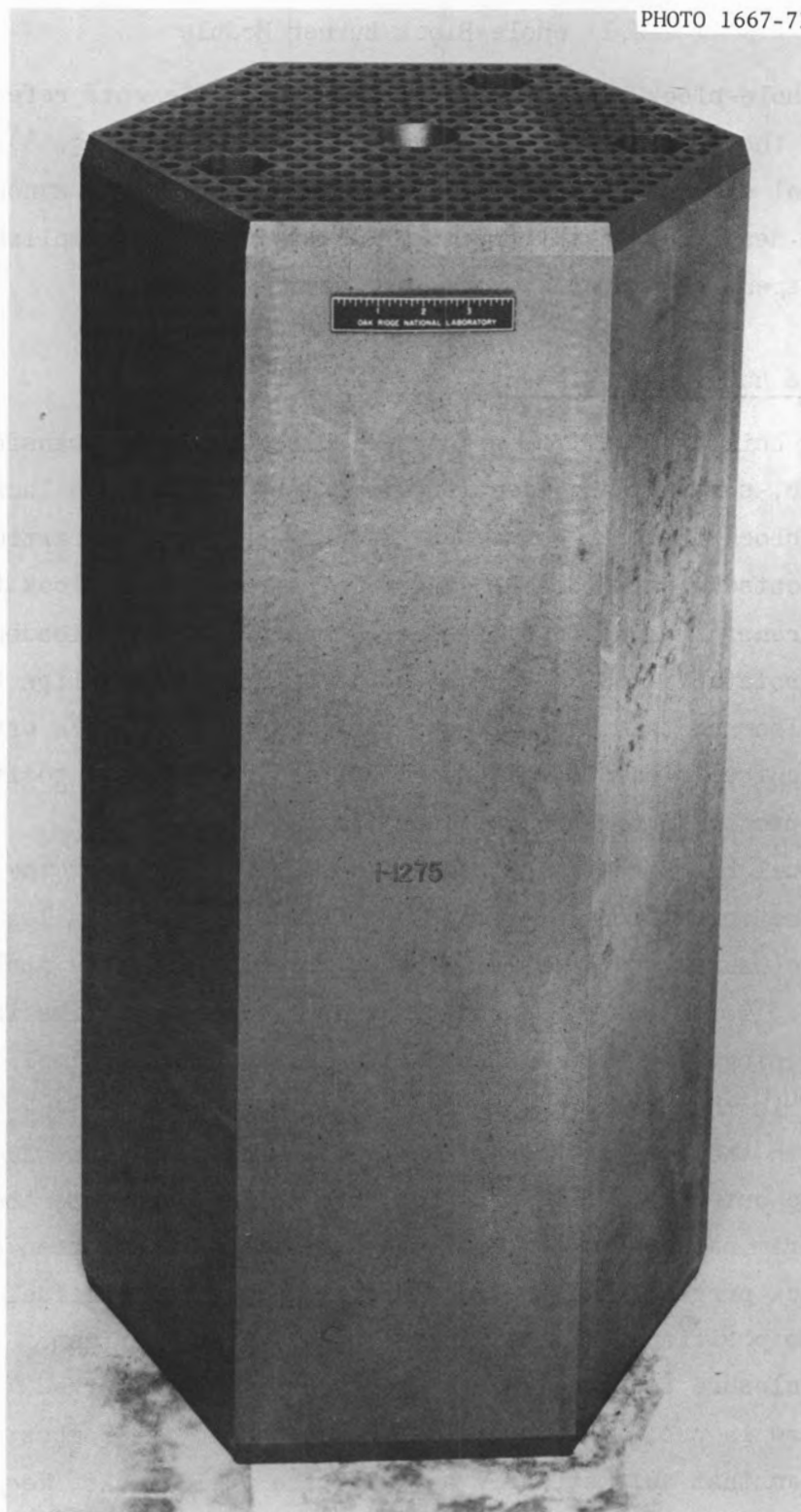


Fig. 3. Photograph of an unfueled HTGR element — Fort St. Vrain type.

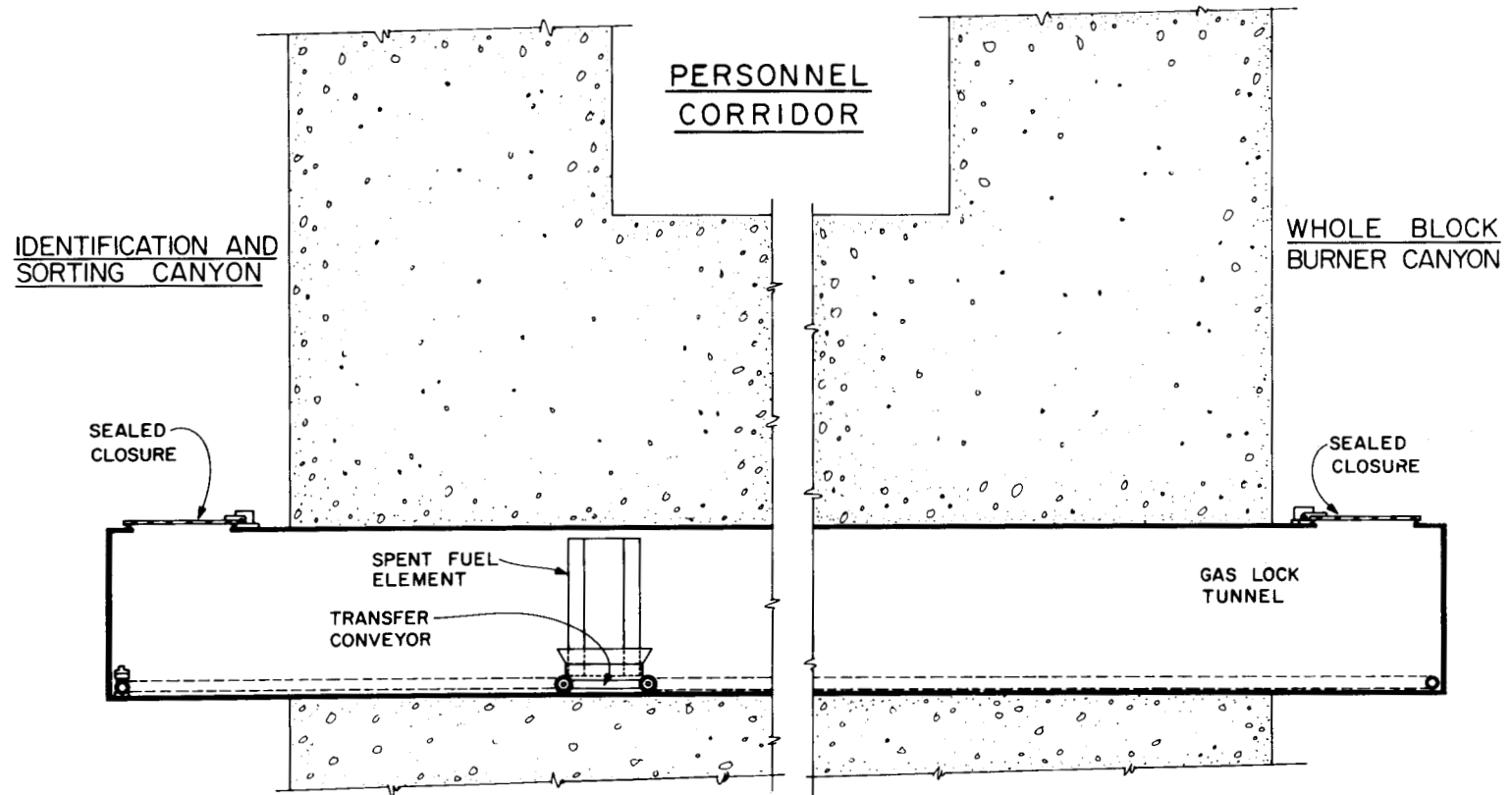


Fig. 4. Sectional view of the fuel block transfer conveyor.

ORNL DWG. 73-11879 RI

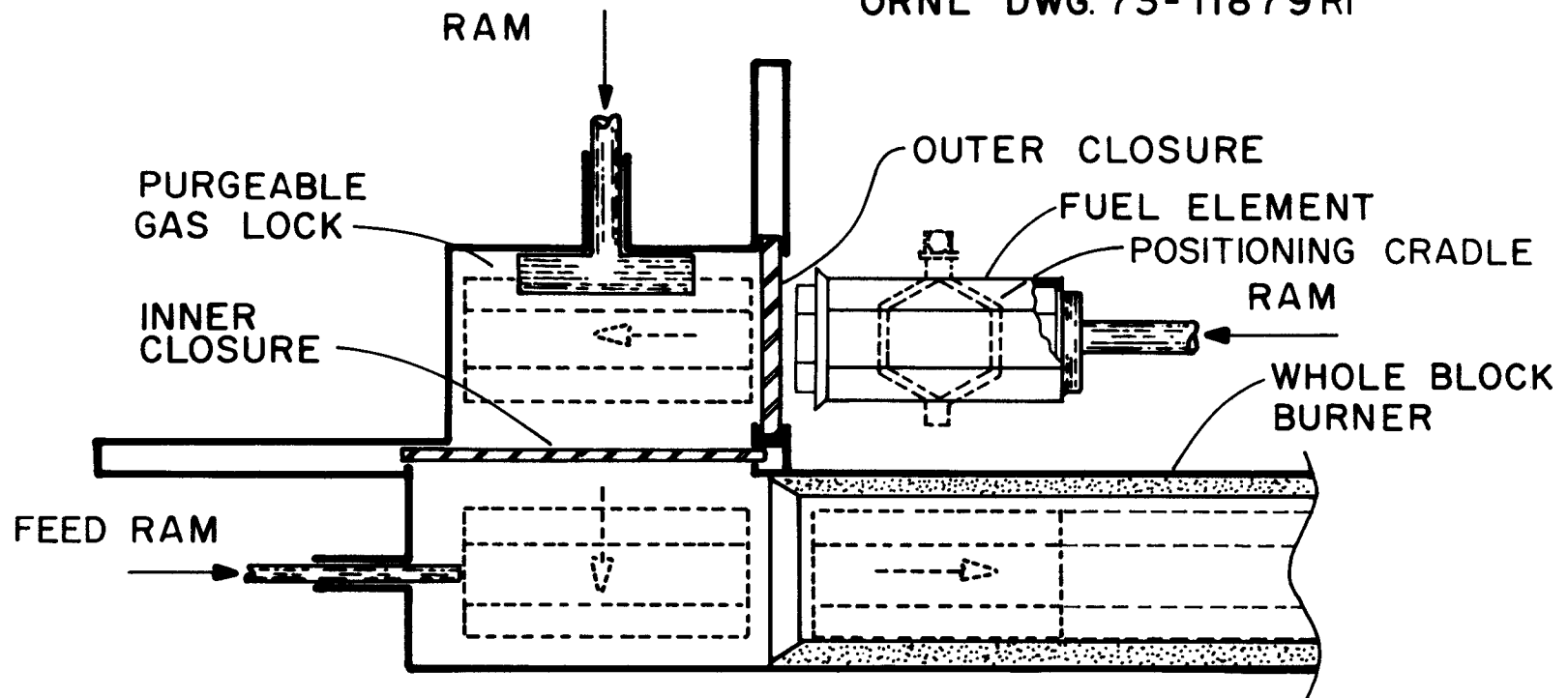


Fig. 5. Schematic representation of the WBB loading system.

### 2.1.2 Whole-block burner

The WBB, shown in Figs. 6 and 7, consists basically of a horizontal chamber constructed of a cylindrical tube (high-temperature, corrosion-resistant alloy), plus a rectangular chamber for charging or loading the fuel elements. The cylindrical tube contains a close-fitting ceramic liner (i.e., its cross-section cavity matches that of the hexagonal shape and size of the fuel blocks) and is surrounded by a cooling jacket, which is shown in Fig. 8. The entire burner is thermally insulated to minimize heat loss to the canyon.

A mixture of oxygen and carbon dioxide is injected at the combustion end of the burner, and the fuel blocks are charged at the other end (see Fig. 6). Carbon dioxide, which makes up the largest fraction of the mixture, is primarily generated by the oxidation of the graphite fuel block and is recirculated through the burner as a diluent gas for both heat removal and temperature control at the burning face of the fuel blocks (referred to as the adiabatic mode). This combustion gas mixture is forced to flow through the fuel block coolant holes because of the close-fitting ceramic liner. The forced flow will tend to cause the fuel block to burn evenly across the face normal to its axis. As the graphite block and carbon matrix are burned away, the fuel particles are released and are swept by the gases into a cyclone separator (see Figs. 6 and 7), along with any unburned carbon particles that are small enough to be fluidized.

The solid product from the cyclone separator is transferred pneumatically to a product hopper. The off-gas from the cyclone is routed through a carbon monoxide oxidizer and a heat exchanger. A blower, located in an adjacent cell, recirculates this off-gas stream back to the inlet end of the WBB or through roughing and HEPA filters to the off-gas decontamination system. A second blower recirculates a gas stream through the cooling jacket surrounding both the cylindrical burning and the rectangular charging portions of the WBB.

The burning chamber will normally contain three or four blocks during burning.<sup>3</sup> After each fuel block has been burned and the feed ram has advanced approximately 32 in., the feed ram is retracted and the next block is charged into the burner in the manner previously described. Subsequent

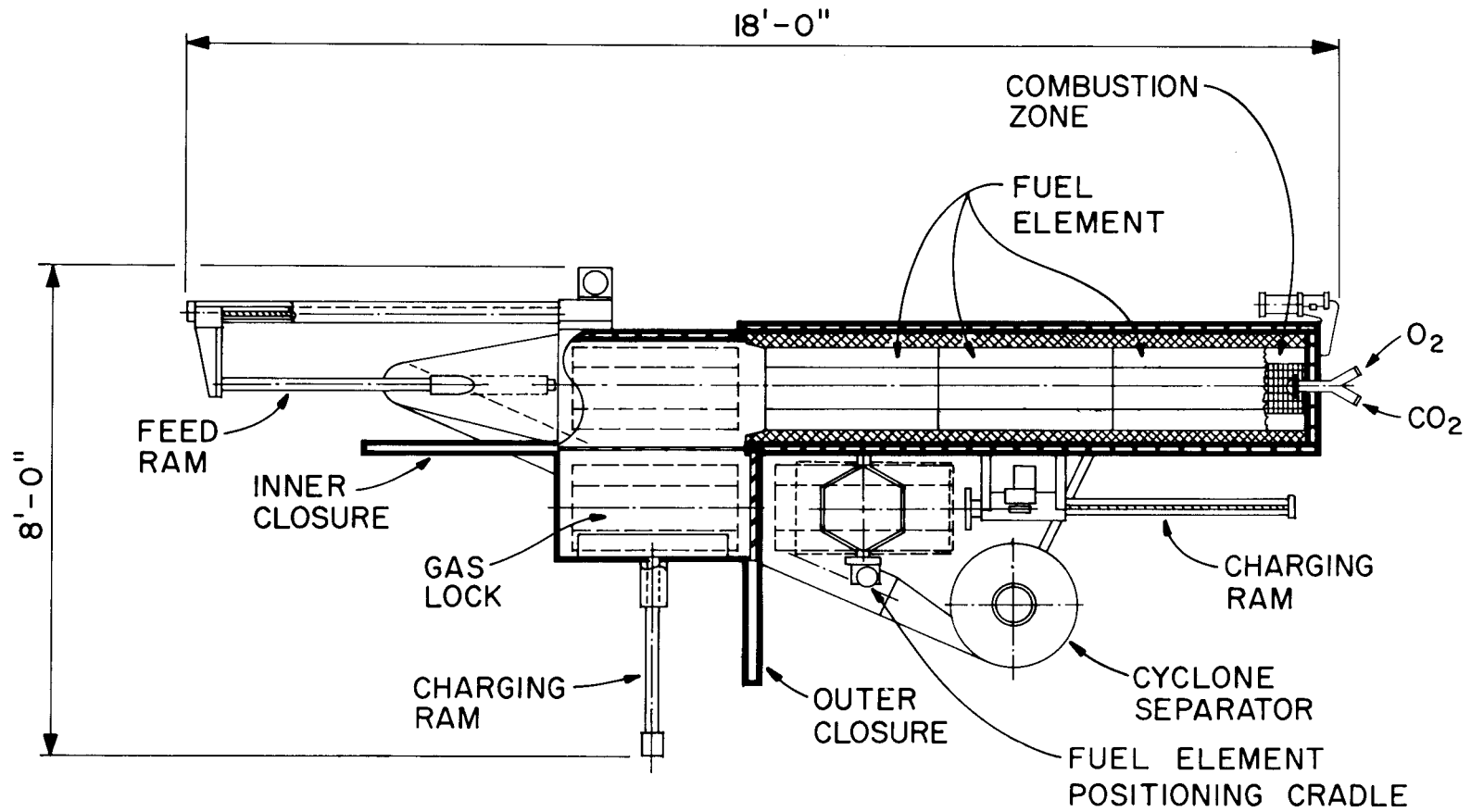


Fig. 6. Conceptual plan view of the WBB.

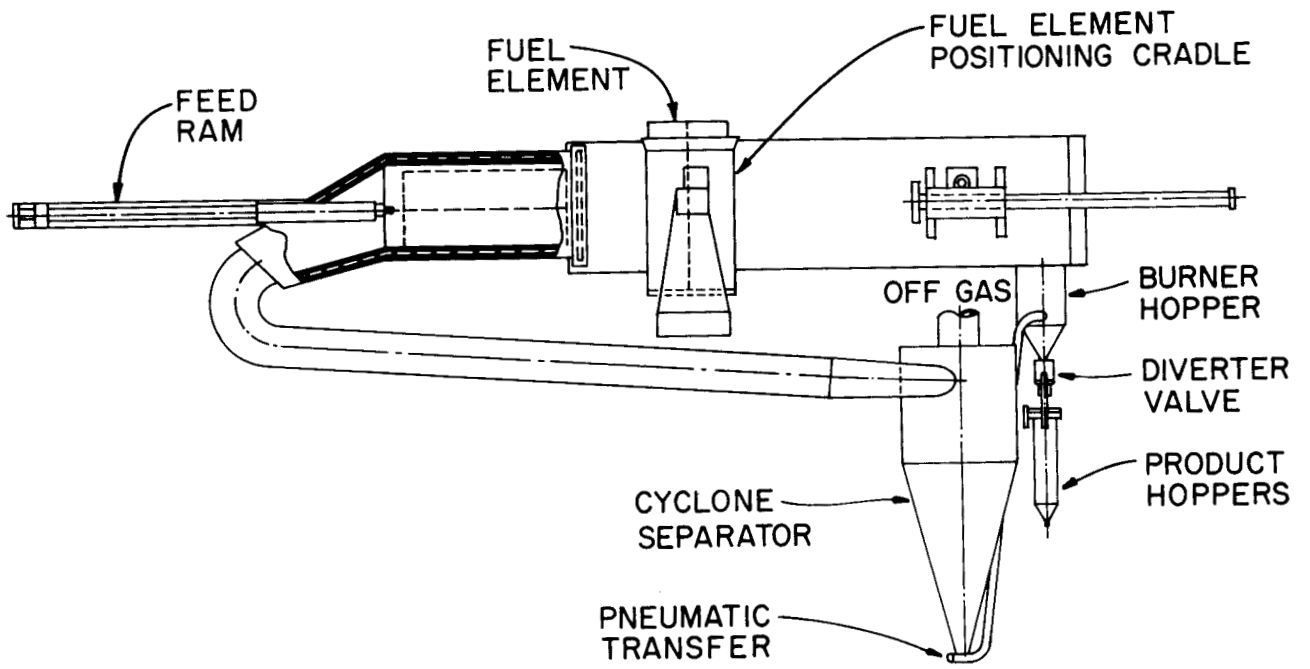


Fig. 7. Conceptual elevation view of the WBB.

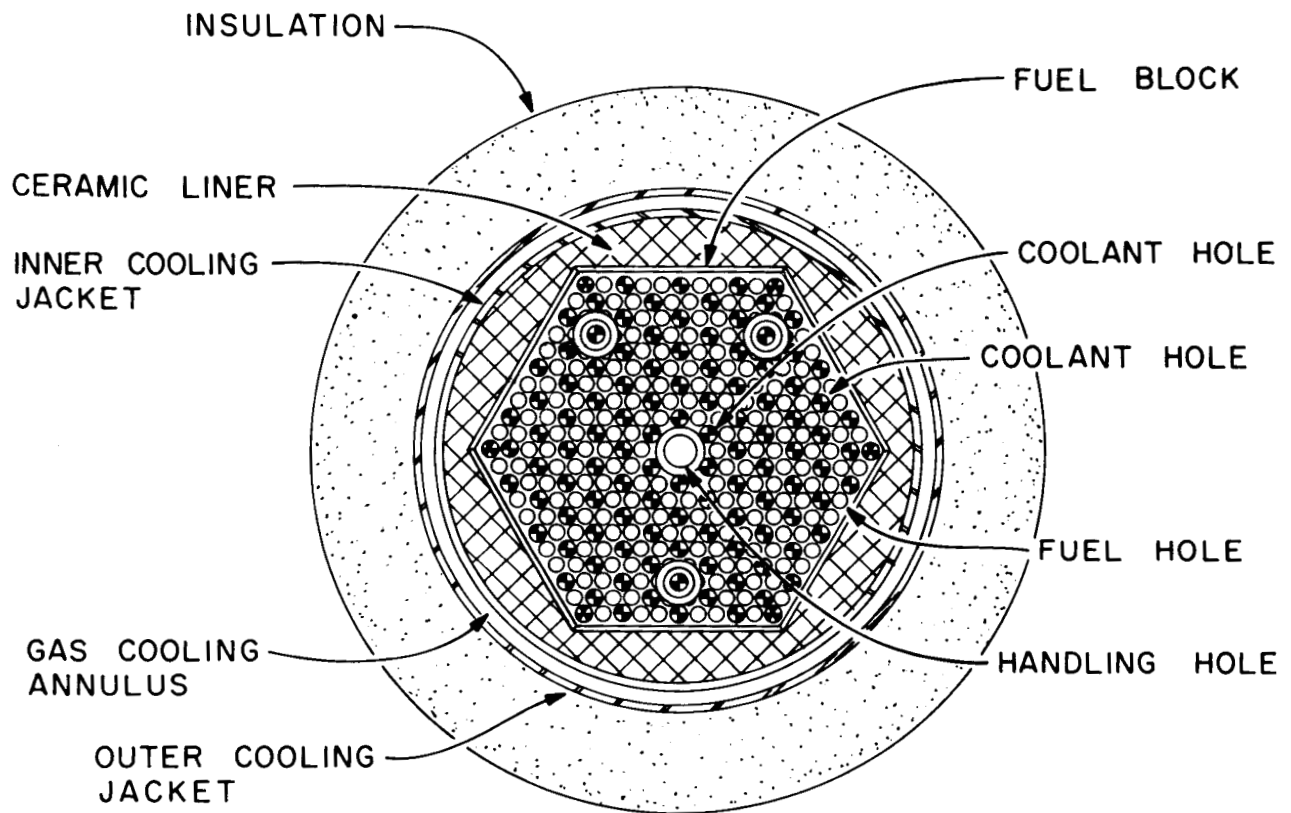


Fig. 8. Sectional view of the conceptual WBB.

fuel blocks are charged, fed, and burned similarly until an entire batch has been charged. At this point, three unburned feed blocks remain in the burning chamber. Whether these three blocks can be satisfactorily burned without the use of off-specification unfueled blocks is uncertain and will require developmental studies. The feeding of three off-specification unfueled blocks would ensure that all of the spent fuel blocks were burned.

After the burning of a batch of blocks is complete, the WBB can be shut down for inspection, cleanout, or maintenance. At this time, the burner, cyclone separator, and hopper zones can be scanned with a portable detector to determine if there is any fuel holdup. Also, a visual inspection of the burning zone of the burner can be made by opening the hinged head through which the oxygen and diluent gas nozzles are mounted.

Maintenance of the WBB is accomplished by, first, releasing the clamps securing the manifold to which all process lines, cooling lines, and electrical leads are connected. Then, the burner is lifted above all the other equipment in the adjacent modules and transported horizontally to a position beyond the burner cells where it can subsequently be conveyed into a decontamination and maintenance cell. An adjacent contact maintenance cell with glove ports can also be utilized for maintenance following decontamination, or for transferring equipment in and out of the burner canyon.

### 2.1.3 Whole-block product burner

To ensure complete burning of the spent fuel block and the outer carbon coatings on the fuel particles, the product from the WBB is pneumatically conveyed into a small fluidized-bed or static-bed endothermic burner. This unit will be electrically heated by resistance heaters to approximately 800°C. All connections will be terminated at the top and mated to corresponding connections in a fixed mounting flange to facilitate remote replacement.

### 2.1.4 Classifiers

After all the carbon has been burned away from a given batch of fuel particles, the 25R or 25W type fuel is separated pneumatically from the

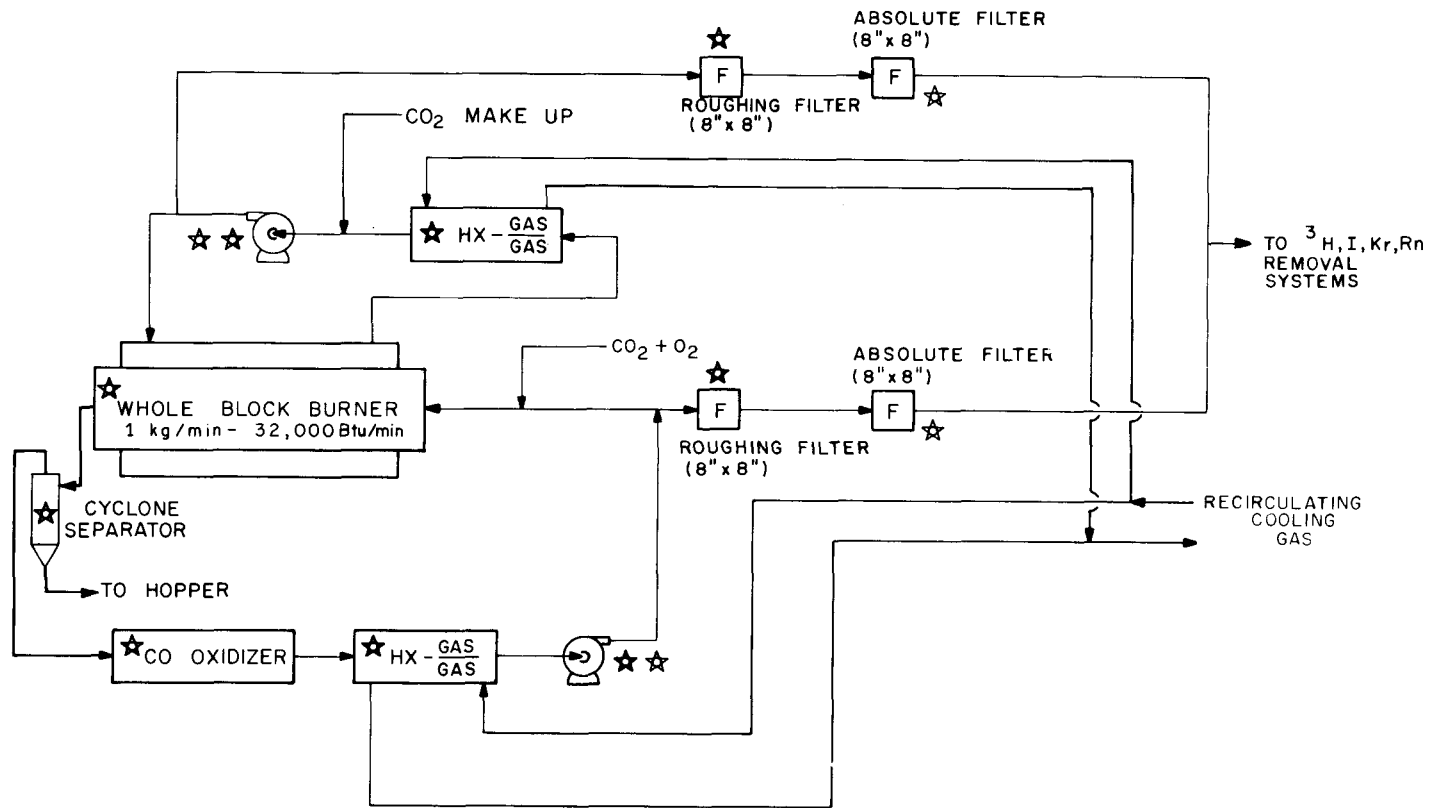
thorium particles by two separator columns or classifiers arranged in series. If a batch contains only  $^{23}\text{R}$  and thorium, the classifiers are bypassed. These classifiers are mounted as a single unit with mating flange connections similar to those for the product burner and other equipment within the cell requiring maintenance or replacement.

#### 2.1.5 Particle crusher

The  $^{25}\text{R}$  particles have a silicon carbide coating (for containment of fission gases) which must be cracked or crushed before the inner (buffer) carbon coating can be burned. The exit stream from the classifier is fed through a double-roll crusher to obtain product which is pneumatically transferred through the cell wall and into the dissolver canyon, where it is weighed, burned in a secondary fluidized-bed crushed particle burner, reweighed, and finally sent to the dissolver. The  $^{25}\text{W}$  particles may be conveyed directly into weigh hoppers and to a canning station without being crushed or burned. The  $^{23}\text{R}$  and thorium streams will be transferred, first, to the weigh hoppers in the dissolver cell, and then into the dissolver.

#### 2.1.6 Auxiliary process equipment

Heat exchangers and CO oxidizer. Two heat exchangers are located in each WBB cubicle. The off-gas from the burner is cooled by the first heat exchanger (gas-to-gas, approximately 27,000 Btu/min). The exchange fluid (probably  $\text{CO}_2$  or  $\text{N}_2$ ) is pumped in a closed circuit to a large common heat exchanger (gas-to-water) located outside the building (recirculating cooling gas stream of Fig. 9). The major portion of the burner flue gas is recycled to the burner where it is used as a diluent gas, while the remainder is filtered and routed to the off-gas decontamination system. A CO oxidizer located immediately ahead of the off-gas heat exchanger will burn the CO in the off-gas. Oxygen injection will be adjusted to give the desired burning rate. This heat exchanger and the CO oxidizer are attached to a manifold for ease in remote removal, replacement, and/or maintenance. The second heat exchanger (gas-to-gas, approximately 5000 Btu/min) cools the gas from the burner cooling jacket.



HX HEAT EXCHANGER  
 ★ LOCATED IN WBB CUBICLE  
 ★★ LOCATED IN BLOWER CANYON

Fig. 9. Flowsheet for the WBB in the adiabatic mode.

Blowers. Two blowers are required for each WBB: one for the normal off-gas circuit, and one for the cooling jacket gas circuit (see Fig. 9). These blowers are located in an adjacent cell or corridor and are thus isolated from the burner cell. The corridor, containing 30 blowers, is served by a separate bridge crane and electromechanical manipulator. This arrangement affords desirable shielding and easier maintenance for the rather large rotating machinery (100 hp and 15 hp, respectively).

Filters. Two 8 x 8 in. roughing filters and two 8 x 8 in. absolute filters are located in each burner cell module. One pair of roughing and absolute filters in series provides filtering for the burner cooling gas circuit in the event that a rupture or leak should occur between the burner wall and its cooling jacket. This filter will, of course, require changing if a leak occurs. The other pair of filters is for normal off-gas or flue gas filtering. These filters can be routinely changed by the manipulator.

#### 2.1.7 Remote handling and maintenance equipment

Specially designed remote tools, as well as a standard general-purpose bridge crane and electromechanical manipulator, will be required to operate and maintain the burner and auxiliary equipment within each WBB cubicle. Transfer of the fuel blocks from the fuel block conveyor gas lock to the burner charging station requires a special tool consisting of an electromechanical arm and hand to engage the centerhole of the fuel block. This unit is mounted on a bridge which spans the burner cubicle and travels on rails installed along the top of the partition walls separating the burner modules.

An electromechanical manipulator will be required in the servicing of the classifiers and roll crusher, as well as in the inspection and cleanout of the burner. Heat exchanger and filter changeout can also be handled by this manipulator. A bridge crane and general-purpose electromechanical manipulator system traveling the entire length of the burner canyon serves all equipment within the canyon with regard to maintenance and replacement. This system is used to convey equipment into the decontamination and maintenance cell located at the end of the canyon. The

blower canyon has a similar system for maintenance and replacement of equipment.

## 2.2 Fluidized-Bed Burner Module

Fluidized-bed burning of spent HTGR fuel elements refers to the burning of crushed materials in an FBB. Each of the fluidized-bed burner modules (1-FBB and 2-FBB) described in this section is designed to accomplish the burning of 24 spent HTGR fuel elements per day.

### 2.2.1 Feed preparation

Crushing system. A crushing system is required to reduce the fuel elements to pieces small enough ( $< 3/16$  in.) for fluidization in the burners. As shown by the schematic diagram in Fig. 10, the system is basically a charging chamber consisting of a gas-lock type of device with an inner and outer closure plus an injection ram. This gas-lock feature is considered essential for containing fine particles produced by the crushers and for maintaining an oxygen-free atmosphere within the crusher train. The fuel blocks are transferred from the identification and sorting area to the crushing area. One fuel element (block) at a time is charged; subsequent charges are not made until the weight monitor on the product hopper being filled indicates that all of the fuel block has reached the hopper. Crushing will be accomplished in three, or possibly four, stages. These stages (i.e., crushers) would be tied together in cascade fashion with a one-fuel-block holdup volume between each. The first two crushers would be of the jaw type, while the third would be a so-called centerroll crusher considered to be very promising by GAC.

The centerroll crusher consists primarily of an 8-in.-diam roller mounted on an eccentric shaft. Although the shaft is motor-driven, the roller is free to rotate independently of its shaft. The crusher housing has fixed plates contoured on either side of the roller to receive larger particles at the top and discharge the finer product at the bottom. The action of this crusher bears no resemblance to that of a jaw crusher. Also, it is unlike a conventional double-roll crusher in that the roller does not necessarily rotate with respect to its housing during actual

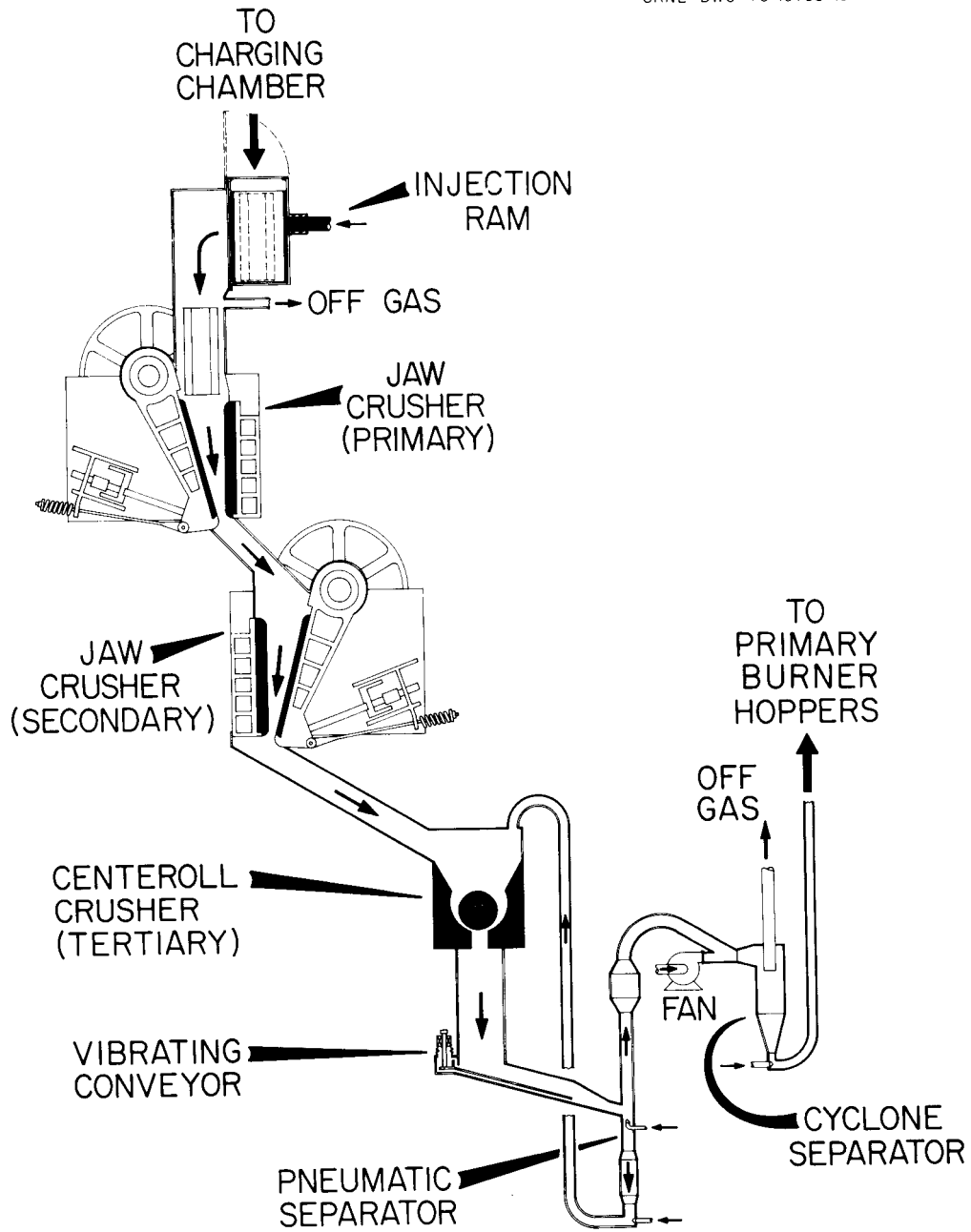


Fig. 10. Schematic of the major equipment items of the crushing train.

crushing. The action most closely resembles that of a gyratory crusher, but with the simplicity in design of the roll crusher. Two stages of the centerroll crusher may be required, although the manufacturer advertises a 12:1 reduction ratio.<sup>4</sup>

Following the last crusher is a pneumatic separator which recycles particles larger than 3/16 in. through the final crushing stage. The product is conveyed via a gas jet to the burner feed hoppers after first being routed through a cyclone separator. The exit gas from the cyclone is filtered before being passed on to the off-gas decontamination system. All gas used to maintain purges (as well as the inert purge) is envisioned to be CO<sub>2</sub>.

One crushing system would have sufficient capacity to operate a 1.5-MTHM/day plant; however, two crushing systems are included. A large bridge crane and an electromechanical manipulator are utilized for maintenance and operate above the crushers. Each crushing system, which is mounted in a common frame, can be disconnected and moved to the maintenance area for repairs.

Burner feed hoppers. After the spent fuel blocks have been crushed to the appropriate size for burning in a FBB, the crushed material must be transferred into the appropriate burners. Portable hoppers were chosen for this operation, primarily because of fuel accountability requirements but also because of the simplicity of their design and operation. There are four 16-in.-diam, 16-ft-tall hoppers at the crushing station holding up to six crushed elements each. The weight of each hopper is continuously monitored as it is filled. If the weight does not correspond to the number of elements fed through the crusher system at any given time, a warning light and/or buzzer is activated, indicating a possible malfunction in the crushing system. After being filled, these hoppers are disengaged from the filling station and transferred through the hopper transfer corridor via a conveyor into the hopper canyon where they can be routed either to a particular burner feed station or to a temporary holding zone. The hoppers are returned to a filling station in the crushing area after being emptied at a burner feed station.

If pneumatic transport of the crusher product to the burner feed hoppers is utilized, the equipment and canyon designs are changed very

slightly. In this case, there are four burner feed hoppers at the burner feed station for each FBB module (see Fig. 11). Each burner feed station has a top flange into which all connections are routed. Such connections are: a filling port, a discharge port (outside the hopper shell) which is connected to the bottom of the hopper by a tube-and-jet-lift device, a line for supplying gas to the jet lift, and a connection for blowback in the event that bridging of particles should hinder the discharge operation. This flange will mate to corresponding flanges at the filling stations and at the burner feed stations. The fixed station flanges will have alignment pins and load cells (weighing devices) combined with vertical lifting and holding devices. Located above each set of four primary feed hoppers is an intermediate hopper (one for each burner module), which enables the burner to be fed from any one of the four primary burner feed hoppers via only one feed line into the burner. Maintenance to, or replacement of, these hoppers and associated equipment is accomplished in a special remote maintenance cell located at the opposite end of the hopper canyon from the crushing area.

### 2.2.2 Fluidized-bed burner

Two fluidized-bed burning systems will be considered. The first of these is the 1-FBB.

Fluidized-bed burning without soot burning. This burner consists basically of a 24-in.-diam cylindrical tube expanding to a 36-in.-diam disengaging section at the top (see Figs. 12 and 13). A conical bottom end accommodates a nozzle for fluidization and a dump valve to a gas jet for unloading the burner. A bank of sintered metal filters with provision for blowback is located at the top of the 36-in. end. Heat is removed by a cooling jacket surrounding the outside shell and, possibly, by some internal heat exchange surfaces within the 36-in. portion.

Fuel is conveyed by pneumatic means from the primary burner feed hoppers successively to a fixed intermediate hopper and to the burner at a point some distance above the actual burning zone (Fig. 14). A given batch of fuel may be fed in large or small increments, as discussed earlier. The filters are periodically blown back to clear away any buildup of soot or fine particles. After most of the carbon in the batch has been

ORNL DWG 73-11907R2

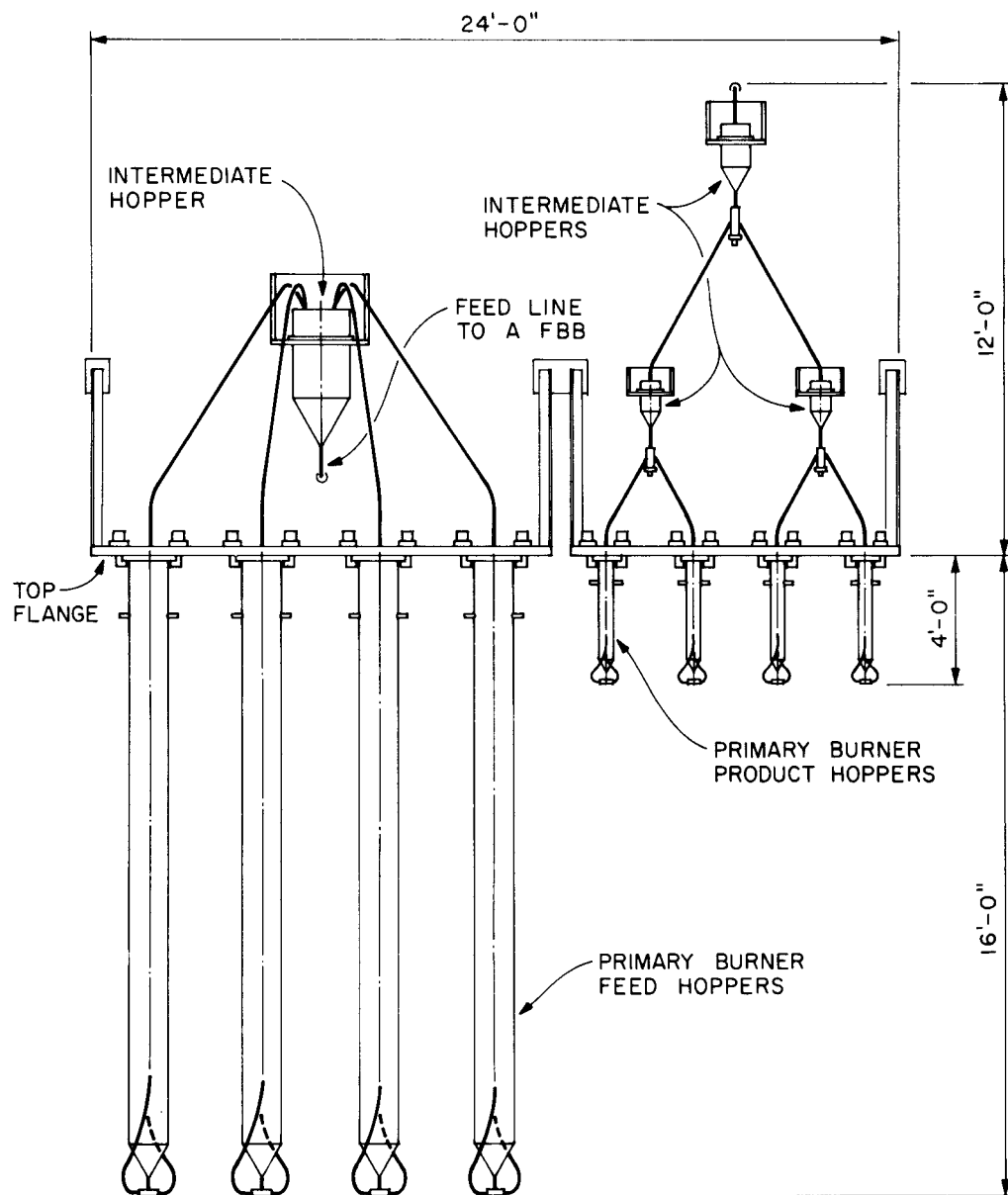


Fig. 11. Elevation view of an FBB feed station.

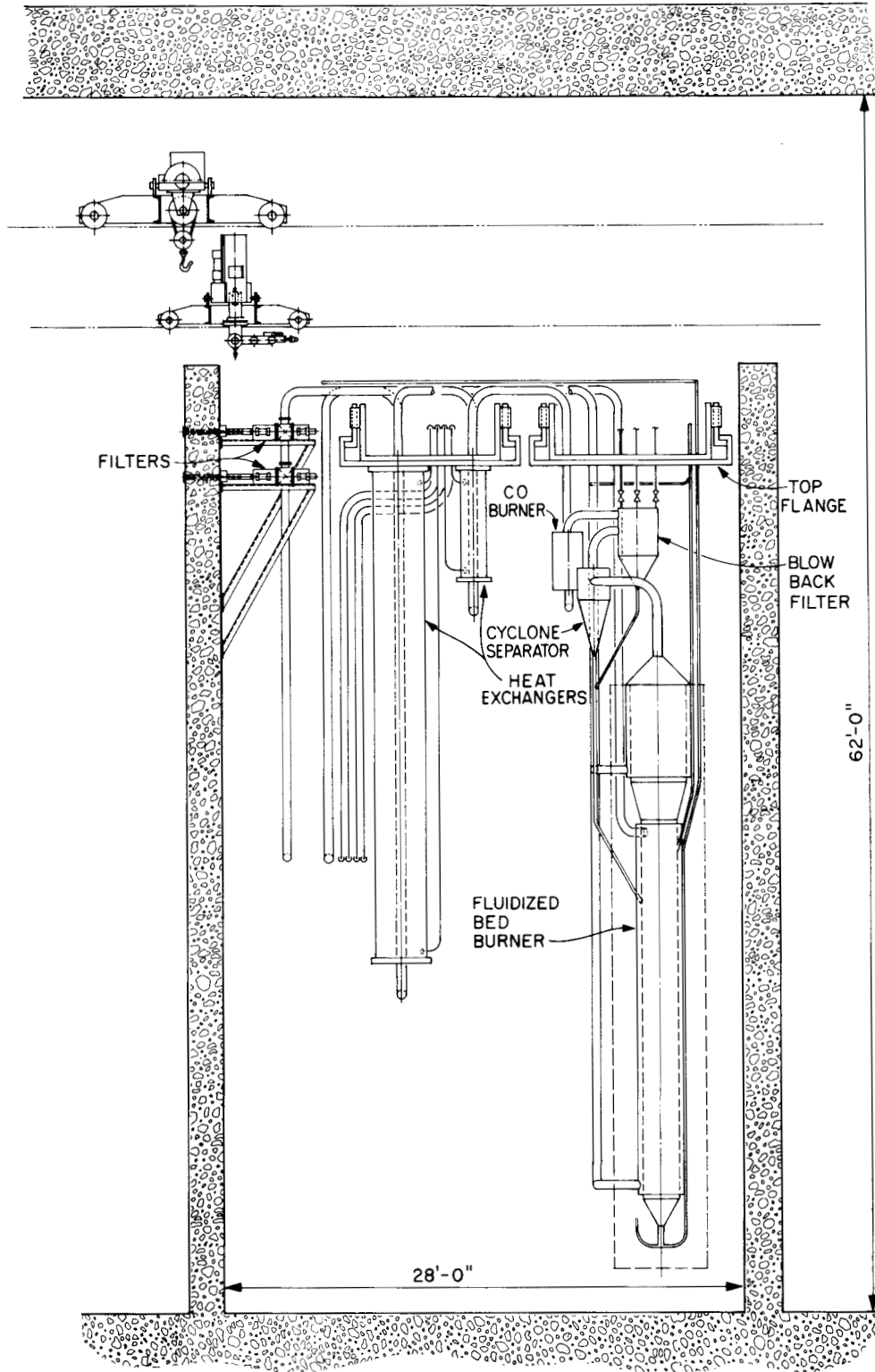


Fig. 12. Elevation view of an FBB module.

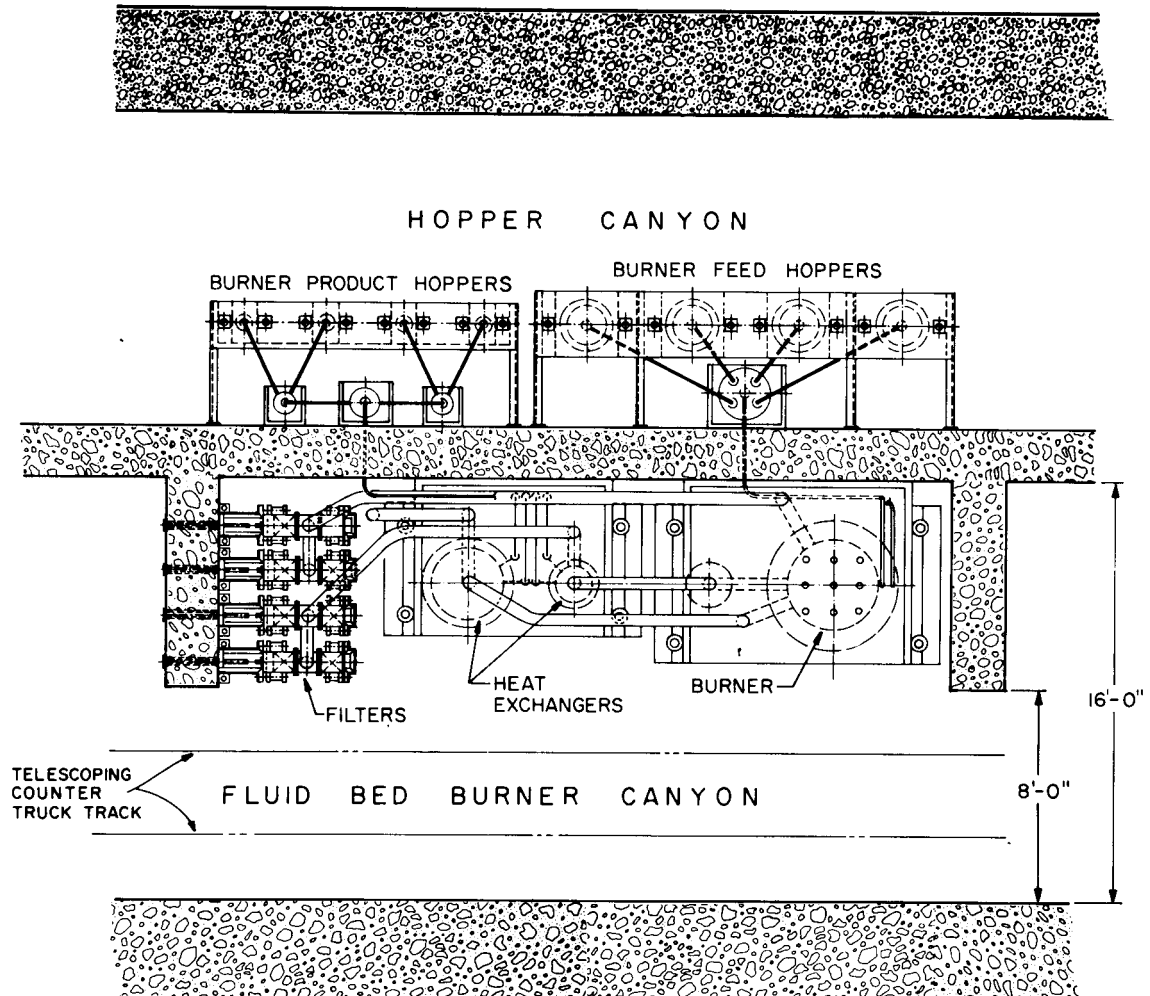


Fig. 13. Plan view of an FBB and feed station.

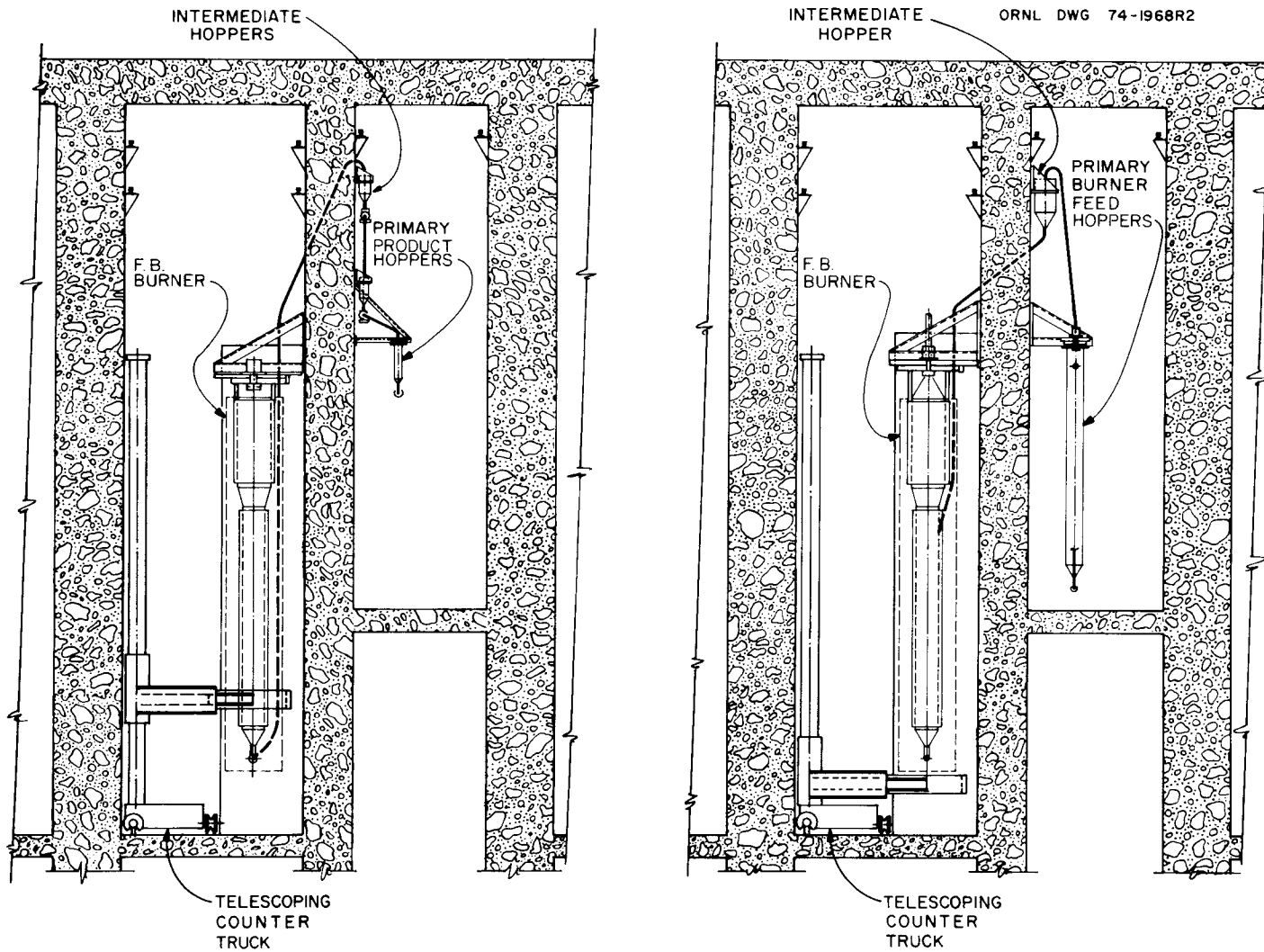


Fig. 14. Elevation view of the FBB showing the relationship of the feed and product hoppers.

consumed (contents of one primary burner hopper, or six spent fuel blocks), the oxygen concentration in the off-gas will increase and the temperature will decrease. The resistance heaters can then be turned on to hold the FBB temperature to  $\geq 800^{\circ}\text{C}$ . In this endothermic burning mode, the residual carbon is oxidized to  $\text{CO}_2$ . At the completion of the endothermic burning step, the particles are pneumatically conveyed from the burner to one of four product hoppers located adjacent to the primary burner feed hoppers in the hopper canyon (see Figs. 14 and 11).

Another primary burner feed hopper is used for recharging the FBB. The resistance heaters are left on (possibly assisted by a CO torch); and, when the temperature for ignition is reached, the oxygen flow rate is increased. The CO torch and the resistance heaters are phased out as combustion commences.

This procedure of shutdown and reignition of the FBB must be repeated four times daily. After a given batch of fuel has been completely burned and the next batch is fed into the FBB, the FBB can be checked with the telescoping counters for holdup. This is accomplished by moving the telescoping counter truck to the FBB station, advancing the horizontal ram to align the counter segment ring with the center line of the FBB, and moving the counter ring upward around the FBB housing. At this time, no significant quantity of product should be located within the cubicle. The shielding walls prevent direct line of sight from the FBB to any other FBB cubicle or feed and product hopper stations (Fig. 13).

Fluidized-bed burner with soot burner. This system (2-FBB) consists basically of an 18-in.-diam fluidized-bed primary burner, a cyclone separator with sintered metal blowback filters on the off-gas side, and a 24-in.-diam fluidized-bed soot burner (see Figs. 15 and 16). Since a high percentage of fines or soot is produced in the fluidized-bed burning of graphite pieces, this system, which contains a separate burner with appropriate fluidizing velocity for the fine material, should be more efficient than the 1-FBB system.

The avoidance of a soot burner has been predicated on the belief that the additional cost associated with it would be prohibitive. In reality, costs for such equipment located within remotely operated hot cells are generally only a small part of the total cost (< 25%), whereas the

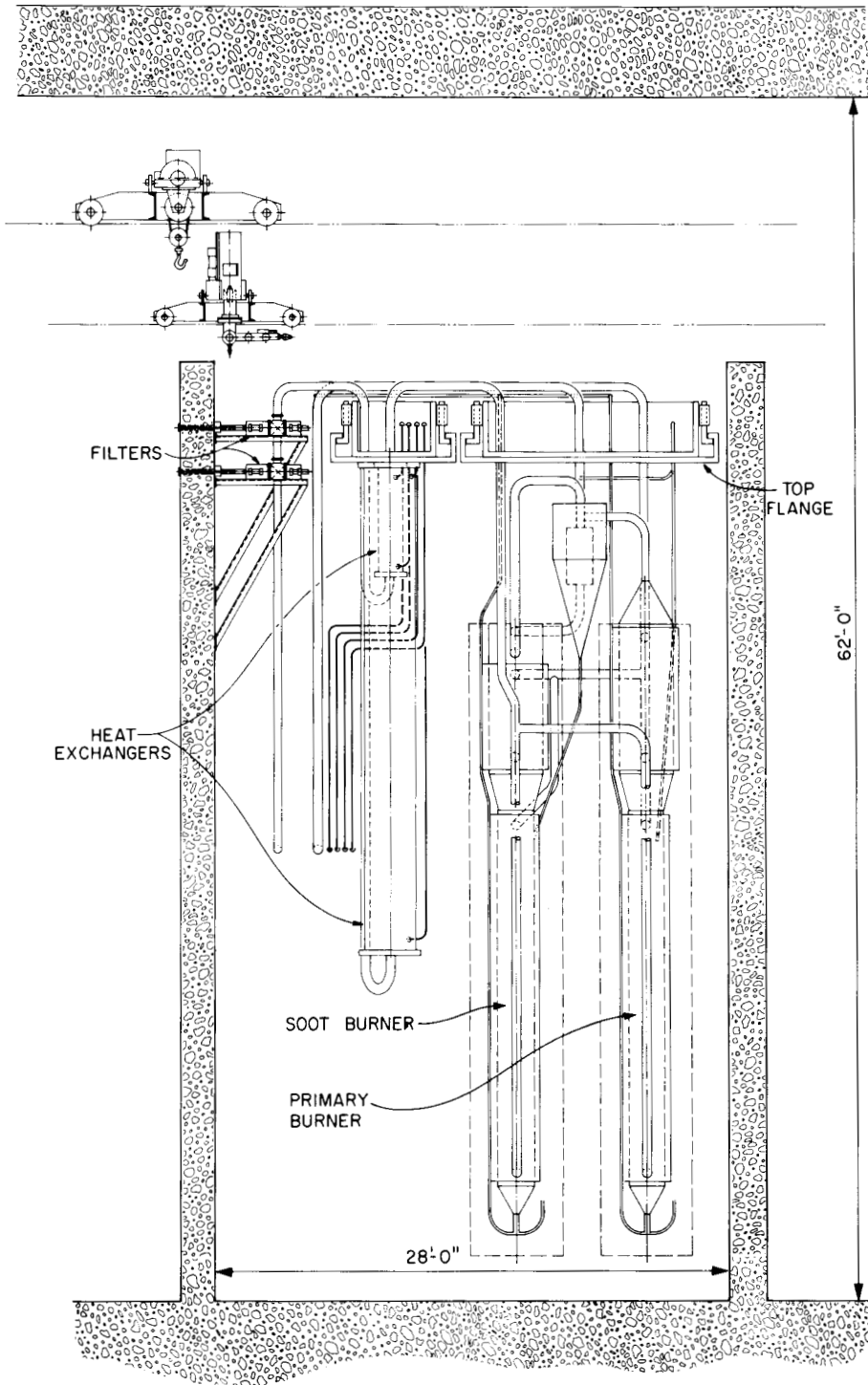


Fig. 15. Elevation view of an FBB module with a separate foot burner.

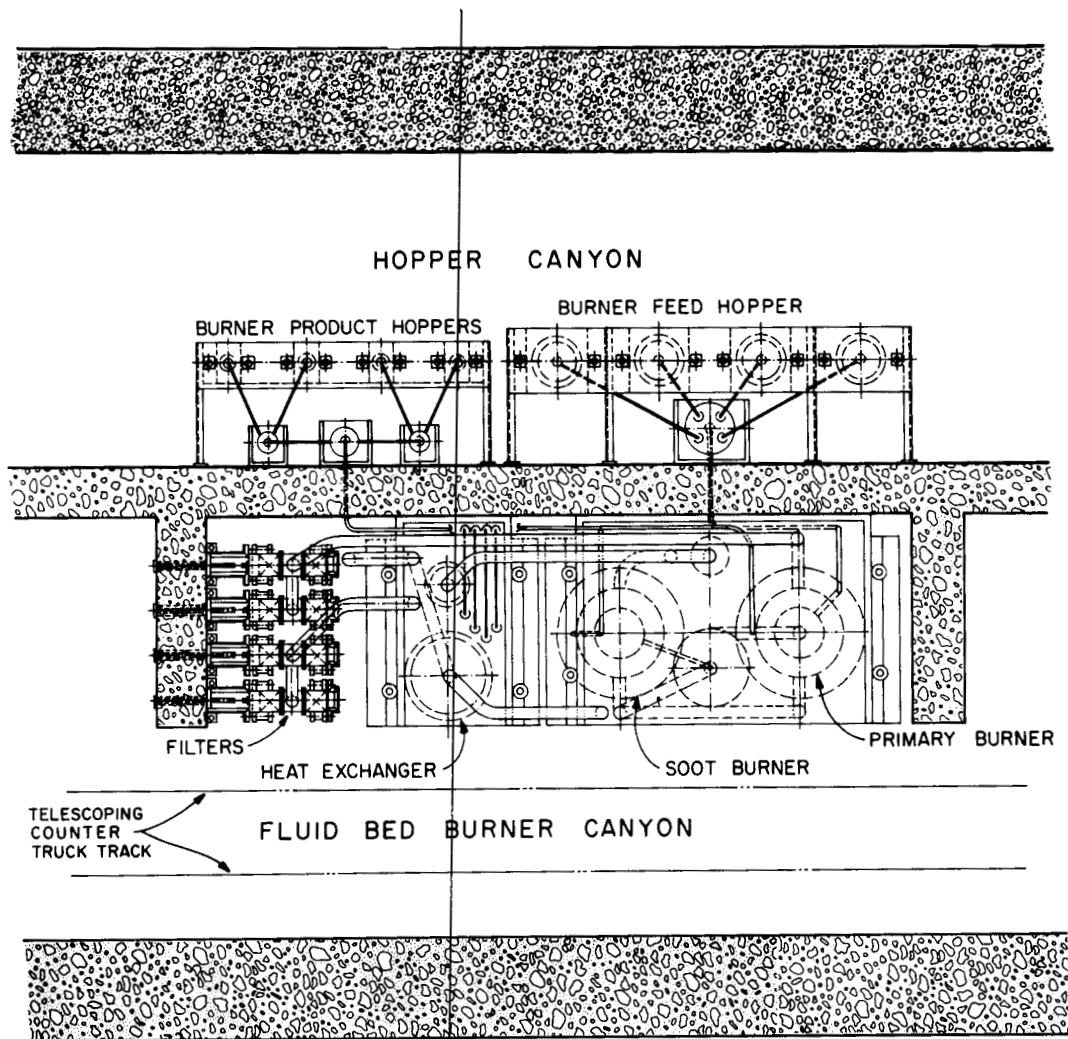


Fig. 16. Plan view of an FBB with separate soot burner and feed station.

building cost (or space required) represents a significant part. The validity of the reasons for not including separate soot burning, which would eliminate several operating difficulties if soot can be burned without a heat transfer medium, is supportive only if the assumption of separate soot burners increasing the hot cell area is correct.

The length of the primary burning module was determined by the lengths required for the primary burner hoppers and primary product hoppers. Since the length of the primary burner module is determined by the space required for hopper supports (four feed and four product hoppers per module), including the extra burner would require no (or limited) additional building expenditures. The benefits of separate soot burning would probably justify the additional equipment expense incurred by including the soot burner.

The operating procedure for the 2-FBB system is similar to that for the 1-FBB. One important difference, however, is the potential capability of the 2-FBB for operating with only one dump-and-reignite cycle per day (or, perhaps, one cycle per annual reactor discharge). It has been determined by GAC that a soot burner requires no extraneous heat transfer media. Thus, no special problems are involved in handling  $Al_2O_3$  or similar materials for this purpose.

The auxiliary equipment required for the 2-FBB system is very similar to that required for the 1-FBB; however, the piping will be slightly more complex to service two burner shells.

### 2.2.3 Primary-burner product hoppers

These hoppers are mounted to a fixed flange similar to that on which the primary burner feed hoppers are mounted (see Figs. 11 and 14). Ahead of these hoppers, however, are three intermediate hoppers with two-way diverter valves for channeling the flow to a particular product hopper. After being filled, a product hopper is disconnected and conveyed down the hopper canyon to a corresponding dissolver loading station. As at the burner modules, each dissolver module has four loading stations from which the product is pneumatically conveyed to an intermediate hopper that feeds two pneumatic separators or classifiers in series. One

stream is routed through a double-roll crusher where the burned-TRISO\* particles are crushed; the other stream feeds into a weigh hopper and finally into a dissolver. The product from the roll crusher (approximately 6-in.-diam rollers) is weighed in a hopper and fed into a small FBB (approximately 4 in. in diameter) where the inner (buffer) coating of carbon is burned. After a given batch has been completely burned, it is pneumatically transferred to a weigh hopper before being dumped into a dissolver. The 25W particles from the classifier can be fed successively through the roll crusher and the crushed-particle burner, and then conveyed to a canning station; alternatively, they can be sent directly from the classifier to a canning station. It should be noted that the WBB and FBB primary burning modules contain different amounts of equipment. However, this is not accounted for in the space requirements for secondary burning and dissolution.

#### 2.2.4 Auxiliary process equipment

Heat exchangers. Two heat exchangers located within each fluidized-bed module are required to remove the heat (see Figs. 17 and 18). A gas-to-gas heat exchanger of approximately 8000-Btu/min capacity will cool the off-gas before it is filtered and sent to the off-gas decontamination facility. Another gas-to-gas heat exchanger with a capacity of approximately 50,000-Btu/min handles the gas from the cooling jacket surrounding the burner. Each of the units is constructed so that all connections terminate in a top flange which mates with a fixed manifold. A special positioning and clamping device makes for easy remote removal and replacement.

These two heat exchangers service only one burner for the 1-FBB system, whereas they service two burners for the 2-FBB system. The latter case will require more pipe connections in the hot cell.

CO oxidizer. The burner off-gas normally contains an excess of CO, which is undesirable in the KALC or off-gas decontamination facility.

---

\*Burned-TRISO particles have a SiC outer layer, a thin sealer layer of carbon, and a porous carbon buffer layer surrounding the fuel kernel.

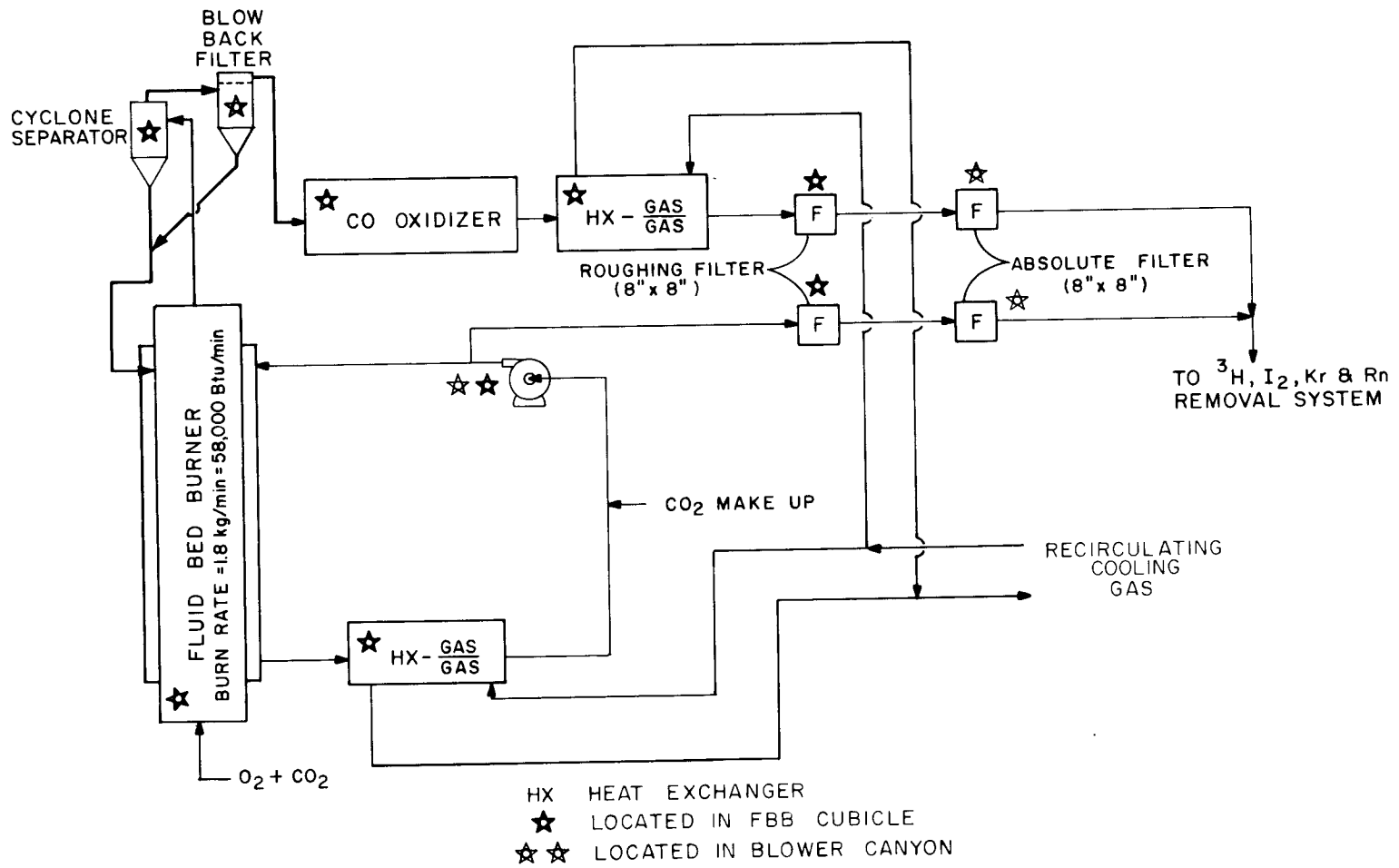


Fig. 17. Flowsheet for fluidized-bed burning.

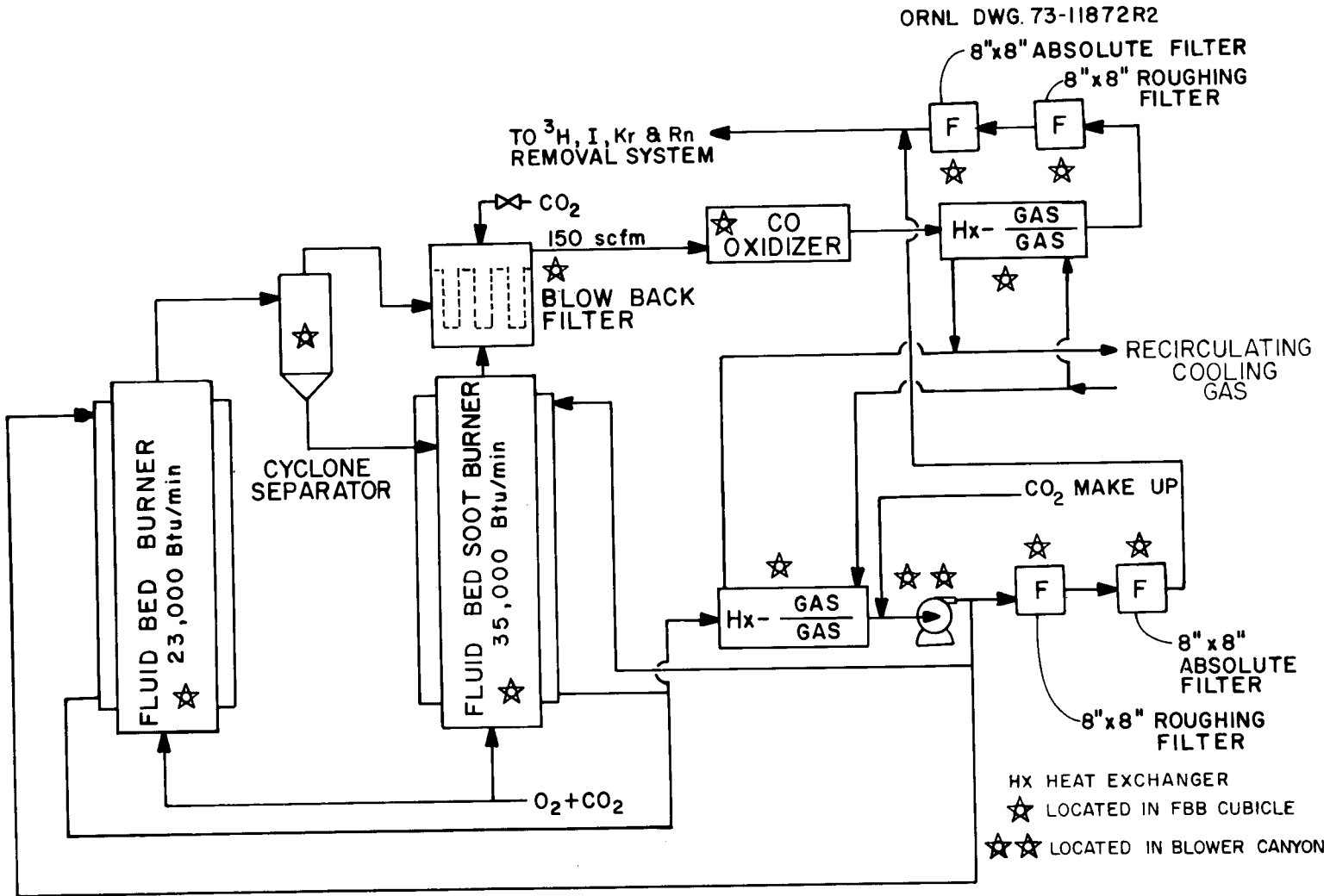


Fig. 18. Flowsheet for fluidized-bed burning with separate soot burning.

Thus, a CO oxidizer (to be developed) is required to burn this excess CO and to maintain approximately 1/2% excess of oxygen. For maintenance purposes, this unit is mounted in a manner similar to that of the heat exchangers.

Filters. Sintered-metal blowback filters are mounted at the top of the burner, and 8 x 8 in. roughing and absolute filters are included in the off-gas line between the heat exchanger and the off-gas decontamination process. A second pair of these filters is installed in a leg of the burner recirculating cooling gas which is connected to the off-gas line. This pair of filters provides filtering and venting of this circuit in the event that a rupture should occur in the burner wall. All of these filters are constructed and positioned so as to facilitate routine remote changeout.

Blowers. A separate canyon adjacent and running parallel to the burner canyon houses a motor-blower combination for each burner module. Each blower (~200 hp) recirculates the cooling gas through the burner cooling jacket and the heat exchanger.

#### 2.2.5 Remote handling and maintenance equipment

Equipment associated with the fluidized-bed burning process is located primarily in four canyons plus a fuel block crushing area. Each of these five zones has an electromechanical manipulator and crane system overhead for either in-cell maintenance or removal and transfer of the equipment to a specific decontamination and maintenance cell.

### 3. SPACE REQUIREMENTS FOR PRIMARY BURNING

If one considers an operating time of 292 days per year (0.8 load factor) and a 12-hr turnaround time between batches, then ten WBBs or seven FBBs will be required for the reprocessing plant, assuming that the spent-fuel element batch sizes are maximized (1000 spent elements per batch). If the number of spent fuel elements per batch is reduced from 1000 to 250, one additional primary burner is required (for all cases, it is assumed that all the spent 25W elements are accumulated

from each reactor before burning). The effect of smaller batch sizes on primary burner requirements is shown in Fig. 19. The lower limit of 48 elements per batch corresponds to the minimum number of spent fuel elements per rail shipment.

It was agreed (with GAC) that we would consider 15 WBBs and 10 FBBs for this study. Therefore, the number of burners included would allow any batch size to be considered. The time required for turnaround may be less than 12 hr; however, for the number of burners considered, there is no incentive for considering shorter turnaround times.

### 3.1 Whole-Block Burning

The use of multiple WBBs, each with a considerable amount of mechanical equipment, suggests a canyon-type structure with simple maintenance equipment provided locally and major or complex maintenance equipment located at the canyon end in a separate maintenance area (Fig. 20). A canyon suitable for containing the 15 WBBs is envisioned as containing 15 cubicles, each of which is 30 ft wide by 15 ft long (including a 2-ft-thick interior wall) by 18 ft high, with a 30-ft-wide by 30-ft-high manipulator-and-crane area traversing above the WBB cubicles (Figs. 21 and 22). Two additional cubicles are included to handle broken fuel elements and one set of spare modular equipment.

Individual rectilinear manipulators with specialized features are supported by the 2-ft-thick cubicle separation walls and service each WBB cubicle for routine operation and maintenance. The 15 specialized rectilinear manipulators and the WBBs (or any major component) can be disconnected and lifted by the crane, assisted by the rectilinear manipulator, and moved through a shield door into the decontamination cell located at one end of the canyon (Fig. 20).

Ventilation of the WBB canyon is accomplished by downflow of air from ceiling diffusers into floor-mounted exhaust ports. The heat liberated from burning (minus losses) is removed by two gas-to-gas heat exchangers located within each WBB cubicle. One of the gas-to-gas heat exchangers removes the heat from the burner off-gas stream, while the

ORNL DWG. 73-11906

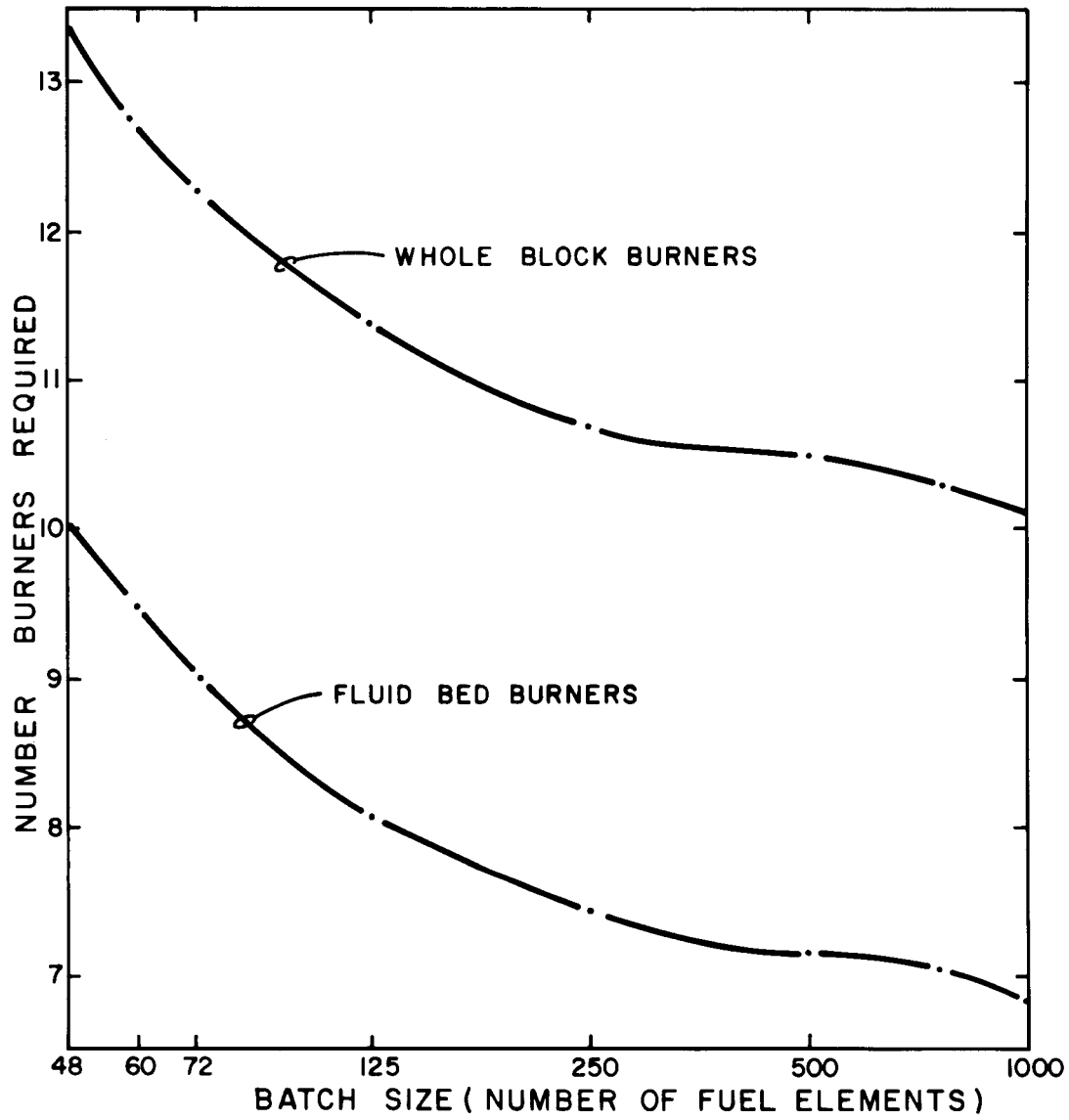


Fig. 19. Number of primary burners required for various batch sizes.

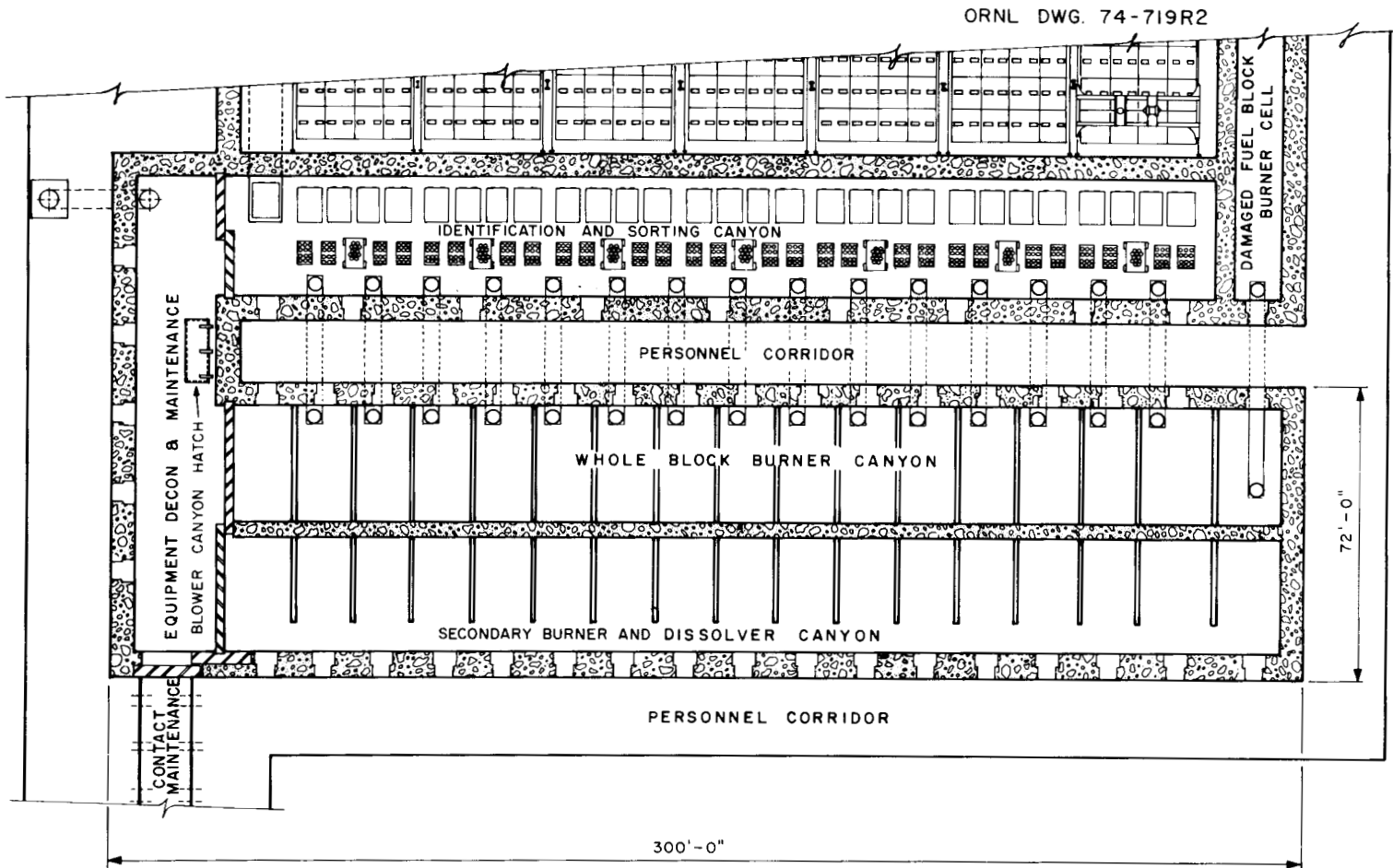


Fig. 20. Plan view of the WBB canyon, the I & S canyon, the equipment decontamination and maintenance area, and the damaged fuel block burner cell.

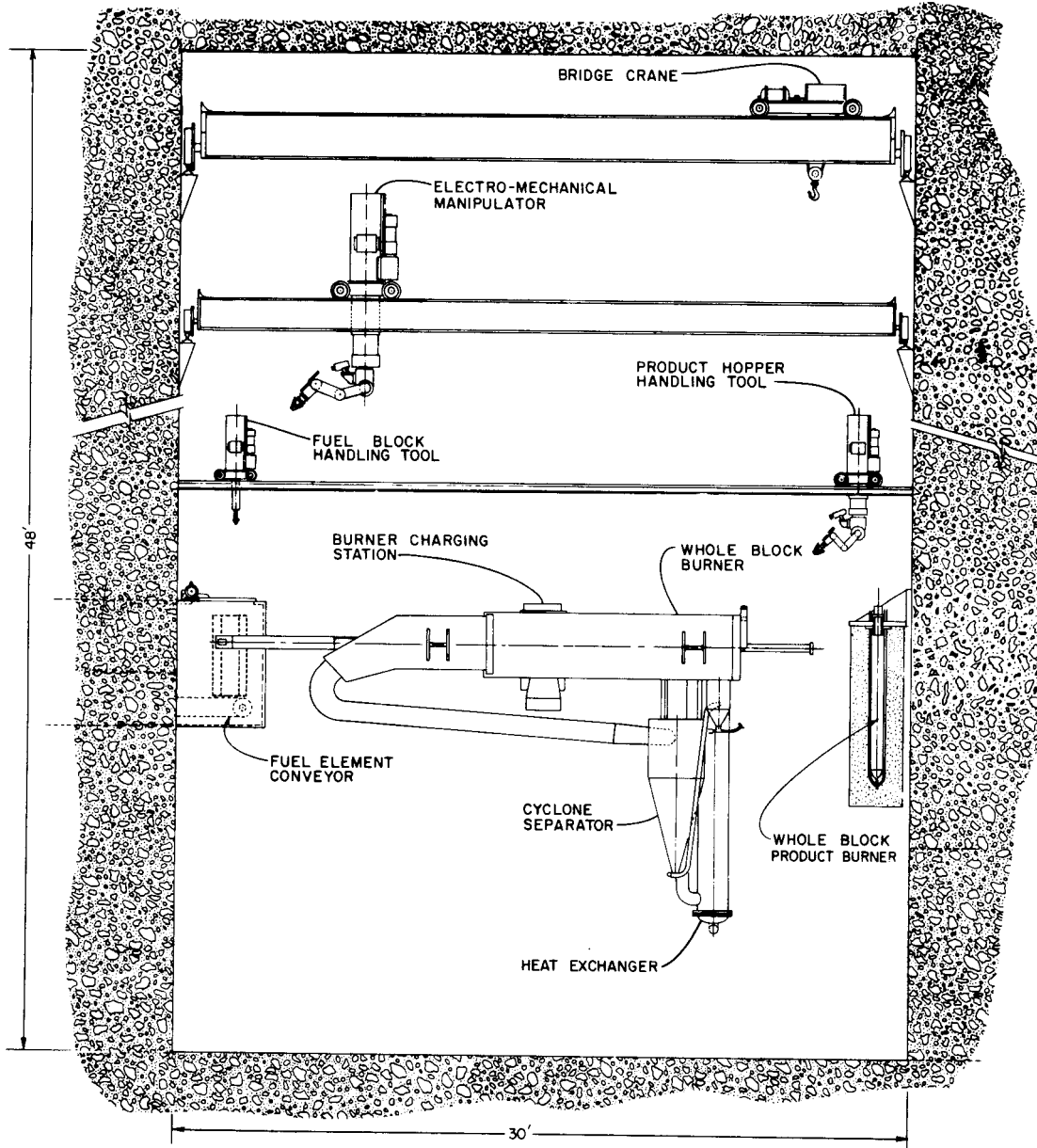


Fig. 21. Elevation view of a WBB module.

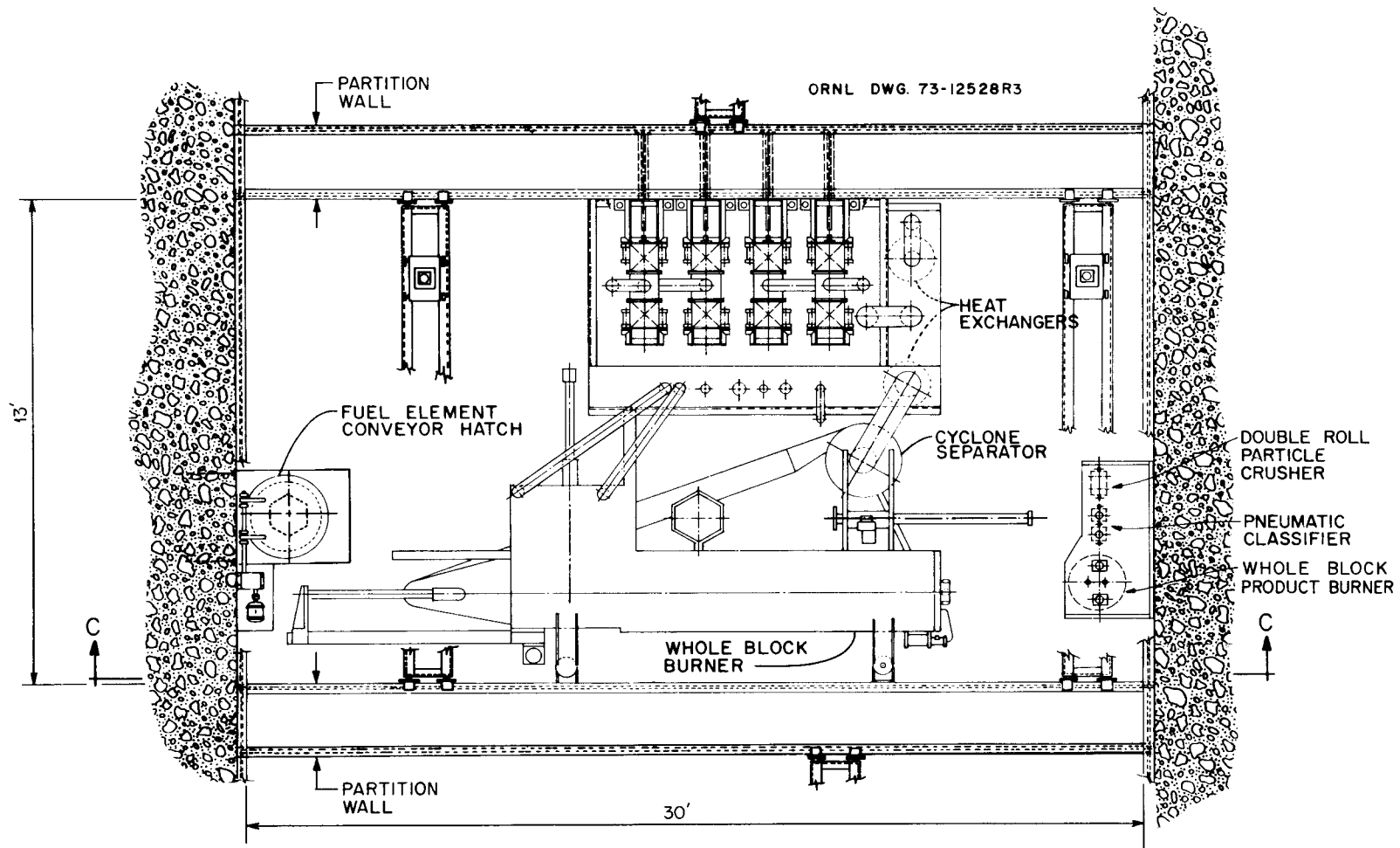


Fig. 22. Plan view of a WBB module.

other removes the heat that is lost through the WBB walls (These heat exchangers are discussed in Sect. 2.1.6.)

The blowers are located in a parallel canyon (referred to as the blower canyon) which is 16 ft wide by 25 ft high (Fig. 23). A maintenance cell is located at one end of the blower canyon for convenience. The blower canyon is equipped with a crane and rectilinear manipulator system to assist in equipment removal and repair. The two blowers required for each WBB are driven by two motors: one 100-hp unit, and one 15-hp unit. The reasons for using the gas-to-gas heat exchangers are: (1) to prevent radioactive material from leaving the building via the main coolant gas stream in the event of a furnace burnthrough, and (2) to exclude water from the primary burners except in the event of two sequential heat exchanger failures. Thus, the criticality problem associated with the WBBs can be reduced to that of a dry system. The use of two closed recirculating-gas loops between the WBBs and the cooling towers affords double containment. Substitution of a closed-liquid recirculating loop for one of these closed gas loops might reduce the capital equipment costs but would have a negligible effect on the building costs.

The larger blower and the larger gas-to-gas heat exchanger will be highly contaminated in this proposed scheme. If HEPA filters are used to maintain a (relatively) clean blower-heat exchanger system, their maintenance and upkeep will add to the complexity of operations to be performed and will also increase the space requirements.

An elevation view of the WBB canyon and blower canyon is shown in Fig. 23. The WBB canyon is located between the I & S and the SB & D canyons. A common personnel corridor is shared between the WBB and the I & S canyons, while a common cell wall is shared between the WBB and the SB & D canyons. It has been assumed that the thickness of the shielding walls between the process canyon and the personnel corridors will average 6 ft.

Figure 20 shows a plan view of these canyons and their common decontamination and equipment repair cells. The 16 WBB cubicles (one spare cubicle) and one special cubicle for handling broken spent fuel block material require a total length of 265 ft. This includes 10 ft for crane parking.

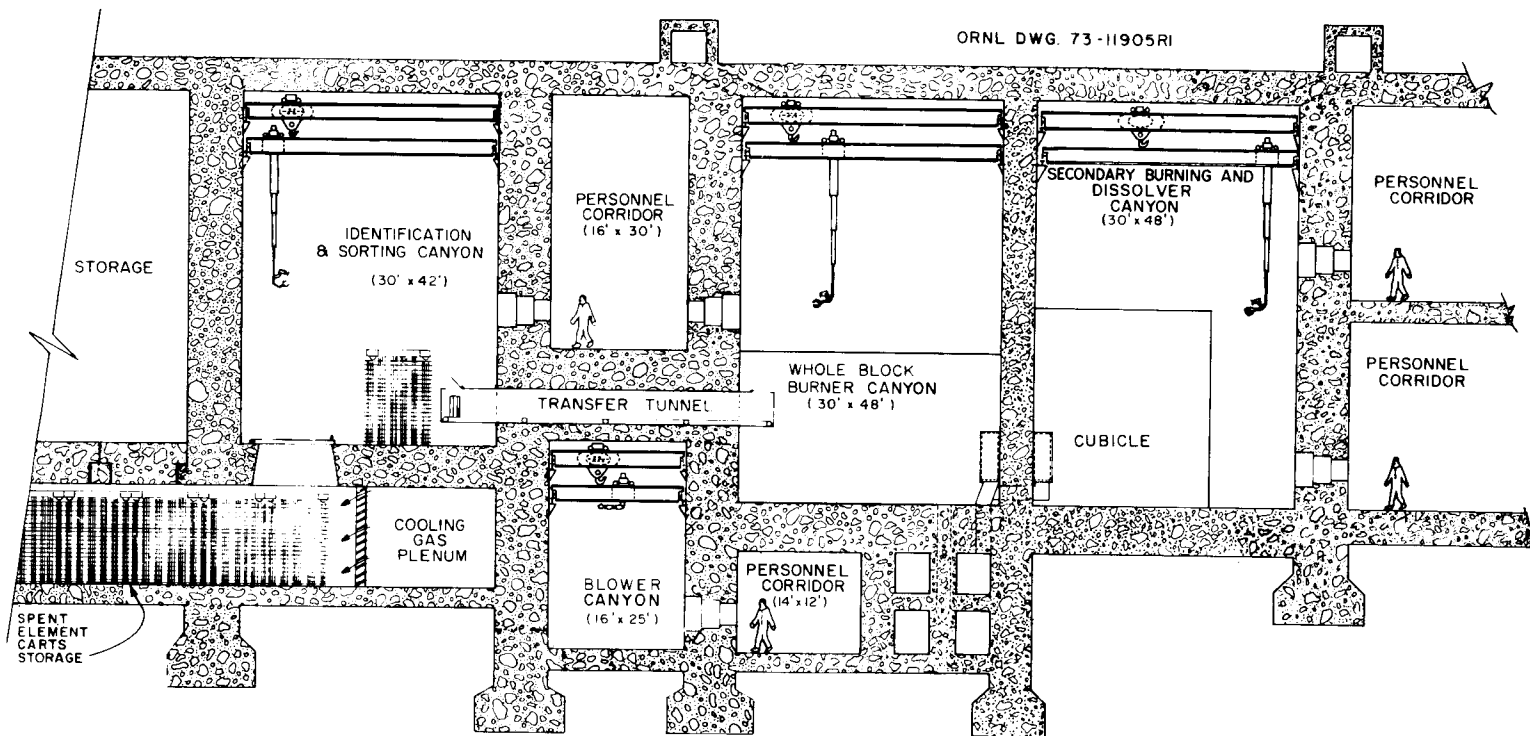


Fig. 23. Elevation view of the WBB showing the relationship of the I & S canyon, the blower canyon, the secondary burning and dissolver canyon, and personnel corridors.

The spent fuel elements move from the I & S canyon, via an element conveyor located in a transfer tunnel below the floor of the personnel corridor, to a WBB cubicle (see Fig. 23).

The product from a WBB may be composed of two streams requiring separation: the 25R or 25W stream (only one exists within any given spent fuel element), and the 23R stream. The reference HTGR fuel particles in the 25R and 25W streams have TRISO coatings. The equipment for classifying and crushing the SiC prior to secondary burning is located within the WBB cubicle for convenience of the dissolver cubicle equipment layout.

Pneumatic transfer of the roll crusher product and the 23R stream is utilized between a WBB cubicle and a dissolver cubicle. The length of the dissolver cubicles can be matched with that of the WBB cubicles so that both the WBB canyon and the SB & D canyon are equally long. In this linear process flow scheme, assurance that the spent fuel elements transferred to a WBB will arrive, eventually, in either the proper Purex product or the proper Thorex product tanks is limited only with respect to the uncertainty of system holdup. Since the burner and dissolver cubicles are connected on a one-to-one basis, batch mix-ups from cubicle to cubicle are not possible. Figure 24 shows the major equipment items and their location in either the WBB canyon, the SB & D canyon, or the blower canyon.

It appears feasible to locate the secondary burning and dissolution equipment in a 30-ft-wide by 15-ft-long cubicle. The two 6-ft-thick shielding walls and the 4-ft-thick wall between the WBB canyon and the SB & D canyon are each about 75 ft high. These massive walls will require approximately 12,000 yd<sup>3</sup> of concrete. It has been assumed that each WBB cubicle and each secondary burner and dissolver cubicle will require at least one viewing window. Thus, at least 32 viewing windows are included in these walls.

From Figs. 20 and 23, it is estimated that the shielded WBB canyon will require approximately 382,000 ft<sup>3</sup> of volume (30 x 48 x 265 ft) and about 16,000 ft<sup>2</sup> of floor space (30 x 265 ft). The blower canyon requires an additional 114,000 ft<sup>3</sup> of canyon volume and occupies an area of 4,560 ft<sup>2</sup>.

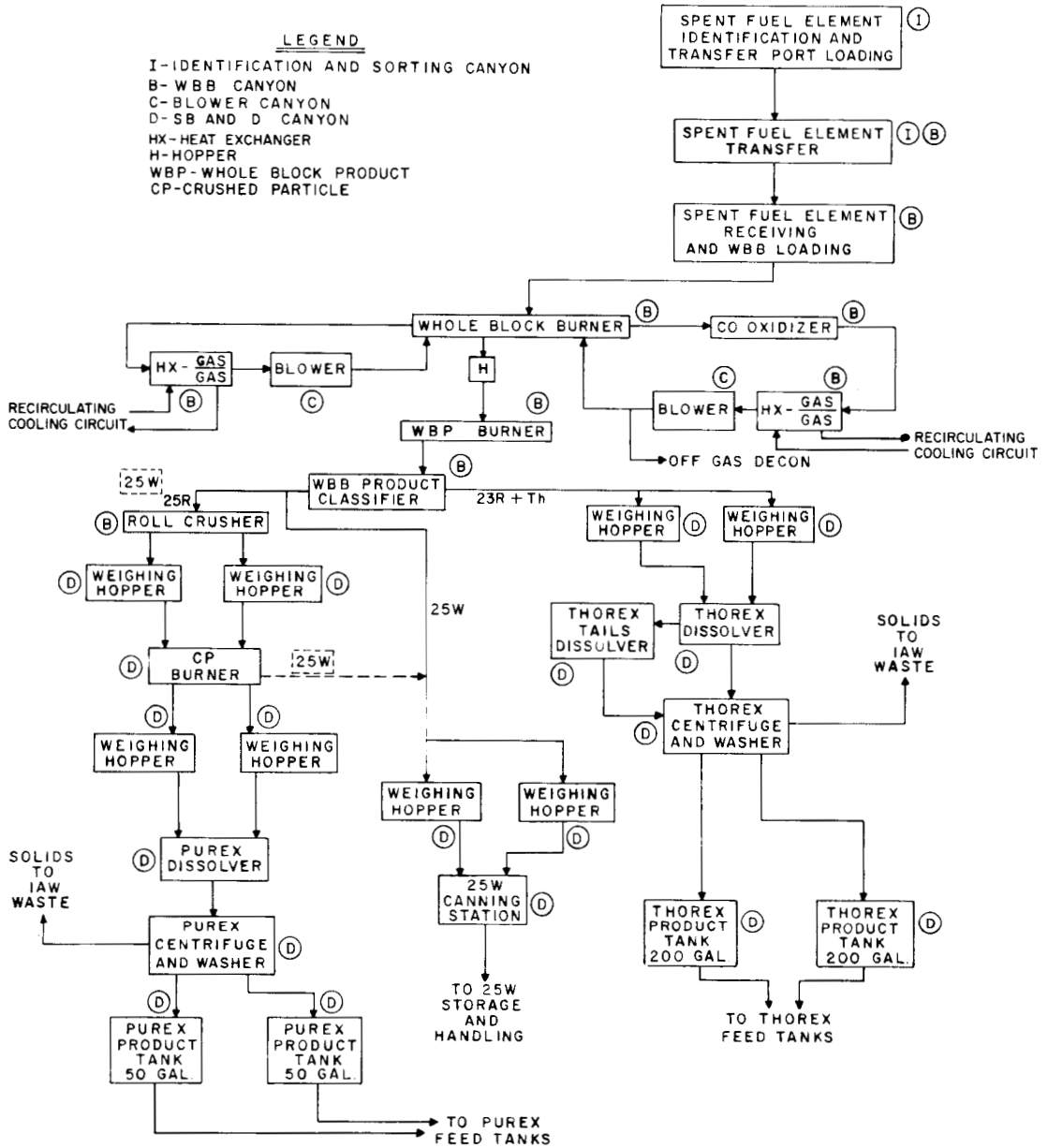


Fig. 24. Flowsheet showing the location of whole-block burning equipment.

### 3.2 Fluidized-Bed Burning

The use of multiple FBBs, each with a considerable amount of mechanical equipment, suggests a canyon-type structure with maintenance equipment provided at the canyon end(s) in a separate maintenance area (Fig. 25). In addition, a canyon-type structure for handling the primary burner hoppers and the FBB product hoppers (hopper canyon) is needed. Also, the two crushing systems (discussed in Sect. 2.2.1) require significant cell space.

A canyon suitable for containing the ten FBBs is envisioned as ten open cubicles, each of which is 30 ft long by 8 ft wide by 48 ft high (see Fig. 12). A corridor 8 ft wide by 48 ft high is required to move the FBBs and the other equipment to and from the maintenance area (Fig. 13). A telescoping detector for checking the FBBs between batches will be mounted on tracks located at the floor of this 8-ft-wide corridor. A 16-ft-wide by 14-ft-high manipulator and crane area traverses above the FBBs and the 8-ft-corridor. The crane, assisted by the manipulator, can remove any FBB or component through a shield door into a decontamination cell located at the end of the FBB canyon (Fig. 25).

A separate canyon for transferring, weighing, storing, and handling the primary burner hoppers and the product hoppers is located parallel to the FBB canyon. This hopper canyon is 12 ft wide by 45 ft high. A crane and manipulator system serves in this canyon in a manner similar to that described for the other canyons.

There are 40 primary burner hoppers, plus a similar number of product hoppers, to be handled each operating day. Each of these must be connected/disconnected, weighed empty/full, and moved twice during each handling cycle. Six operations are carried out by each hopper, for a total of 480 hopper operations daily; each operation requires an average of 3 min. Thus, the necessity for using automatic equipment or multiple handling equipment becomes apparent. Further, the equipment must be highly reliable to avoid plant stoppage. If pneumatic transport of the crushed product is found to be acceptable, the envisioned hopper canyon will be necessary due to maintenance requirements.

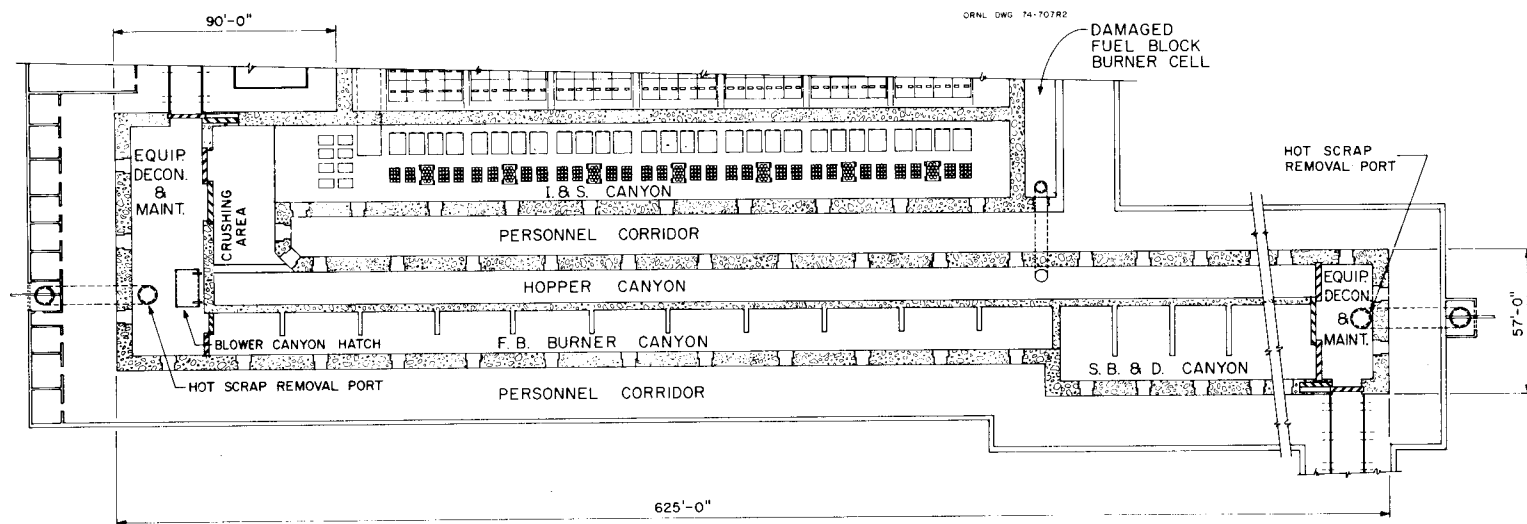


Fig. 25. Plan view of the FBB canyon, the hopper canyon, the I & S canyon, the equipment decontamination and maintenance cell(s), and the damaged fuel block burner cell.

45

An area for the two crushing trains is also required. The best location for these trains appears to be at the end of the I & S canyon, with a smaller canyon (crushing area) connecting the I & S canyon and the hopper canyon for transferring the primary burner feed from the tertiary crusher to the hopper canyon. Figure 26 is an elevation view of one of the crushing trains.

Ventilation of the FBB canyon, the hopper canyon, and the crushing area will be accomplished in a downflow manner as described for the WBB. The heat liberated from burning (minus losses) is removed by two gas-to-gas heat exchangers located within each FBB cubicle (Fig. 17). One of these removes the heat from the FBB off-gas stream; the other removes the heat that is lost through the FBB walls.

The FBB blowers are located in a blower canyon, 12 ft wide by 20 ft high, which is located below the hopper canyon (Fig. 27). A maintenance cell is located at one end of the blower canyon for maintenance (Fig. 25). The blower canyon is also equipped with a crane and manipulator. The blower for each FBB is driven by a 200-hp motor. (Thus, the blower canyon contains ten electric motor-blower systems of 200 hp each.) The blower canyon serves the same function for the FBB as it did for the WBB (see Sect. 3.1).

An elevation view of the FBB canyon, the hopper canyon, and the blower canyon is shown in Figs. 27 and 28. The hopper canyon is located between the I & S and the FBB canyons. A common personnel corridor is shared between the hopper and the I & S canyons, while a common wall is shared between the FBB and the hopper canyons.

It has been assumed that each hopper station located in the hopper canyon and each FBB cubicle will require a viewing window. Thus, it will be necessary to have a personnel corridor adjacent to the FBB corridor. It is also assumed that each crushing train requires a viewing window. Hence, 25 viewing windows are required for this part of the FBB system.

The comparison between the FBB and WBB must include the SB & D canyon for completeness. The arrangement of this canyon is shown in Fig. 25. The 11 FBB cubicles (one spare cubicle) require 340 ft of length; this includes 10 ft for crane parking. The SB & D canyon requires 230 ft of length.

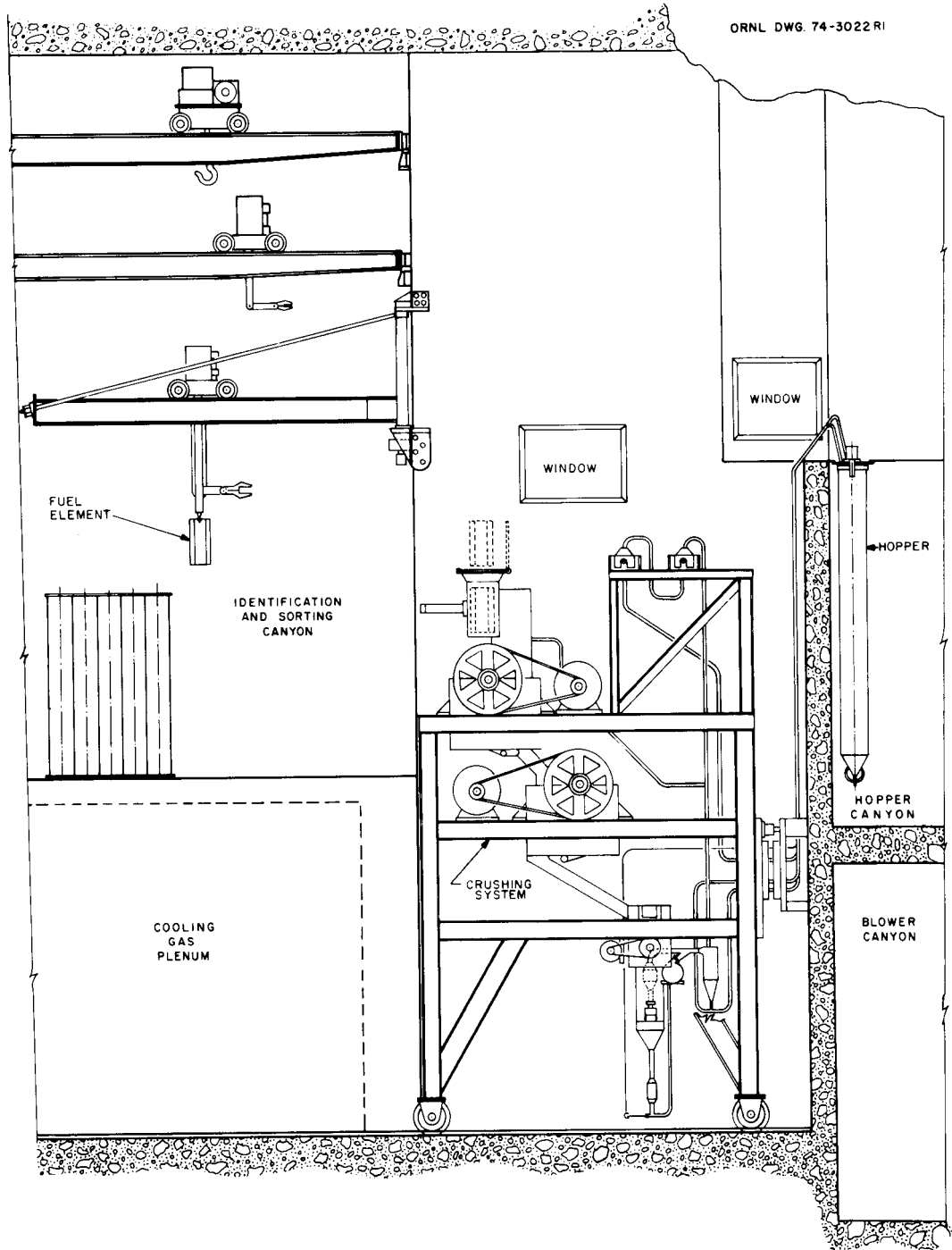


Fig. 26. Elevation view of a crushing train located within the cells.

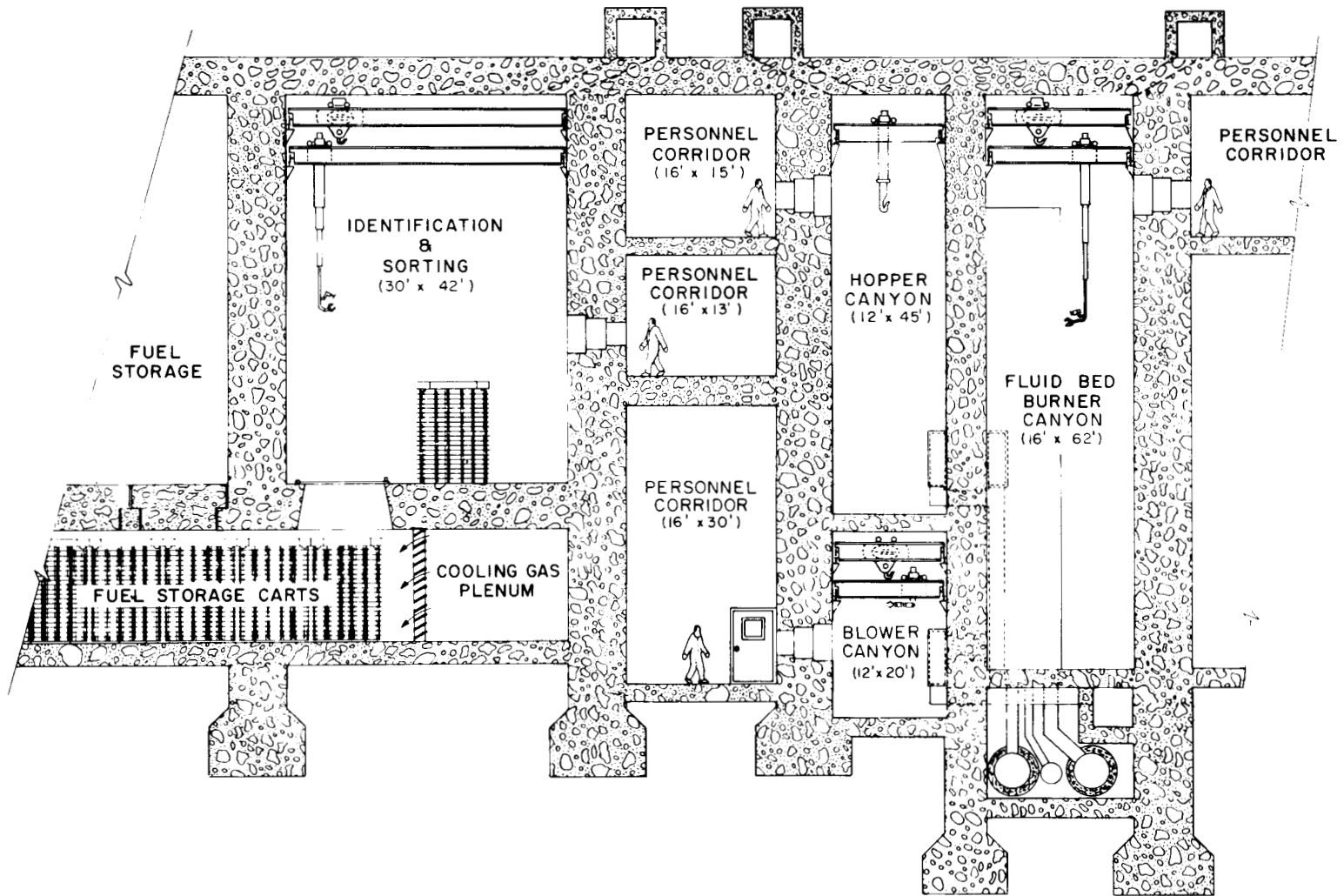


Fig. 27. Elevation view of the FBB showing the relationship of the I & S canyon, the blower canyon, and personnel corridors.

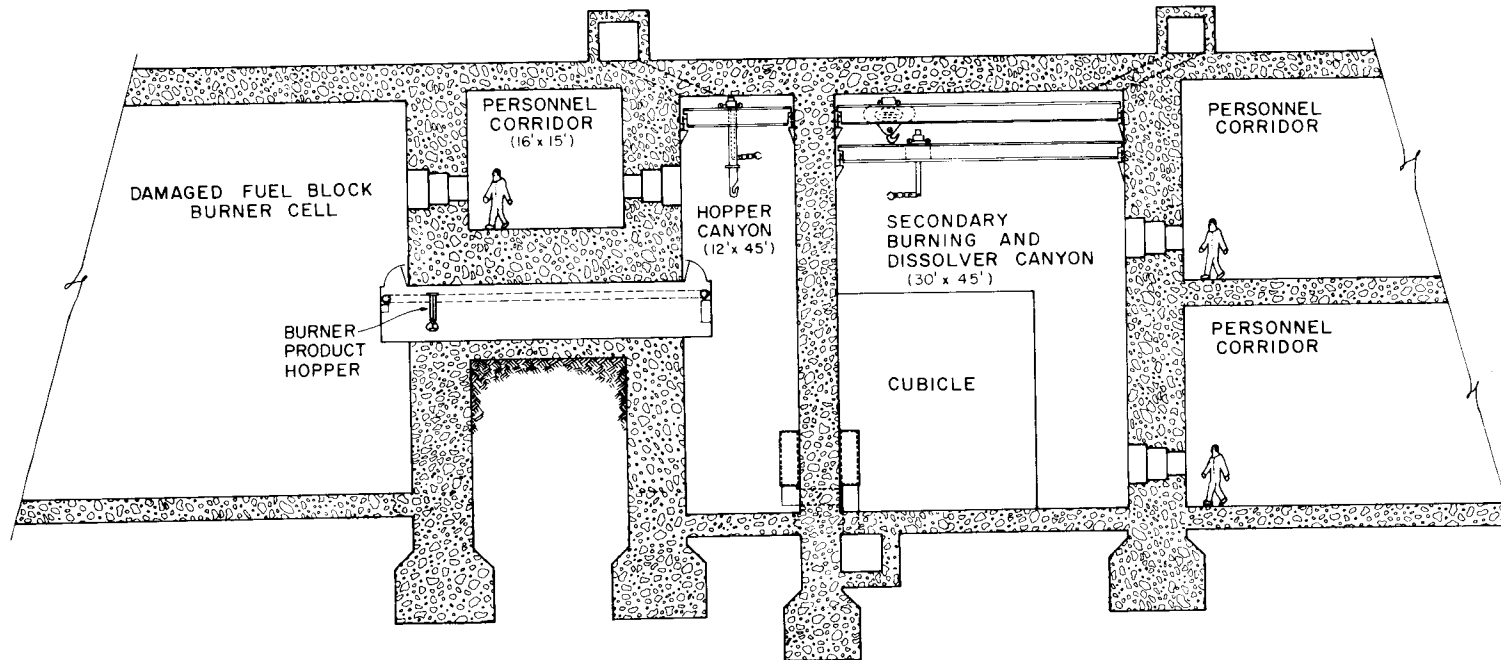


Fig. 28. Elevation view of the hopper canyon showing the relationship of the SB & D canyon, the damaged fuel burner cell, and personnel corridors.

The spent fuel elements move from the I & S canyon into a queuing area (located at one end of the canyon) for crushing. A "crushing batch", which has been assumed to be one day's feed for a FBB (24 elements), is handled in groups of six elements. (The six crushed elements fill one primary burner hopper.) A running inventory check is made after each group of elements has been crushed, and a final inventory is made to ensure that the crusher train is empty after each entire batch of elements has been crushed.

The four primary hoppers are moved, inventoried (weighed), transferred to the appropriate hopper station, and connected for burning. The primary burner burns the contents of one primary burner hopper, and the burned product is emptied into a primary burner product hopper. The primary burner product hopper is disconnected, weighed, moved down the hopper corridor to the appropriate secondary burner and dissolver station, and connected for emptying.

The equipment for classification and crushing is located in the SB & D cubicles. If this equipment is located at the FBB cubicles, the number of product hoppers to be handled is doubled.

Pneumatic transfer of the contents of the primary burner hoppers and the primary burner product hoppers was assumed for this study. Pneumatic transfer of the crusher product into the primary burner hoppers was also assumed.

In order to maintain operating flexibility and separation of each reactor's product, the number of secondary burners and dissolvers is equal to the number of primary burners. The length of the SB & D canyon is 230 ft, assuming a 30-ft-wide canyon. Each cubicle is 20 ft long. This necessitates that the hopper canyon be extended an additional 250 ft beyond the FBB canyon in order to service the secondary burner and dissolver cubicles.

This arrangement provides assurance that the sorted elements on a dolly located in the queuing area will be transferred into the four desired primary burner hoppers. It also gives assurance that the product in a primary burner hopper will be transferred into the desired primary burner product hopper, and that the product in a primary burner product hopper will be eventually transferred into the proper Purex

product or Thorex product tanks. Such assurances are limited by the uncertainty of systems holdups; however, whenever the primary burner hoppers or the primary burner product hoppers are moved from a loading to an unloading station, there is no inherent assurance that the proper transfer will be made unless each set of four hoppers can only be connected to a particular station. This compromises operating flexibility too severely, and administrative control is preferable. Figure 29 shows the major equipment items and their location between the several canyons.

The arrangement of the various canyons precludes the use of a common decontamination cell by all canyons. Thus, one common maintenance and decontamination cell serves the I & S canyon (including the crushing equipment), the FBB canyon, and the blower canyon, while a second cell serves the hopper canyon and the SB & D canyon. Study of the additional functions of an HTGR reprocessing-refabrication facility would probably show that this latter decontamination and maintenance cell could be shared with some other process step.

The 6-ft-thick shielding walls enclosing the FBB canyon and the matching length of the hopper canyon are about 75 ft high, as is the common 4-ft-thick wall separating these two canyons. The two 6-ft-thick shielding walls enclosing the SB & D canyon and the matching length of the hopper canyon are about 60 ft high; the common 4-ft-thick wall separating these two canyons is also 60 ft high. The 75-ft-high section extends 340 ft, and the 60-ft-high section extends 230 ft. These three massive walls will require approximately 16,400 yd<sup>3</sup> of concrete.

If the same considerations with regard to viewing are included for the secondary burner and dissolver cubicles (plus that matching portion of the hopper corridor) as were made for the WBB, then 22 windows must be associated with these operations. These, added to the 25 already considered, make a total of 47 viewing windows associated with FBB burning and dissolution. Since the viewing windows associated with the hopper canyon can be smaller, it is assumed that they are equivalent to seven normal viewing windows. Thus, 32 viewing windows (or equivalent) are required for the FBB system (same number as required for the WBB system).

LEGEND  
 I = IDENTIFICATION AND SORTING CANYON  
 H = HOPPER CANYON  
 B = BURNER CANYON  
 F = BLOWER CANYON  
 D = SB & D CANYON  
 C = CRUSHING AREA  
 HX = HEAT EXCHANGER

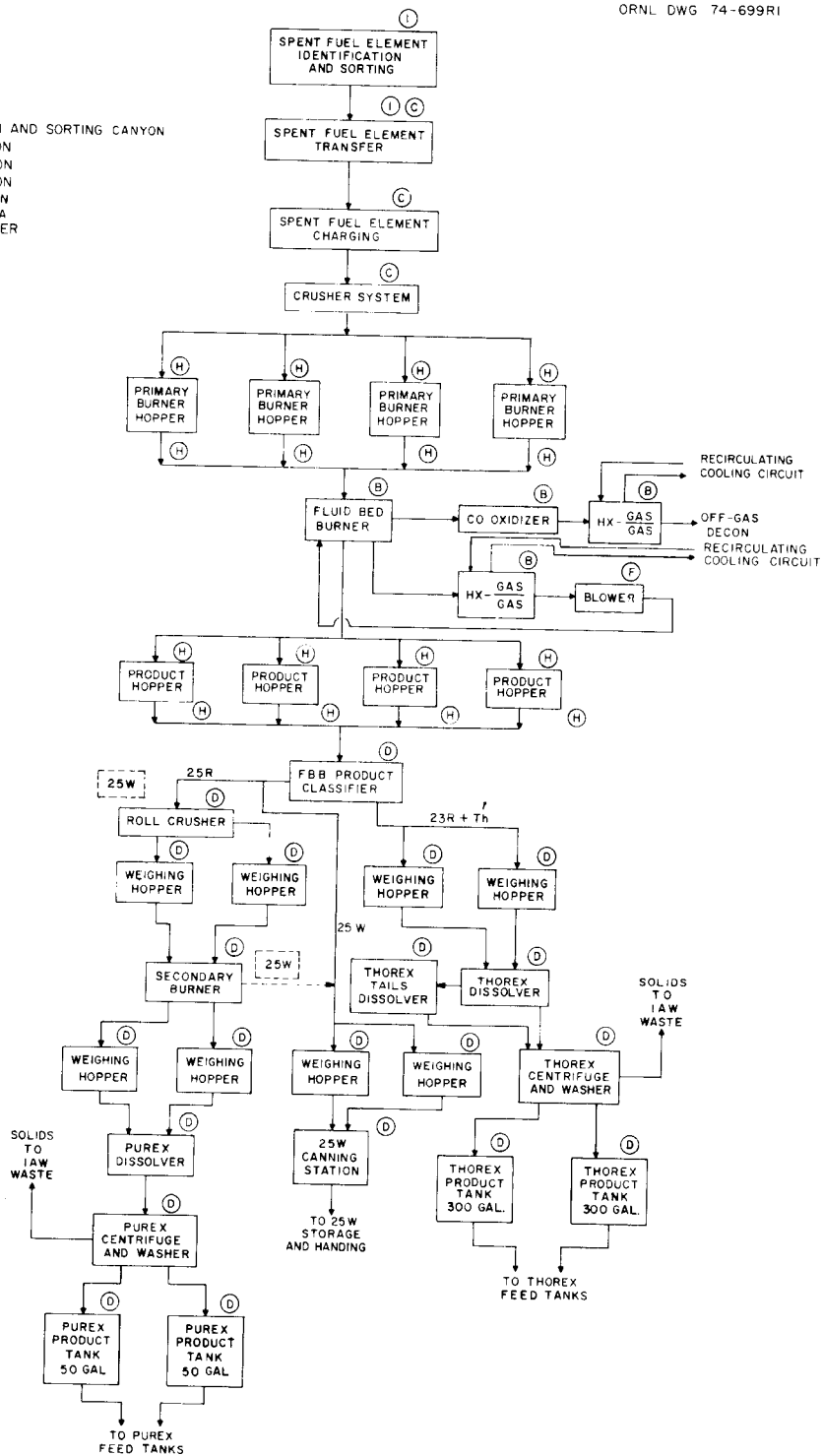


Fig. 29. Flowsheet showing the location of FBB equipment.

From Figs. 25, 27, and 28, the shielded canyon volume required for the FBBs, hoppers, and crushers is estimated to be approximately 720,000 ft<sup>3</sup>. The amount of canyon floor space is about 14,000 ft<sup>2</sup>. The blower canyon requires an additional 86,000 ft<sup>3</sup> of volume and occupies 4320 ft<sup>2</sup> of area.

#### 4. COST ESTIMATES

Preliminary cost estimates, based on 1975 costs, have been made for the installed modular equipment, including instrumentation, heat removal system, and building costs associated with the WBB and the 2-FBB systems. Factors are applied to the sum of these costs to estimate other direct construction costs, indirect construction costs, and owner's costs.

The fabrication of multiple modular equipment items reduces the unit cost for fabrication. This is brought about by savings in procurement, prorating the costs of jigs and fixtures among several items, reduced labor cost due to familiarization of the tasks, etc. A similar savings in certain indirect construction costs, especially engineering, is also recognized.

The method used in making cost estimates consists of determining the cost of a single module of equipment on an installed basis. Each time the number of items fabricated is doubled, a fractional cost factor (FCF) which reduces the cost by 15% is multiplied by the cost of a single module to obtain the cost of additional modules.

The following equation, which is continuous through these points, is useful in calculating the fractional cost factor for a given number of units:

$$FCF = \frac{(0.85)(1.7)^{\frac{\ln x}{\ln 2}} - 0.15}{0.7 x},$$

where

$x$  = number of units fabricated.

Figure 30 is a plot of the FCF as a function of  $x$ . As shown, the value of the FCF is 0.63 for 15 units and 0.69 for 10 units. Thus, the

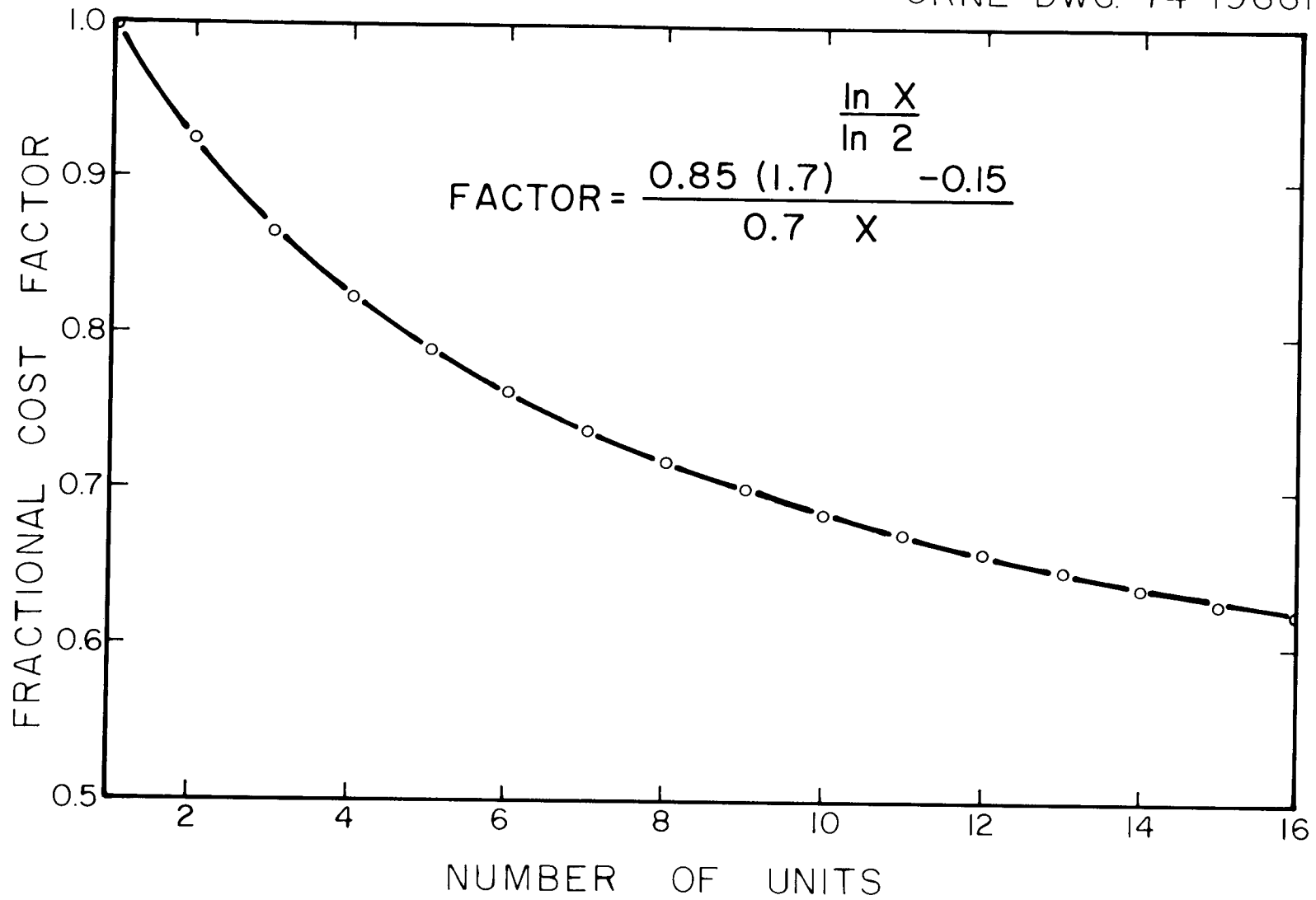


Fig. 30. Fractional cost factor vs number of units.

51

"learning factor" reduces the cost of 15 units by 27% (1 - 0.63) of that calculated using the straight-line method.

#### 4.1 Equipment Costs

##### 4.1.1 Whole-block burning

The estimated installed equipment cost for a WBB module is shown in Table 1. The cost of the equipment located within the WBB canyon and the blower canyon associated with one WBB is included. The installed modular equipment cost for 15 WBB modules is found as follows:

$$\begin{aligned} \text{WBB modular equipment cost} &= \$ 1,665,000 \times \text{FCF} \times 15 \\ &= \$ 1,665,000 \times 0.63 \times 15 \\ &= \$ 15,734,250 \end{aligned}$$

##### 4.1.2 Fluidized-bed burning

The installed equipment cost for a 2-FBB module is shown in Table 2. The cost of the equipment located within the FBB canyon, the hopper canyon, and the blower canyon associated with one FBB is included. The installed modular equipment cost for ten FBB modules is found as follows:

$$\begin{aligned} \text{FBB modular equipment cost} &= \$ 1,705,000 \times \text{FCF} \times 10 \\ &= \$ 1,705,000 \times 0.69 \times 10 \\ &= \$ 11,764,000 \end{aligned}$$

However, the cost of the crushing and weighing station equipment (Table 3) must be added. Thus, the installed equipment cost for ten FBB modules is:

$$\$ 11,764,000 + \$ 1,305,000 = \$ 13,069,000$$

#### 4.2 Cost of Heat Removal System

The heat removal system is the system that transports the heat from the burner heat exchangers to a heat exchanger located outside the building. It is envisioned that the HTGR reprocessing-refabrication complex is U-shaped (Fig. 31), with the heat-transfer equipment located within the "U". This arrangement affords the opportunity of sharing common heat-transfer facilities for the burning and coating operations with minimum runs of ducting.

Table 1. Estimated installed equipment cost for a WBB module

Item	Cost (\$)
WBB	500,000
CO oxidizer	60,000
Two blowers	25,000
Two heat exchangers	75,000
Piping	250,000
Manipulator	200,000
Transfer tunnel	30,000
Instrumentation	300,000
Filters	150,000
Special connectors	<u>75,000</u>
Total	<u>1,665,000</u>

Table 2. Estimated installed equipment cost for a 2-FBB module

Item	Cost (\$)
Burner Equipment	
2-FBB	400,000
CO oxidizer	40,000
Blower	20,000
Two heat exchangers	125,000
Piping	250,000
Instrumentation	150,000
Filters	150,000
Special connectors	<u>60,000</u>
Subtotal	1,195,000
Hopper Equipment	
Four primary burner hoppers	100,000
Four product hoppers	60,000
Diverters and feeders	20,000
Piping	120,000
Instrumentation	100,000
Filters	50,000
Special connectors	<u>60,000</u>
Subtotal	510,000
Total	<u>1,705,000</u>

Table 3. Estimated installed equipment cost for  
crushing and hopper weighing

Item	Cost (\$)
Crushers	500,000
Piping	75,000
Instrumentation	100,000
Filters	50,000
Special connectors	80,000
Hopper weighing stations	<u>500,000</u>
Total	1,305,000

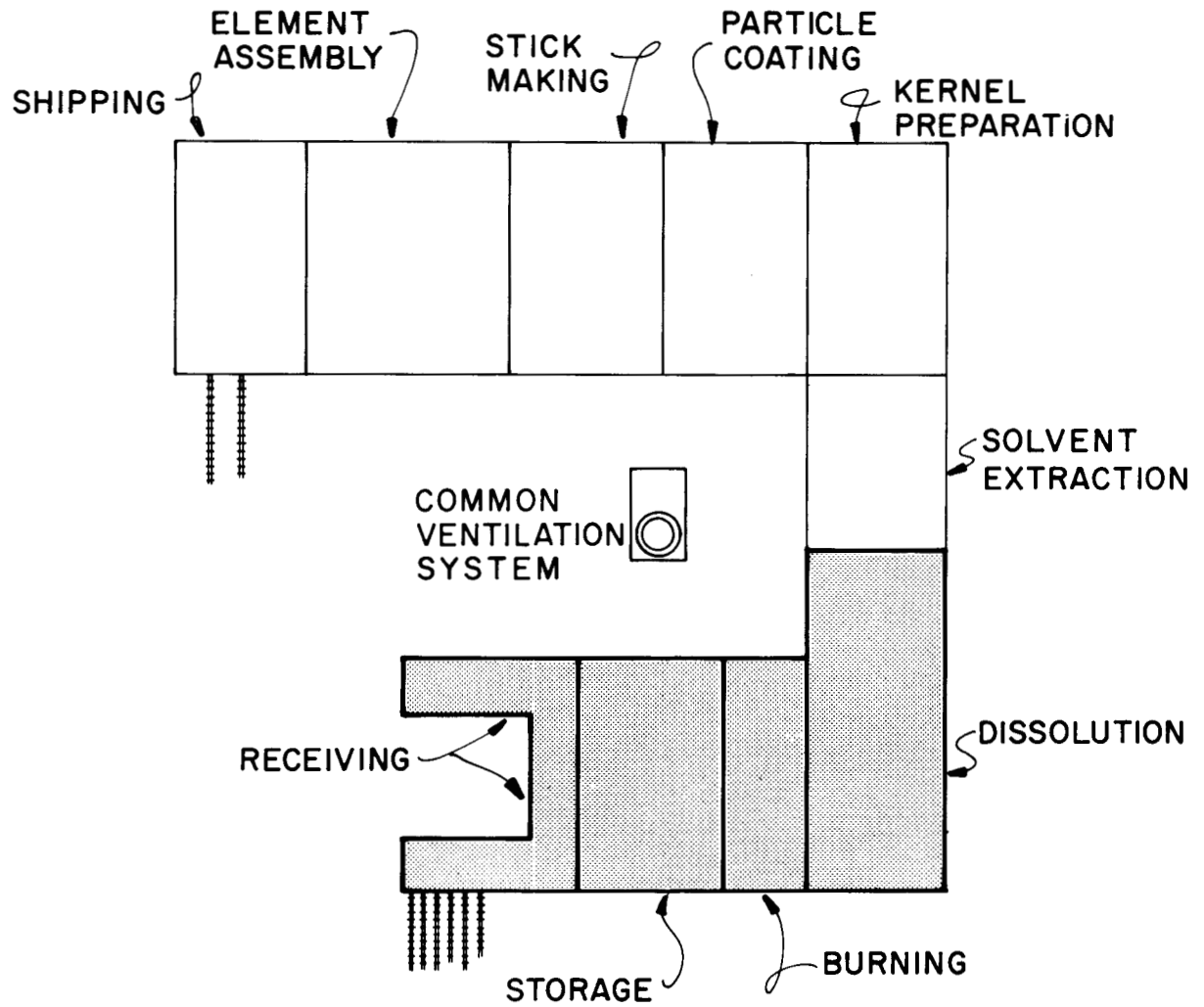


Fig. 31. A generalized HTGR reprocessing-refabrication plant layout.

The temperature of the gas leaving the heat exchangers in the blower canyon will be too high for concrete duct-type construction. Therefore, an insulated metal duct system is envisioned. The estimated cost of the heat removal system is shown in Table 4. This estimate is applicable to either the WBB or the 2-FBB system.

Table 4. Estimated installed equipment cost for the heat removal system

Item	Cost (\$)
Ducting	750,000
Insulation	1,000,000
Cooling tower and heat exchanger system	<u>1,750,000</u>
Total	3,500,000

#### 4.3 Building Cost

The cost of the portion of the reprocessing plant directly associated with burning was estimated by assuming that personnel corridor costs are shared with other process steps (identification and sorting, secondary burning, and dissolving, etc.). The cost associated with the decontamination and maintenance areas is not included in the estimate. The portion of the facility included in the building costs for the WBB is shown in Figs. 32 and 33; the portion included in the building costs for the FBB is shown in Figs. 34-36.

The building costs were estimated using the following factors:

- (1) Concrete for cell structures      \$ 300/yd<sup>3</sup>
- (2) Personnel corridors                \$ 100/ft<sup>2</sup>
- (3) Crane bay (atop cell structure)   \$ 100/ft<sup>2</sup>
- (4) Viewing windows                    \$ 30,000 each

ORNL DWG. 74-1366

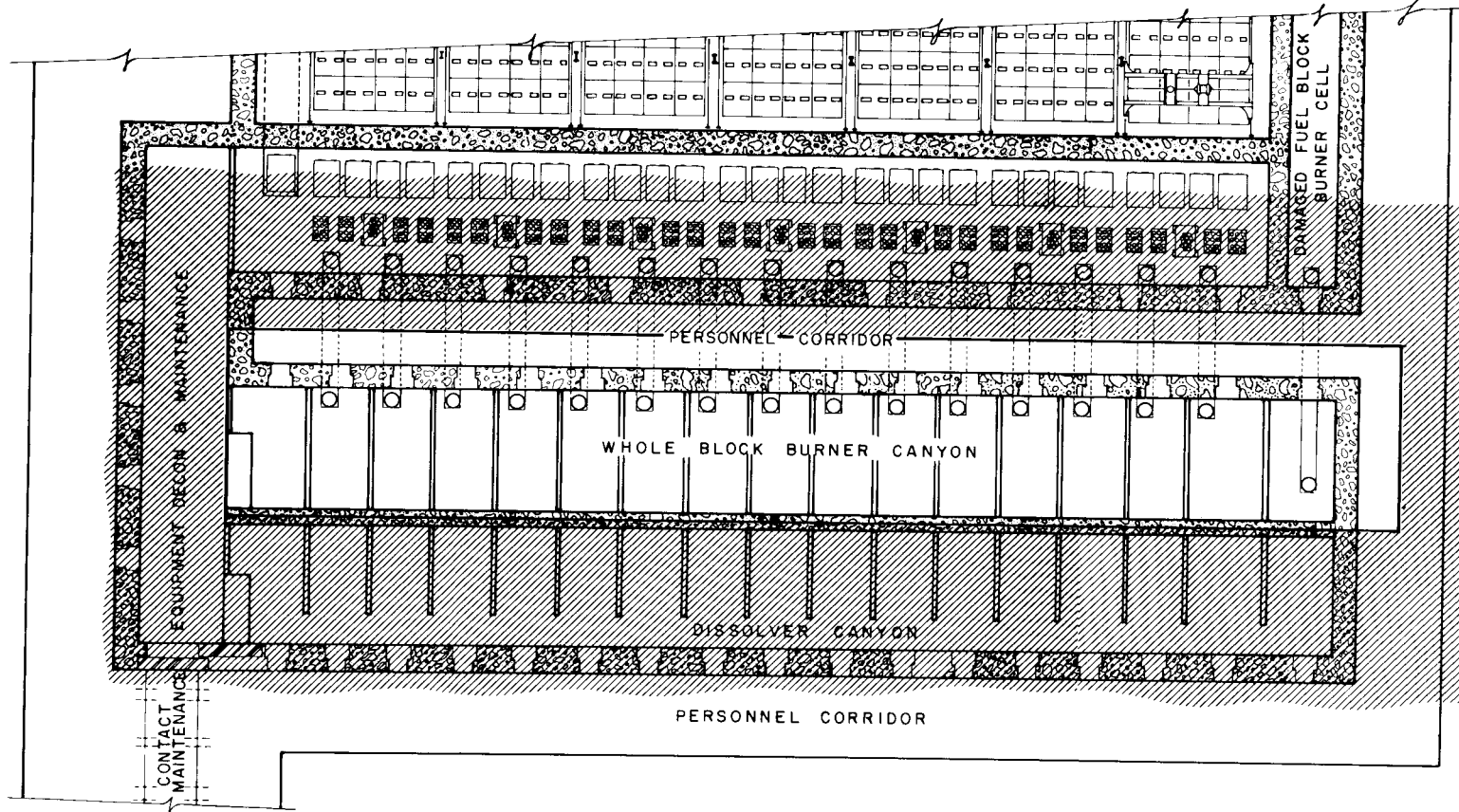


Fig. 32. Plan view of that portion of the facility included in the building costs for whole-block burning.

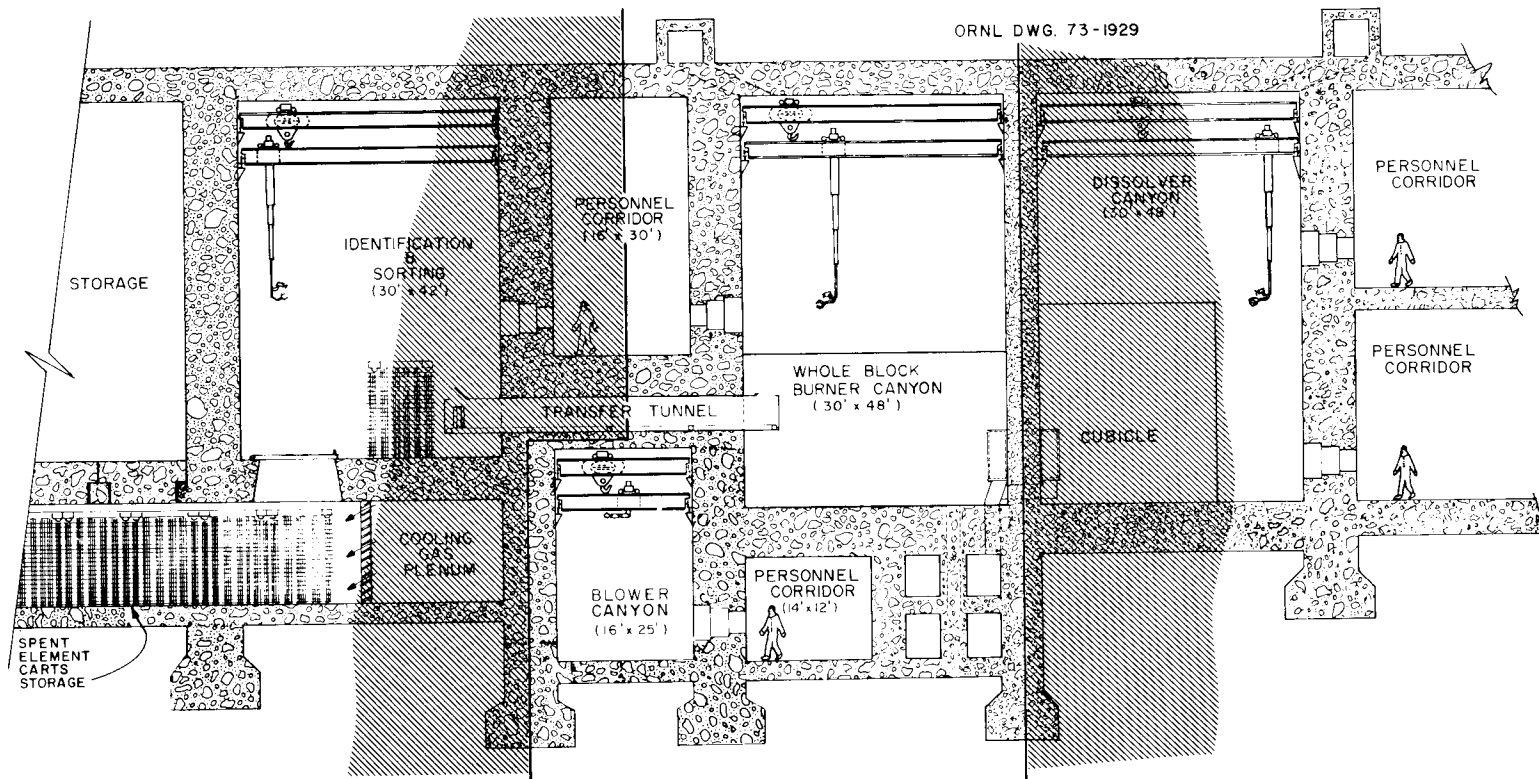


Fig. 33. Elevation view of that portion of the facility included in the building costs for whole-block burning.

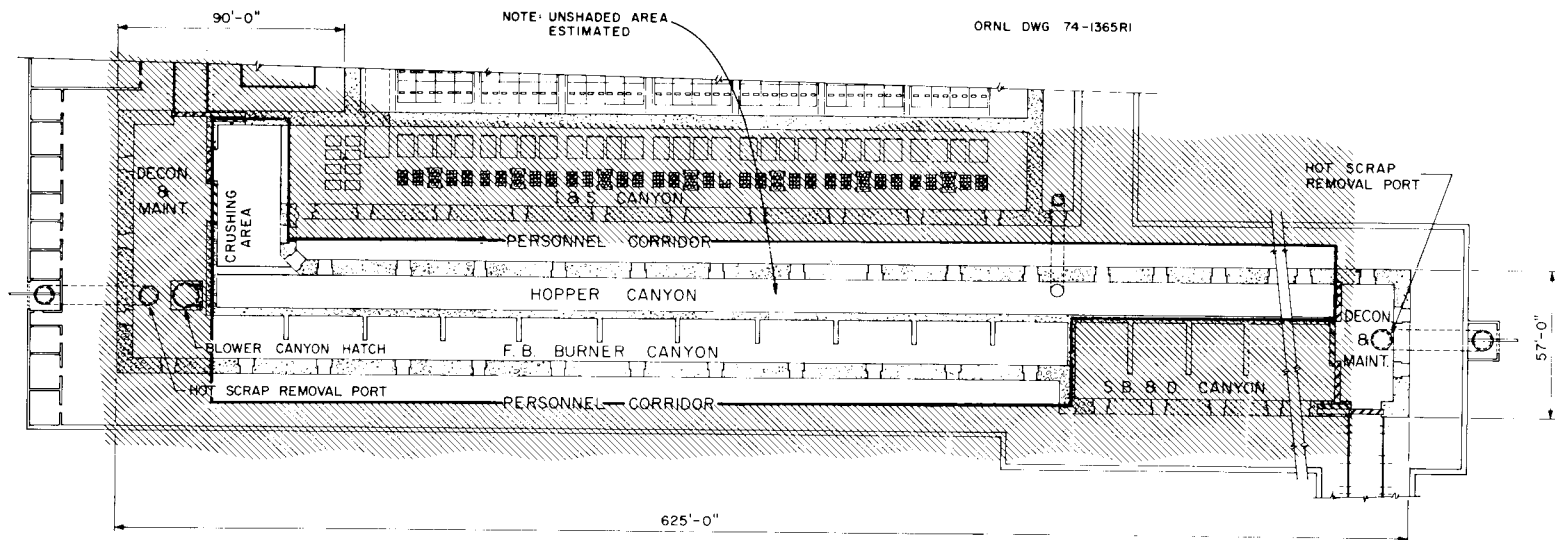
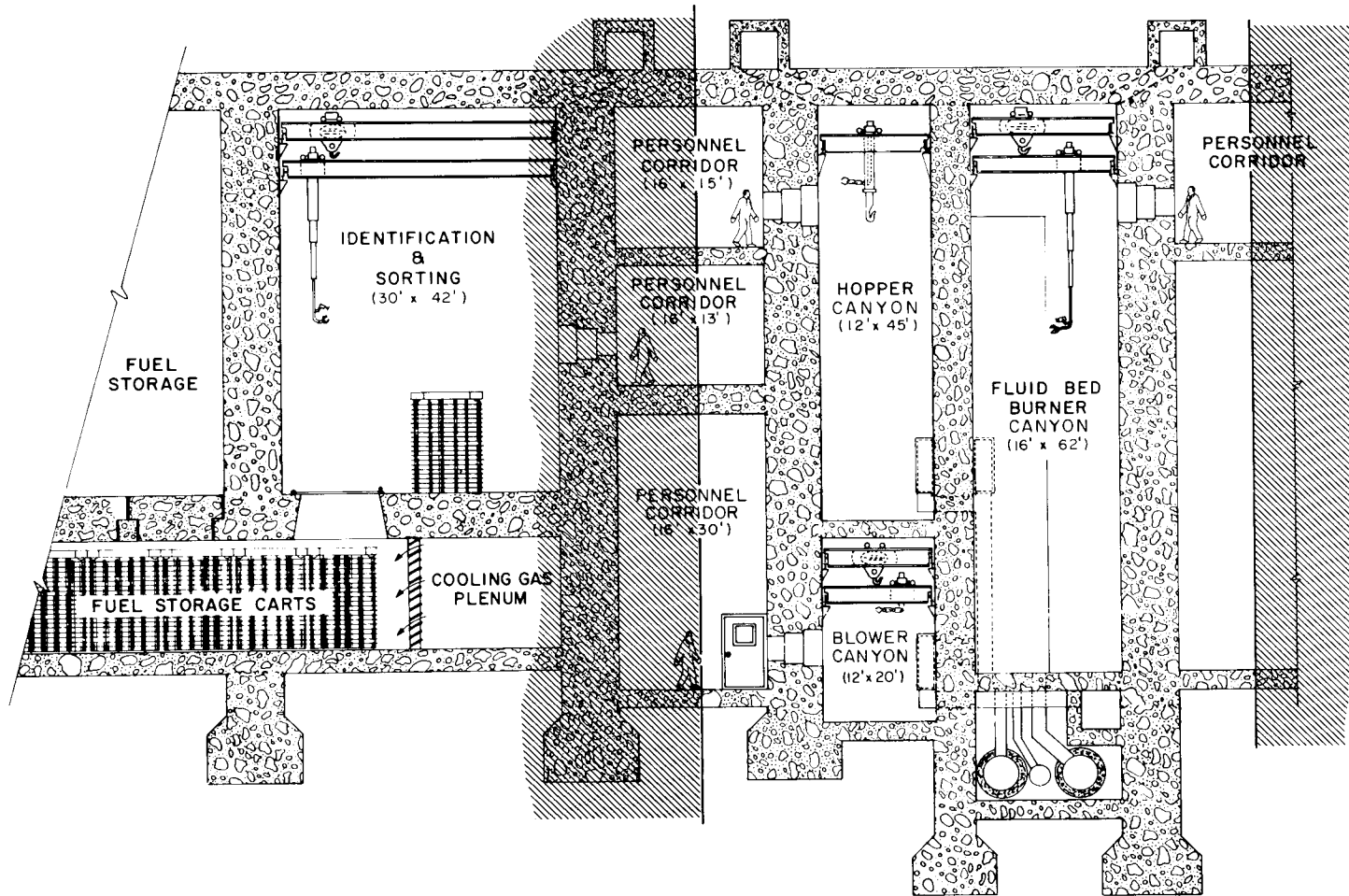


Fig. 34. Plan view of the portion of the facility utilized in estimating the cost of the 2-FBB system.



79

Fig. 35. Portion of the facility utilized in estimating the cost of the 2-FBB system - elevation through the FBB.

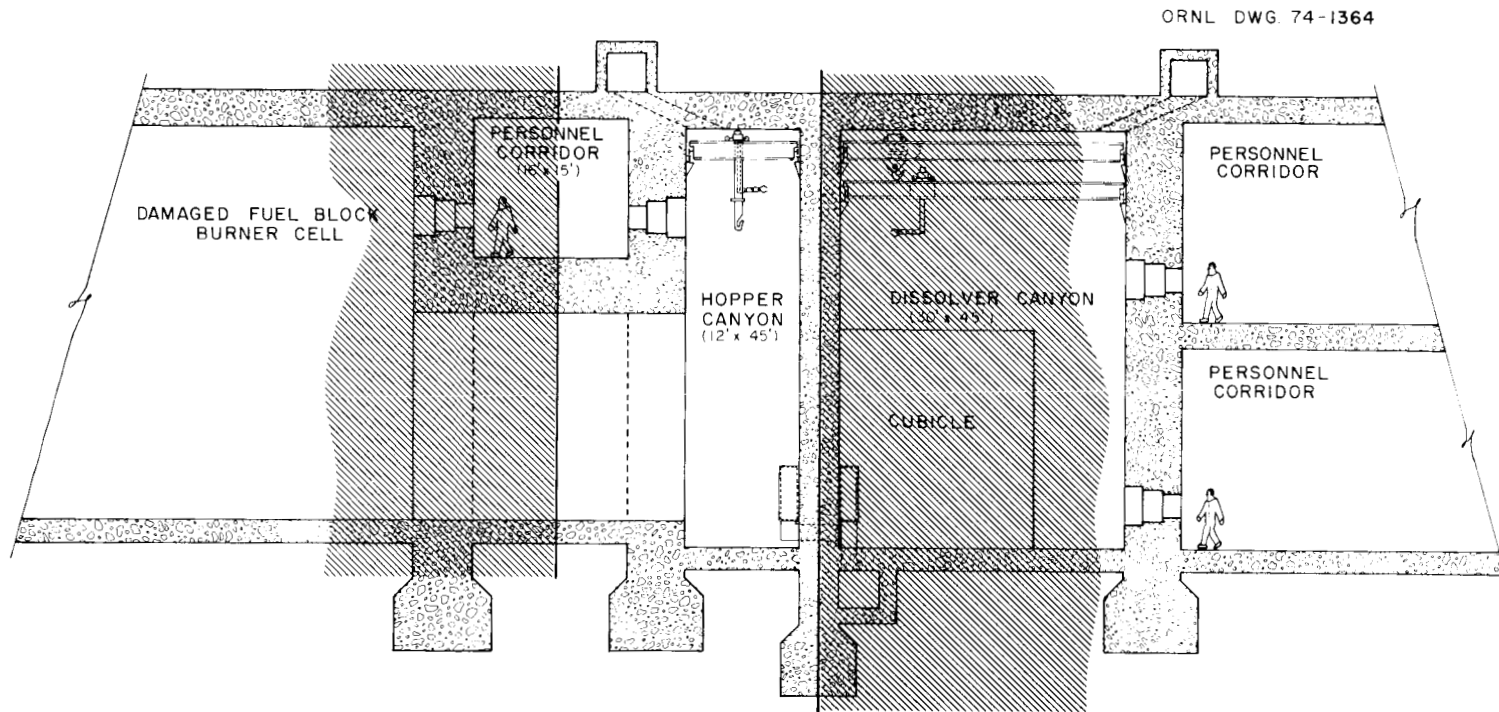


Fig. 36. Portion of the facility utilized in estimating the cost of the 2-FBB system - elevation through the hopper canyon.

#### 4.3.1 Whole-block burning

The estimated volume of concrete associated with the WBB shielding walls, roofs, and floors is 17,000 yd<sup>3</sup>. The WBB canyon and the blower canyon each contain a crane and rectilinear manipulator, which is included in the building costs. The estimated WBB building cost is summarized in Table 5.

Table 5. Estimated building cost for whole-block burning

Item	Cost (\$)
Concrete (17,000 yd <sup>3</sup> )	5,100,000
Windows (15)	450,000
Crane and manipulators	600,000
Service penetrations	1,500,000
Personnel corridors (6000 ft <sup>2</sup> )	600,000
Crane bay (12,720 ft <sup>2</sup> )	<u>1,272,000</u>
Total	9,522,000

#### 4.3.2 Fluidized-bed burning

The estimated volume of concrete associated with the 2-FBB shielding walls, roofs, and floors is 29,000 yd<sup>3</sup>. The FBB canyon, the hopper canyon, and the blower canyon each contain a crane and rectilinear manipulator. The FBB building costs are summarized in Table 6.

Table 6. Estimated building cost for fluidized-bed burning

Item	Cost (\$)
Concrete (29,000 yd <sup>3</sup> )	8,700,000
Windows (15)	450,000
Cranes and manipulators	900,000
Service penetrations	1,800,000
Personnel corridors (17,000 ft <sup>2</sup> )	1,700,000
Crane bay (28,600 ft <sup>2</sup> )	<u>2,860,000</u>
Total	16,410,000

#### 4.4 Other Direct Construction Costs

The costs for site improvement and outside utilities (excluding the heat removal system) were estimated as 1% and 10% of the estimated direct construction cost, respectively. Using the estimates of direct construction costs as shown in Table 7 and the factors given above yields other construction costs of \$3,190,000 for the WBB and \$3,630,000 for the 2-FBB.

Table 7. Summary of direct construction costs

	Cost (\$)	
	WBB	FBB
Process equipment	15,734,250	13,069,500
Heat removal system	3,500,000	3,500,000
Building	<u>9,522,000</u>	<u>16,410,000</u>
Total	28,756,250	32,979,000
Assume	29,000,000	33,000,000

#### 4.5 Total Direct Construction Cost

The total estimated direct construction cost associated with the WBB is \$32,190,000; that associated with the FBB is \$36,630,000.

#### 4.6 Estimates of Indirect Construction Costs

Indirect construction costs are estimated as a fraction of the direct construction cost. The factors used are those currently being utilized in the ORNL HTGR Program cost estimates of a commercial facility. The sum of these factors is 0.647 (see Table 8).

#### 4.7 Owner's Cost Estimates

Owner's costs are also estimated as a fraction of the direct construction cost. The factors used are those currently being utilized in the ORNL HTGR Program cost estimates of a commercial facility. The sum of these factors is 0.47 (see Table 9).

Table 8. Indirect construction cost factors to be applied to the total direct construction cost

Item	Factor
General and administrative	0.10
Engineering	0.20
Miscellaneous construction	0.05
Contingency	0.20
Spare parts	0.007
Noninstalled spare equipment	0.03
Quality assurance	<u>0.06</u>
Total	0.647

Table 9. Owner's cost factors to be applied to the total direct construction cost

Item	Factor
Land	0.01
Project management	0.02
Licensing	0.04
Taxes, insurance, and interest	0.20
Preoperational testing and startup	<u>0.20</u>
Total	0.47

#### 4.8 Total Estimated Cost

The total estimated costs of primary burning are \$68,000,000 for the WBB and \$78,000,000 for the 2-FBB, respectively (see Table 10). The total estimated cost of primary burning using the WBB is about 15% less than that of the 2-FBB.

Table 10. Total estimated costs of primary burning

Type of cost	WBB	FBB
Direct construction	32,190,000	36,630,000
Indirect construction	20,827,000	23,700,000
Owner's	<u>15,129,000</u>	<u>17,216,000</u>
Total	68,146,000	77,546,000
Assume	68,000,000	78,000,000

The HTGR reprocessing plant will handle about 1330 kg of heavy metal per day. Assuming a 15-yr plant life and a load factor of 0.8, the unit costs of primary burning are \$11.67/kg for the WBB and \$13.39 kg for the FBB.

#### 4.9 Cost Sensitivities

The cost estimates presented in this section can more properly be referred to as cost guesstimates since they are simply guesses and not costs derived by obtaining fabrication quotations. Therefore, it is of benefit to consider the effect of inaccurate guesses on the total estimated costs.

##### 4.9.1 Sensitivity to module costs

As was stated in the introduction, "the amount of technical information on which the evaluation is based is unequal for the two systems." Therefore, one would expect this fact to be reflected in the cost estimates for the equipment. Using the fluidized-bed system as a base, what error in the WBB equipment cost would make the two systems equal in total

cost? If the cost estimate for the whole-block burning equipment is increased by 30%, then the total costs of the WBB and the FBB are equal at about  $\$78 \times 10^6$ .

Another approach is to assume that the modular equipment estimates are equal for the two cases and to consider the effect of underestimations on the total costs. As one increases the modular equipment costs (equally) from 0 to 100%, the ratio of total costs for the FBB to the WBB decreases from 1.15 to 1.04 (see Fig. 37). At an increase of about 200% in the estimated modular equipment cost, the two systems are equal in estimated total cost. Figure 38 is a plot of the effects of modular equipment cost increase on the total estimated cost in absolute values.

#### 4.9.2 Sensitivity to building cost

The estimate on construction cost for shielded facilities has been made by prorating the cost between the shielded cell structure (cubic yards of concrete) and the unshielded space around the cells (area of floor space). In the base case, values of \$300 per cubic yard of concrete and \$100 per square foot of floor space were used. Figure 39 is a plot of the total cost vs concrete cost (\$100 to \$500 per cubic yard) and area costs of \$100 and \$200 per square foot. The WBB system is less sensitive to variations in these factors than is the FBB system, which is a result of the larger building required for the FBB.

## 5. CONCLUSIONS AND RECOMMENDATIONS

Two methods have been studied for accomplishing the primary burning of HTGR fuels for a plant which will handle about 50,000 MW(e). These methods are the reference process, fluidized-bed burning, and an undeveloped backup process, whole-block burning.

Within the accuracy of this study, one may draw the conclusion that, in evaluating a process step, the total plant must be considered. Each of the two systems evaluated for primary burning may appear the least costly, depending on the amount of consideration given to the related process steps. Thus, it is recommended that the total plant be considered in making such future comparisons of process alternatives.

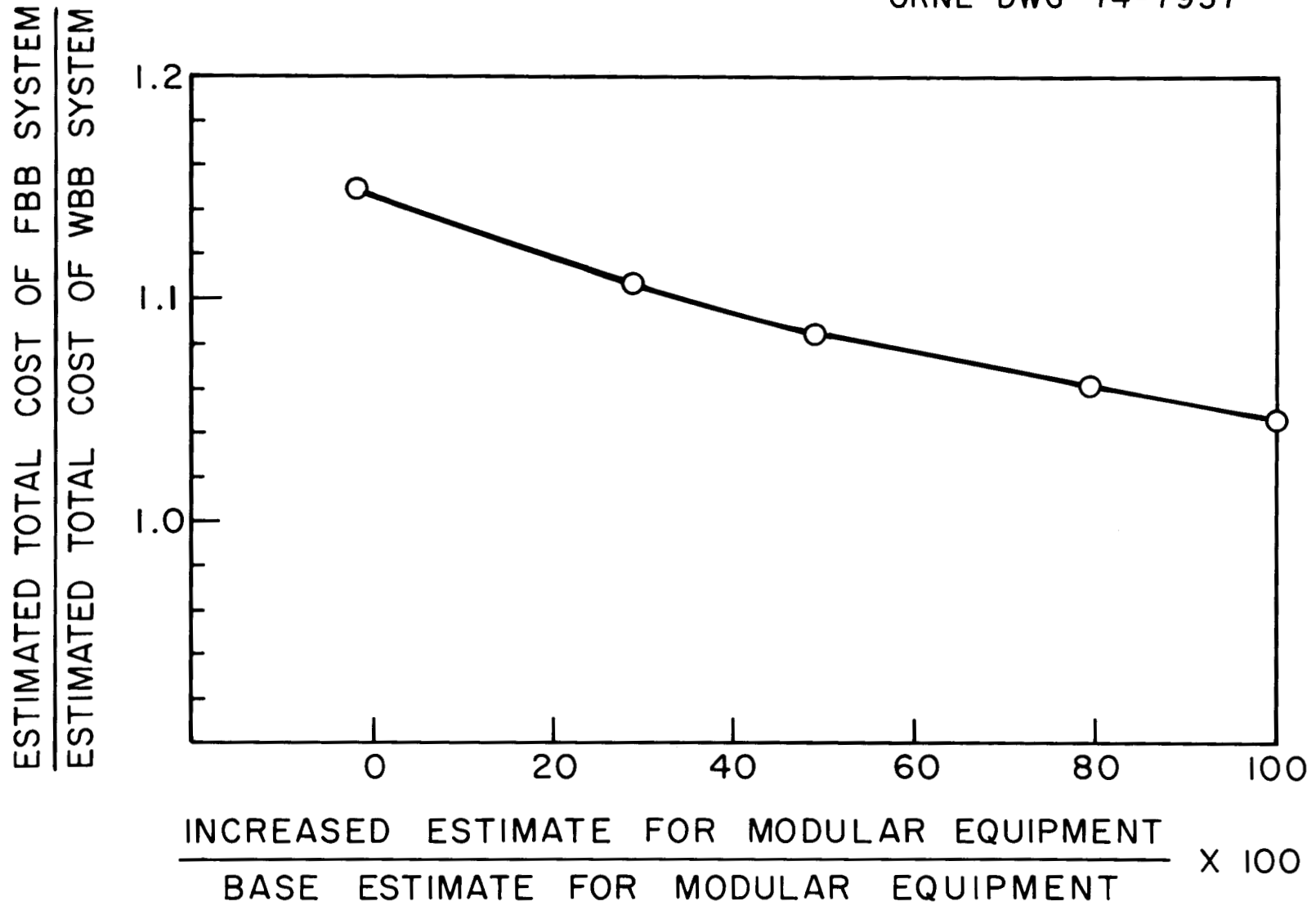


Fig. 37. Relative effect of underestimation of modular equipment cost on the total cost.

ORNL DWG 74-7958

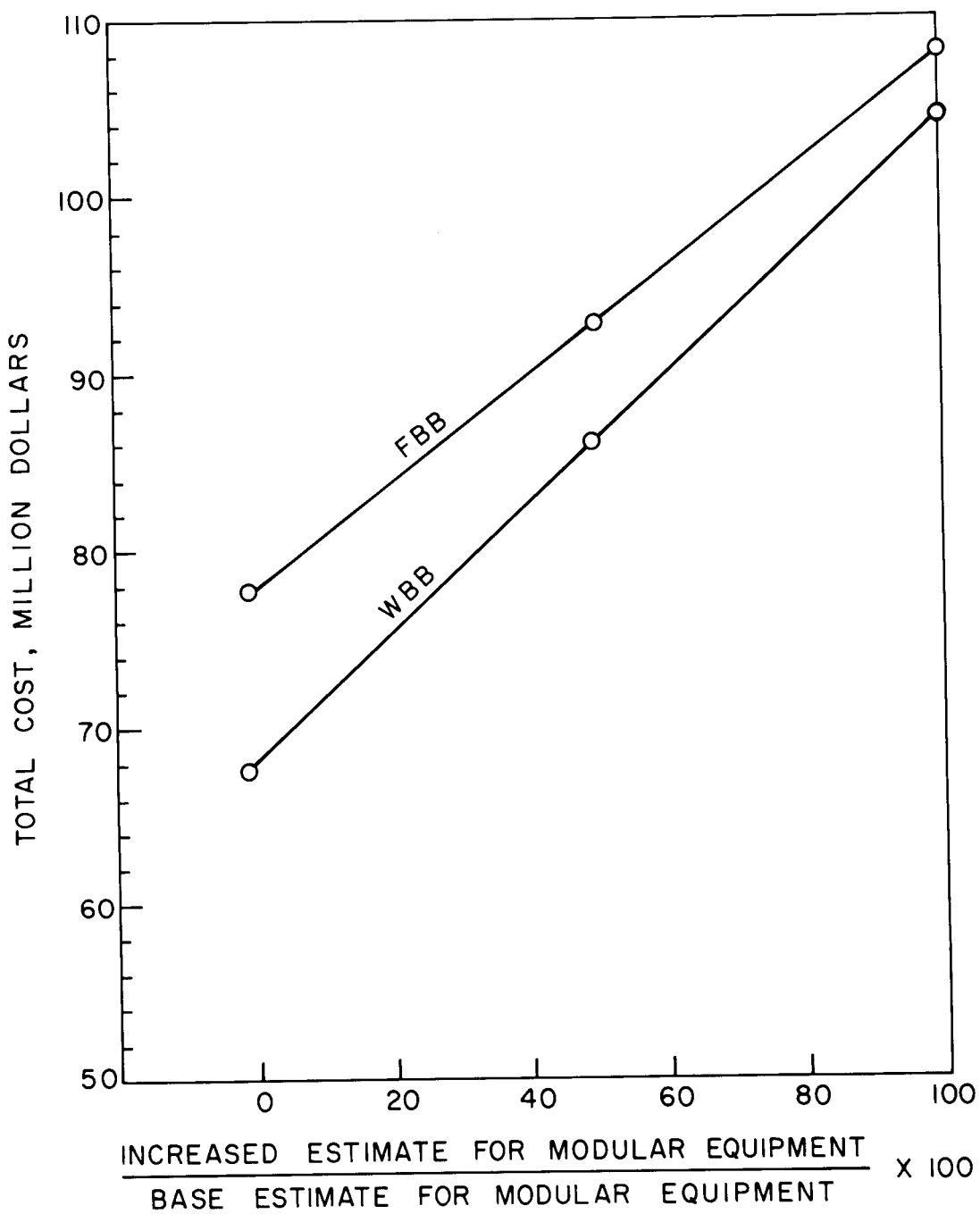


Fig. 38. Effect of underestimation of modular WBB and FBB equipment cost on the total cost.

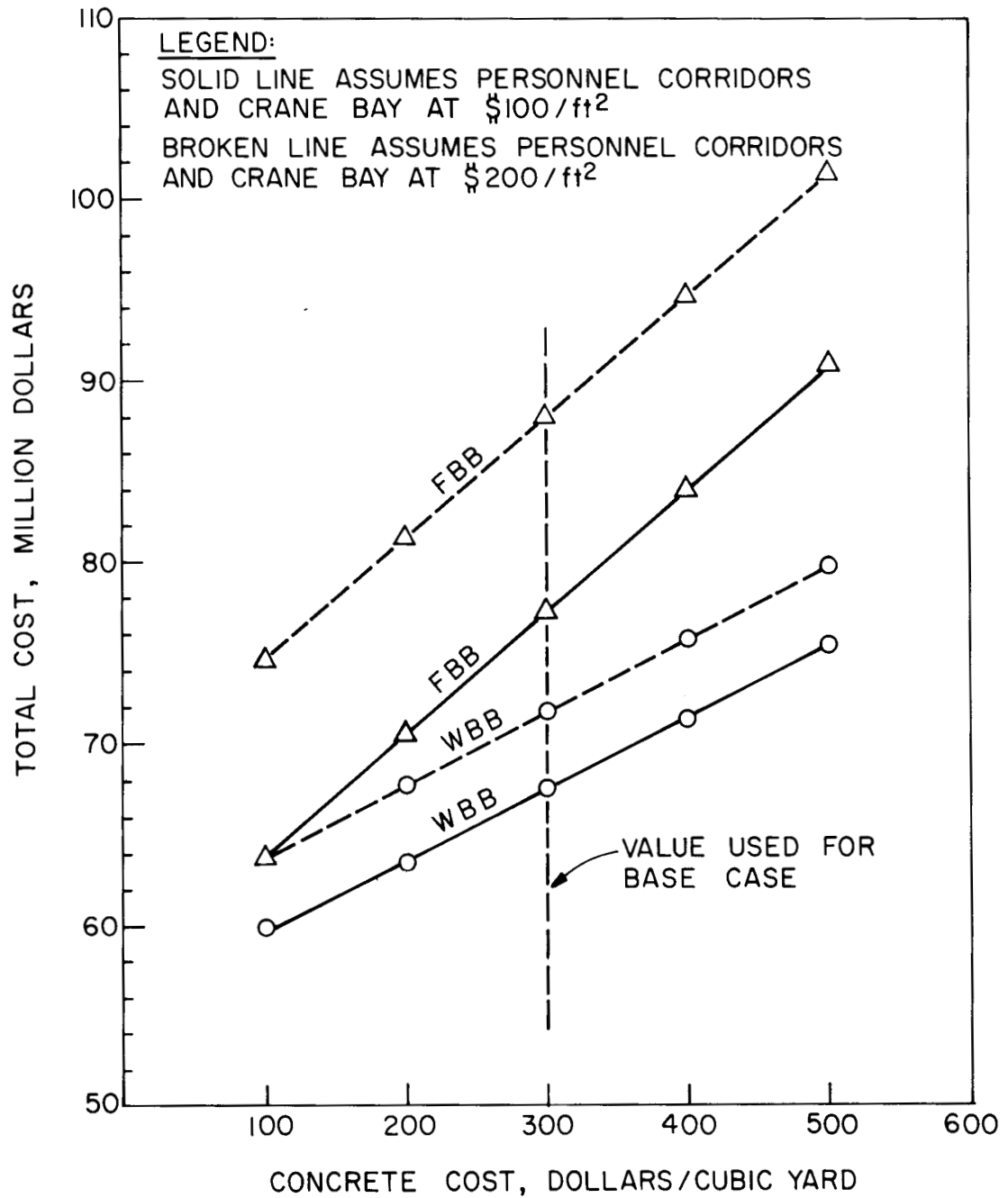


Fig. 39. Effects of concrete and building area costs on the total cost of the WBB and FBB systems.

Results of the study show that the canyon-type structure has the remote maintenance flexibility required to protect the capital investment of a primary burner system; failed equipment can be removed, replaced, and/or modified as required. Within the accuracy of the estimate, one can draw the following conclusions:

1. The estimated cost of the process equipment associated with whole-block burning is higher than that associated with fluidized-bed burning.
2. The cost of the hoppers for handling the crusher product and the primary burner product amounts to about 30% of the modular cost of a FBB.
3. If the estimated equipment cost associated with whole-block burning is increased by about 30% relative to fluidized-bed burning, the difference between the total costs for the two methods is negligible.
4. If the estimated equipment cost for each burning method is increased by about 200%, the cost difference between the total costs of the two methods is negligible.
5. The estimated cost of the building and hot cell(s) associated with fluidized-bed burning is higher than that associated with whole-block burning. This conclusion results from some starting assumptions about the interrelationship with equipment and canyons. The primary fluidized-bed burner is too long to be handled above other burner modular equipment. This necessitates that an unobstructed aisle be retained for moving these long burners to and from the maintenance area. In effect, the same assumption was applied to the feed hoppers more for the sake of convenience than from the standpoint of a firm requirement.
6. If the cost factors for estimating the cost of the cell structures and unshielded area(s) around them are higher

than the base case values ( $\$300/\text{yd}^3$  and  $\$100/\text{ft}^2$ ), the total cost for the FBB system will escalate faster than that for the WBB system. This is simply an effect of the larger building space required for the FBB system.

7. The best guess as to the cost of primary burning for a 50,000 MW(e) economy is \$100 million. This cost estimate is based on 1975 funding and does not include any escalation factors. It is the best guess for both WBB and FBB.

From a different point of view, this study evaluated a short and a long primary burner. A short burner which can be removed above other modular burner equipment has a definite economic advantage as related to building cost. Thus, the development program should have an objective to reduce the length/diameter ratio.

From an operational point of view it is recommended that a reliable pneumatic transport system be developed. Very little attention has been devoted to this within the present FBB development program.

The choice between the WBB and the FBB system could perhaps be made by considering differences in the ease of operation and reliability of the two systems. However, additional developmental studies will be required on the WBB before such a choice can be made.

A very important parameter not explicitly considered in this study is the interrelationship of the spent HTGR fuel storage area and all head-end operations through dissolution. One attractive approach would be to design the process steps in a modular manner to allow for future expansions. If this approach is practical, the huge penalties associated with either oversizing or undersizing of the HTGR reprocessing plant can be minimized by building the initial plant small and then adding-on capacity as near-term projections are made later.

The type of structure considered for the WBB canyon, which has provisions for maintenance located at one end, can, if properly designed, be extended incrementally in length at the opposite end; on the other hand, the arrangement considered for the FBB canyon and its associated hopper

canyon cannot easily be extended incrementally in length due to maintenance requirements at both ends. From an investor's viewpoint, this is perhaps the most important consideration to be made in choosing between the WBB and the FBB systems.

## 6. REFERENCES

1. Staffs of the Oak Ridge National Laboratory, Gulf General Atomic and Allied Chemical Corporation, National HTGR Fuel Recycle Development Program Plan as of August 1973 (Draft), ORNL-4702, Rev. 1 (Aug. 11, 1973).
2. L. M. Ferris, "Head-End Processes for Graphite-Base and Carbide Reactor Fuels," pp. 121-70 in Progress in Nuclear Energy, Ser. III, Vol. 4, Pergamon, New York, 1969.
3. P. A. Haas, HTGR Fuel Reprocessing: A Whole-Block Burner with Recycle of Cooled Gas for Temperature Control, ORNL-TM-4519 (August 1974).
4. Denver Equipment, A Division of Joy Manufacturing Co., Denver, Colo.
5. C. D. Scott, Ind. Eng. Chem., Process Design Develop. 5, 223-33 (June 1966).
6. National Bureau of Standards Research Paper RP 1634 (February 1945), Table 8.
7. L. Bonnetain, X. Duval, and M. Letort, "On the Role of Surface Oxides in the Graphite-Oxygen Reaction," pp. 107-114 in Proceedings of the Fourth Conference on Carbon, 1959.
8. J. B. Lewis, "The Thermal Reactivity of Nuclear Grade Graphite to Oxygen," in Progress in Nuclear Energy, Ser. IV, Vol. 5, Pergamon, New York, 1963.
9. T. J. Clark et al., "Gas-Graphite Systems," Chap. 14 of Nuclear Graphite, ed. by R. E. Nightingale, Academic, New York, 1962.
10. J. Nagle and R. F. Strickland-Constable, "Oxidation of Carbon Between 1000-2000°C," pp. 154-64 in Proceedings of the Fifth Conference on Carbon, 1961.

11. B. Lewis and G. von Elbe, Combustion, Flames, and Explosive Gases, Academic, New York, 1961.
12. M. Rossberg, Z. Elektrochem. 46, 952-56 (1954).
13. P. L. Walker, F. Rusinko, and L. G. Austin, Advan. Catalysis 11, 133-221 (1959).
14. G. von Elbe, B. Lewis, and W. Roth, "Problem of the Second Explosion Limit in the Carbon Monoxide-Oxygen System," in Fifth Symposium (International) on Combustion, 1954.
15. Gmelin's Handbuch der Anorganischen Chemie, Vol. 14-C2, "Kohlenstoff," p. 108, 1972.
16. H. R. W. Cobb, G. B. Engle, and F. T. S. Parry, Characterization of Production-Grade H-327 Graphite for HTGR Design, GA-10389 (Nov. 4, 1970).
17. M. E. Whatley, Calculations of the Performance of the KALC Process, ORNL-4859 (May 1973).
18. J. G. Arquette and R. Blanchard, Fixed Bed Combustion of HTGR Graphite Core - An Analysis of Heat and Mass Transfer, ORNL-MIT-172 (May 1, 1973).
19. H. Barnert-Wiemer, unpublished calculations, WBB Files, Oak Ridge National Laboratory, 1973.
20. H. B. Beutler, R. L. Hammer, and J. W. Prados, GCR Semiannu. Progr. Rep. Sept. 30, 1966, ORNL-4036, pp. 10-22.
21. T. B. Lindemer, ORNL, personal communication, Sept. 26, 1974.
22. C. C. Haws and J. W. Snider, A Vertical Tube Furnace for Continuously Calcining Sol-Gel-Derived  $\text{ThO}_2\text{-UO}_2$  at a Rate of 35 Kilograms per Day, ORNL-3894 (January 1969).
23. Chem. Technol. Div. Annu. Progr. Rep. May 31, 1969, ORNL-4422, pp. 109-10.
24. L. H. Brooks, GAC, personal communication, Aug. 22, 1972.
25. M. E. Speath, GAC, personal communication, May 22, 1973.

26. V. C. A. Vaughen, ORNL, unpublished calculations, 1973.
27. D. E. Ferguson, P. A. Haas, and R. E. Leuze, U.S. Patent 3,742,720 (July 3, 1973).
28. C. A. Burchsted and A. B. Fuller, Design, Construction, and Testing of High-Efficiency Filtration Systems for Nuclear Applications, USAEC Report ORNL-NSIC-65, Oak Ridge National Laboratory, Nuclear Safety Information Center (January 1970).
29. R. D. Zimmerman, GAC, personal communication, Sept. 20, 1973.

APPENDIX A: PRELIMINARY EXPERIMENTAL STUDIES OF A  
ONE-SIXTH-SCALE WHOLE-BLOCK BURNER

H. Barnert-Wierner\*

## A.1 Introduction

Recovery of bred  $^{233}\text{U}$  and unburned  $^{235}\text{U}$  from spent high-temperature gas-cooled reactor (HTGR) fuel elements requires separation of the fissile and fertile particles from the much larger amount of graphite. In the reference reprocessing flowsheet, this is accomplished by crushing the fuel element and then burning the crushed material in a fluidized bed of alumina. Since the crushing and burning steps release fission products in both gaseous and particulate form, complete containment and decontamination of the cover gas of the crushers and of the burner off-gas are necessary. Further, crushing and fluidized-bed burning are difficult operations to carry out in hot cells. For these reasons, we have continued a small development effort relative to burning the whole fuel block as a backup to block crushing and fluidized-bed burning. The primary aim of this effort has been to show that practical burning rates are attainable in a whole-block burner. Secondary objectives are to develop preliminary concepts for full-scale whole-block burners and to pinpoint the areas in which further development effort is needed.

The proposed reprocessing pilot plant at ACC, which will have a capacity of 12 Fort St. Vrain (FSV) reactor fuel elements per day, will require an average burning rate of 0.83 kg of graphite per minute. A full-scale reprocessing plant handling the fuel from a 55,000-MW(e) economy will require a burning rate about thirteen times as great. A full-scale plant will use multiple burners; the minimum graphite burning capacity of a single unit should be at least the 0.83 kg/min that is required for the pilot plant at ACC.

We have demonstrated a carbon burning rate of 136 g/min in a one-sixth-scale block burner. Depending on the method used to calculate the corresponding burning rate for a full-scale whole-block burner, values ranging from 800 to 1100 g/min may be calculated from the demonstrated

---

\*Present address: KFA, Jülich, West Germany.

The experiments reported here were completed over a period during which the author was a guest scientist at the Oak Ridge National Laboratory.

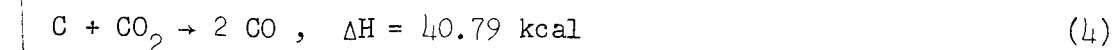
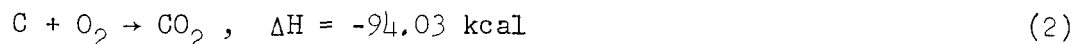
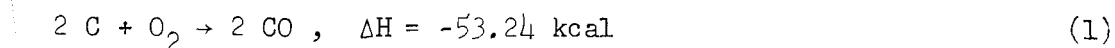
rate. (This is equivalent to 30 to 40 kg of carbon per hour per square foot for a 17-in.-diam burner.) The expected rate for the fluidized-bed burner is 30 kg of carbon per hour per square foot. Thus, a single WBB could handle the throughput required for the ACC pilot plant or for a 4000-MW(e) economy.

The reaction kinetics and mechanisms of heat transfer were considered and reported for burning of early graphite-uranium fuels.<sup>5</sup> Numerical solutions for a mathematical model showed reasonable agreement with experimental results, and potential operational problems were revealed. An adiabatic flow reactor concept, with recycle of cooled gas to provide temperature control and heat removal, has now been proposed.<sup>3</sup> Mathematical analyses were made for this control concept using a simplified model to calculate gas compositions and temperatures throughout a whole-block burner for HTGR fuel.<sup>3</sup>

## A.2 Literature Survey

The literature contains voluminous references to graphite-oxygen reactions. However, there is little agreement between the findings of many investigators because the rates, and perhaps even the mechanisms, of the reactions depend strongly on the nature of the carbon, impurities present, degree of graphitization, particle size, and other factors. These vary widely from one grade of graphite to another.

Four reactions are important in the carbon-oxygen system ( $\Delta H$ 's are at 18°C):



The heats of reaction as a function of temperature<sup>6</sup> show little change up to the 1800°K of concern in a burner. The CO and CO<sub>2</sub> from reactions (1) and (2) are both primary reaction products. It is assumed that both CO and CO<sub>2</sub> molecules are formed when surface oxides decompose. The rates of production of CO and CO<sub>2</sub> are either proportional to each other ( $V_{\text{CO}} = m_o V_{\text{CO}_2}$ ) or related on a linear basis ( $V_{\text{CO}} = m_o V_{\text{CO}_2} + b$ ). The composition

and structure of the surface oxides are not known. The ratio of CO to CO<sub>2</sub> increases approximately exponentially with temperature.

Whether the CO/CO<sub>2</sub> ratio depends on the graphite type has not yet been established. Catalytic impurities such as sodium, iron, and vanadium in concentrations as low as tens of ppm can markedly influence the rate of oxidation and the proportions of CO and CO<sub>2</sub> formed.<sup>8</sup> Other effective catalysts which increase the reaction rate are cobalt, manganese, nickel, and copper.

In many graphites the impurity atoms are found in local deposits so that discrete pits are produced during oxidation of the graphite. Water is also known to act as a catalyst in oxidation reactions, but only when other catalysts are already present. The catalytic effect increases with water concentration in the gas up to approximately 100 ppm.

The oxidation of graphite shows three regimes.<sup>9</sup> Below 800°C, the surface reaction is of zero order with an activation energy of 80 kcal/mole. On samples thicker than 0.1 mm, the diffusion of oxygen into the pores of the graphite results in an observed half-order reaction with an activation energy of 42 kcal/mole. Above 1200°C the chemical reaction is so fast that the rate is determined by boundary layer diffusion. The activation energy is that of gas diffusion and thus very low, the order of reaction being generally found to be unity. A continuous transition region, or intermediate regime, exists between 800 and 1200°C.

In the high-temperature region, the chemical rate undergoes another change.<sup>(10)</sup> The activation energy decreases and becomes negative at a temperature of about 1500°C so that, even in the absence of gas transport control, there will be a maximum in the rate at this temperature. Such a phenomenon is ascribed to self-heating of active sites on the graphite surface. At a still higher temperature, the activation energy is again positive.

The secondary reaction of CO with O<sub>2</sub> to form CO<sub>2</sub> is significant for temperatures above about 750°C. Carbon monoxide is readily oxidized at the surface of suitable catalysts such as the oxides of transition metals. Lewis and von Elbe<sup>11</sup> have shown the importance of water as a catalyst. In a nearly dry gas the oxidation rate is substantially independent of

the oxygen pressure but is directly proportional to the partial pressure of the water vapor. In a wet gas the rate becomes proportional to the oxygen pressure and has an activation energy of 24 kcal/mole.

Reaction (4), ( $\text{CO}_2 + \text{C} \rightarrow 2 \text{CO}$ ), becomes important only at high temperatures. The "threshold oxidation temperature" (which is defined as that at which a sample loses 1% of its weight in 24 hr) for graphite in  $\text{CO}_2$  is  $900^\circ\text{C}$ , as compared with  $400^\circ\text{C}$  in air.<sup>9</sup>

The reaction of carbon and oxygen in the presence of excess carbon has been studied extensively by the French chemist O. L. Boudouard, and the  $\text{CO}/\text{CO}_2$  ratio as a function of temperature and pressure in a system with surplus carbon is usually called the Boudouard equilibrium in European literature. His data at 1-atm pressure show 1% CO and 99%  $\text{CO}_2$  at  $400^\circ\text{C}$ , and 1%  $\text{CO}_2$  and 99% CO at  $1000^\circ\text{C}$ . Rossberg,<sup>12</sup> on the other hand, found the  $\text{CO}/\text{CO}_2$  ratio to be independent of the Boudouard equilibrium when oxidizing tubes, made from nuclear graphite, in a dry oxygen stream. He found that the  $\text{CO}/\text{CO}_2$  ratio followed the equation

$$\text{CO}/\text{CO}_2 = 10^{3.86} \exp(-18,700/\text{RT})$$

T, K	CO/CO <sub>2</sub>
1700	0.5
1000	0.02
750	

between  $520$  and  $1420^\circ\text{C}$ . At gas velocities greater than 50 m/sec, the  $\text{CO}/\text{CO}_2$  ratio was found to be independent of the gas velocity and the oxygen concentration in the gas. At lower gas velocities, the CO was not removed rapidly enough and oxidized in the gas phase.<sup>13</sup>

An explosion is possible if the off-gas contains both CO and  $\text{O}_2$ . It is assumed that the pressures and temperatures at which a  $\text{CO}-\text{O}_2$  mixture explodes occupy a peninsula-shaped region in a pressure-temperature diagram.<sup>14</sup> Along the lower bound of this region (the first explosion limit) the pressure decreases with increasing temperature, whereas along the upper bound (the second explosion limit) the pressure increases with increasing temperature. The existence of such peninsulas may be taken as evidence of a branched-chain reaction which is competing with two chain-breaking reactions, one predominating at low pressure and the other at high pressure.

This assumption is valid for H-containing mixtures. It has not yet been verified for a  $\text{CO}-\text{O}_2$  mixture that is absolutely free of H-containing impurities (e.g.,  $\text{H}_2$ ,  $\text{H}_2\text{O}$ ,  $\text{CH}_4$ , etc.). A selection of explosion limits

for the ternary system CO-O<sub>2</sub>-CO<sub>2</sub> is given in Table A.1.<sup>15</sup> The values for G<sub>1</sub> (lower limit) and G<sub>2</sub> (upper limit) are given in mole % CO.

Table A.1. Explosion limits for the ternary system CO-O<sub>2</sub>-CO<sub>2</sub>

CO <sub>2</sub> (mole %)	G <sub>1</sub> (mole % CO)	O <sub>2</sub> (mole %)	CO <sub>2</sub> (mole %)	G <sub>2</sub> (mole % CO)	O <sub>2</sub> (mole %)
0	16.7	83.3	55.1	37.8	7.1
20.4	19.4	60.2	39.9	52.2	7.9
38.8	22.2	39.0	20.0	73.0	7.0
55.5	25.0	20.0	0	93.9	6.1

### A.3 Description of the Equipment

The experimental whole-block burner (experimental WBB) for this study was, in reality, sized to hold one-sixth of a whole block and had been built to use portions of an existing facility for testing fluidized-bed burners. Thus the gas supply system, the off-gas system with the gas analyzers, and the recorders for temperatures and pressures were already installed. The size of the off-gas system limited the gas flow rates for the experimental WBB.

The burner and the off-gas system were located in a concrete cell which was 16 ft long, 6 ft wide, and 30 ft high. This cell was ventilated with 6000 cfm of air, which entered at the bottom through a louver and was exhausted near the top by two fans. The burner was operated from a control room where the gas analyzers and all recording and controlling instruments were installed. Figure A.1 shows a schematic flowsheet for the burner system. The torch gases CO and O<sub>2</sub>, the feed gases O<sub>2</sub> and CO<sub>2</sub>, the purge gas N<sub>2</sub>, and the gases for calibrating the gas analyzers were supplied from cylinders. The pressurized air for the cooling came from the central laboratory supply. All flows were measured by rotameters. The gases entered the burner at the top and left it at the bottom. Between the burner and the filters, a line branched off to the gas analyzer. The main off-gas stream entered the combined cyclone--filter vessel. The two porous metal filters could be blown back with N<sub>2</sub>. Collected dust was removed through

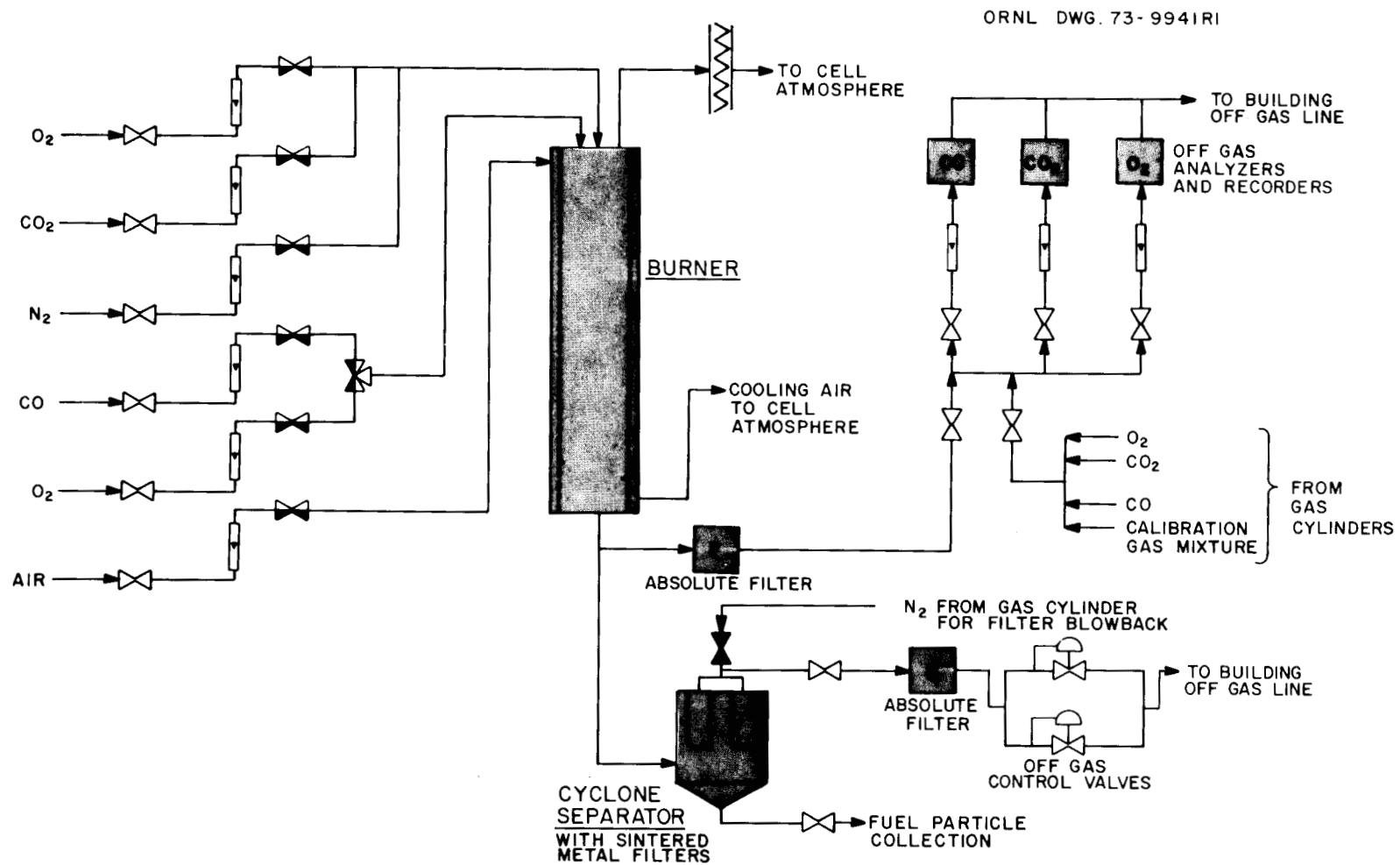


Fig. A.1. Schematic of the experimental one-sixth-scale whole-block burner.

a ball valve at the bottom of the cyclone. After the porous metal filters, a filter filled with glass wool extracted the remainder of the graphite dust from the off-gas.

The two parallel off-gas control valves maintained the pressure in the system at a set valve. The off-gas was then released to the building off-gas line.

### A.3.1 The HTGR fuel block

The fuel element used in the Fort St. Vrain reactor (Fig. A.2) is a hexagonal graphite block, about 14 in. across the flats and 31 in. high. It contains two hundred ten 0.5-in.-diam fuel holes, one hundred two 0.625-in.-diam coolant holes, and six 0.5-in.-diam coolant holes.

The proposed HTGR 3000/2000-MW reference fuel block is of similar size but contains sixty-six 0.826-in.-diam coolant holes, six 0.717-in.-diam coolant holes, and one hundred thirty-two 0.624-in.-diam fuel holes (Figs. A.3 and A.4). Compared with the Fort St. Vrain block, the cross-sectional area of all coolant holes is 16% greater, the volume of the fuel sticks is 2% greater, and the volume of the graphite is 4% smaller.

The HTGR fuel element can be cut axially into six pieces without penetrating the fuel sticks. The experimental WBB was sized to hold one-sixth of a Fort St. Vrain block [Fig. A.5(a)]. Such a segment would normally have 18 coolant holes; however, since we cut through two rows of holes to obtain one-sixth of a block, only 13 coolant holes are intact in the segment.

Table A.2 lists the properties of H-327 graphite, the principal core graphite of the Fort St. Vrain reactor. Tables A.3 and A.4 give the concentrations of the impurities in this material.<sup>16</sup>

Graphite blocks without fuel were used for the most of the runs. Three one-sixth blocks contained extruded fuel rods, which were made by the ORNL Metals and Ceramics Division by using rejected TRISO-coated  $\text{ThC}_2$  particles supplied by the General Atomic Company. Five one-sixth-block segments were filled with fuel sticks, which were also fabricated by the ORNL Metals and Ceramics Division and contained different types of coated

ORNL DWG 71-9528

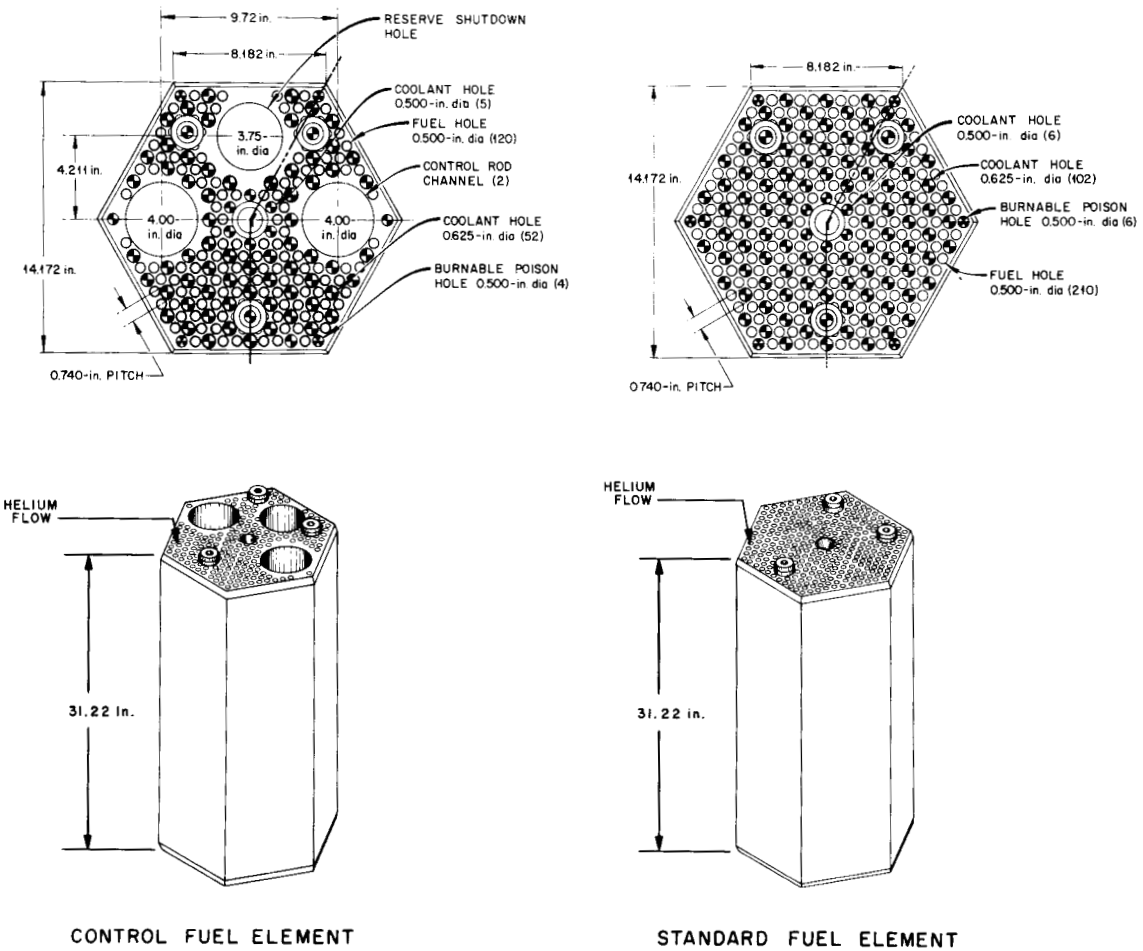


Fig. A.2. Schematic of the Fort St. Vrain HTGR reactor fuel elements.

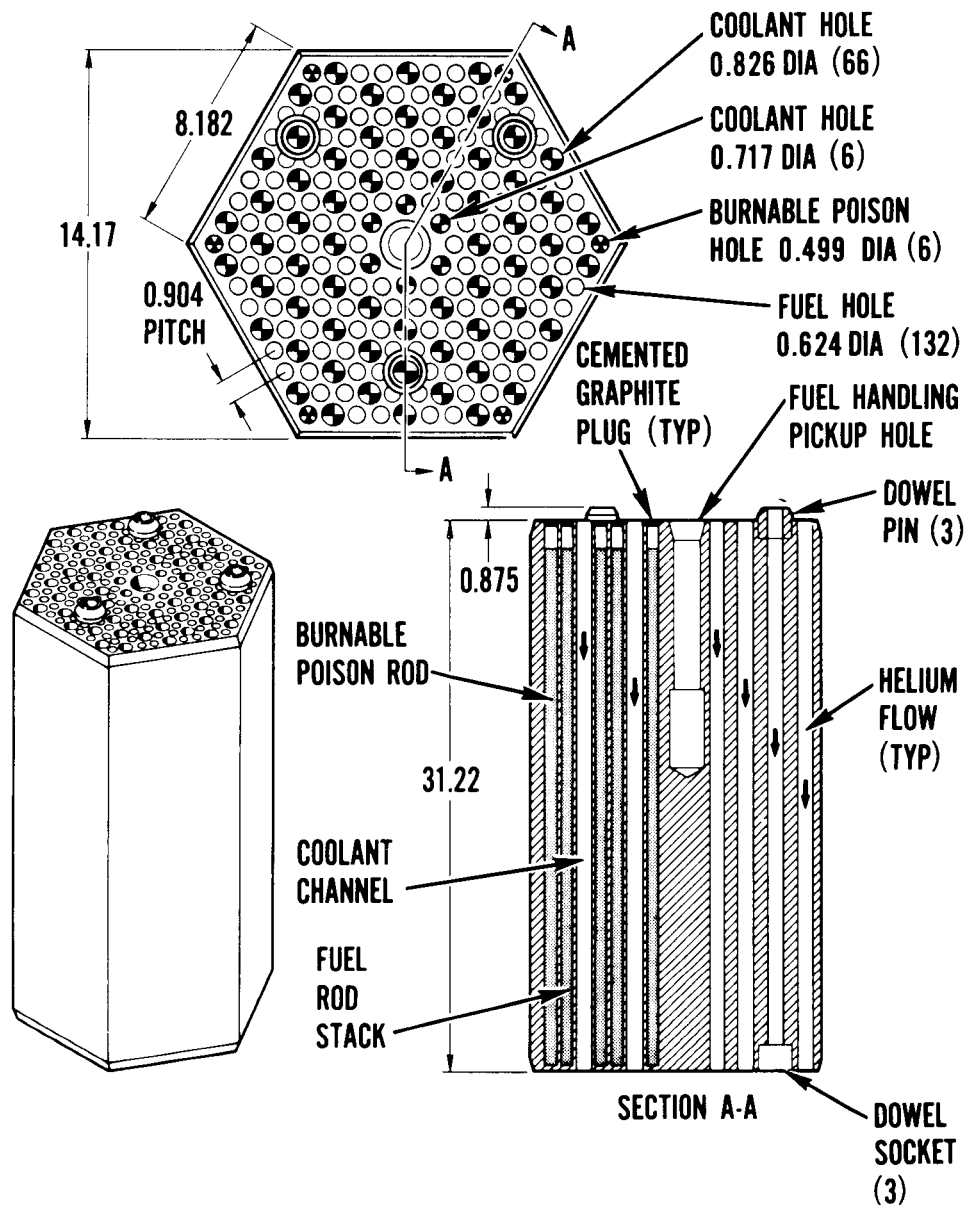


Fig. A.3. Typical 1160-MW(e) modified fuel element.

# CONTROL FUEL ELEMENT

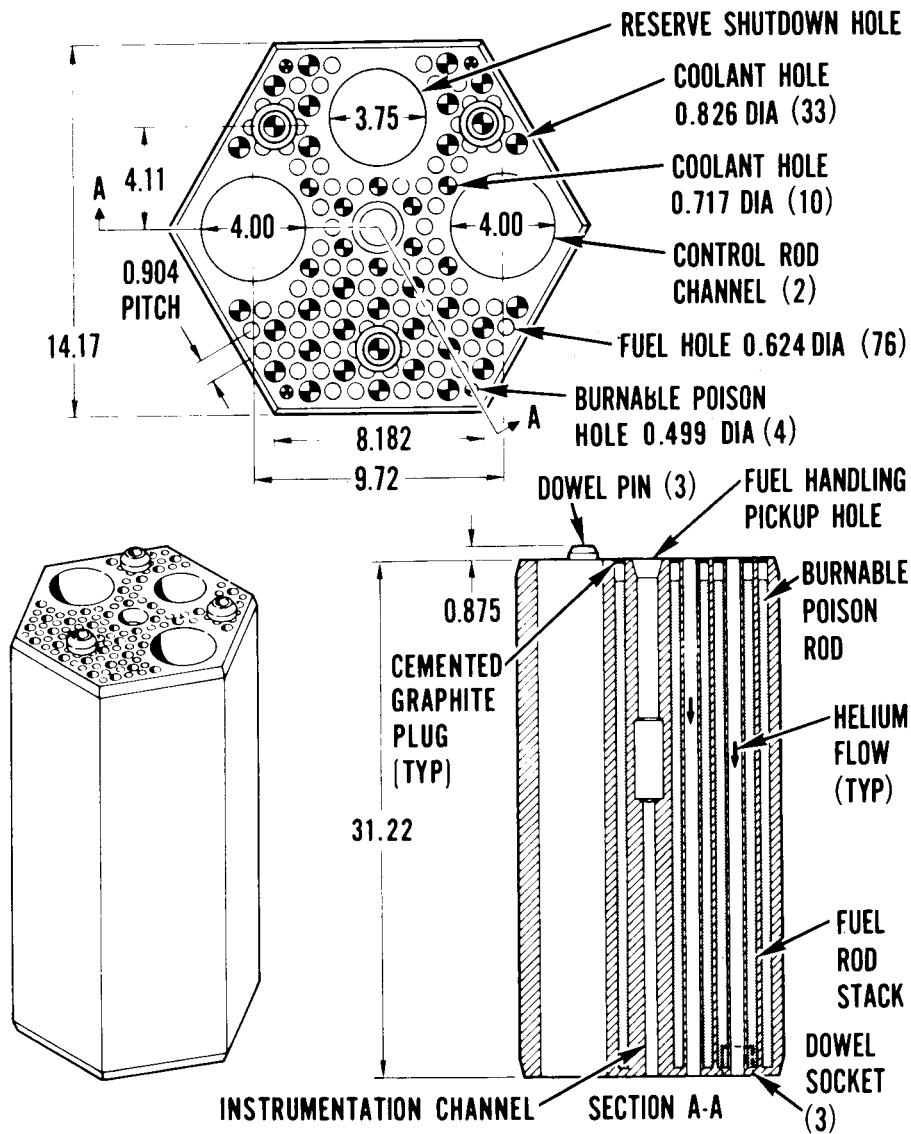


Fig. A.4. Typical 1160-MW(e) modified fuel element with control rod passage.

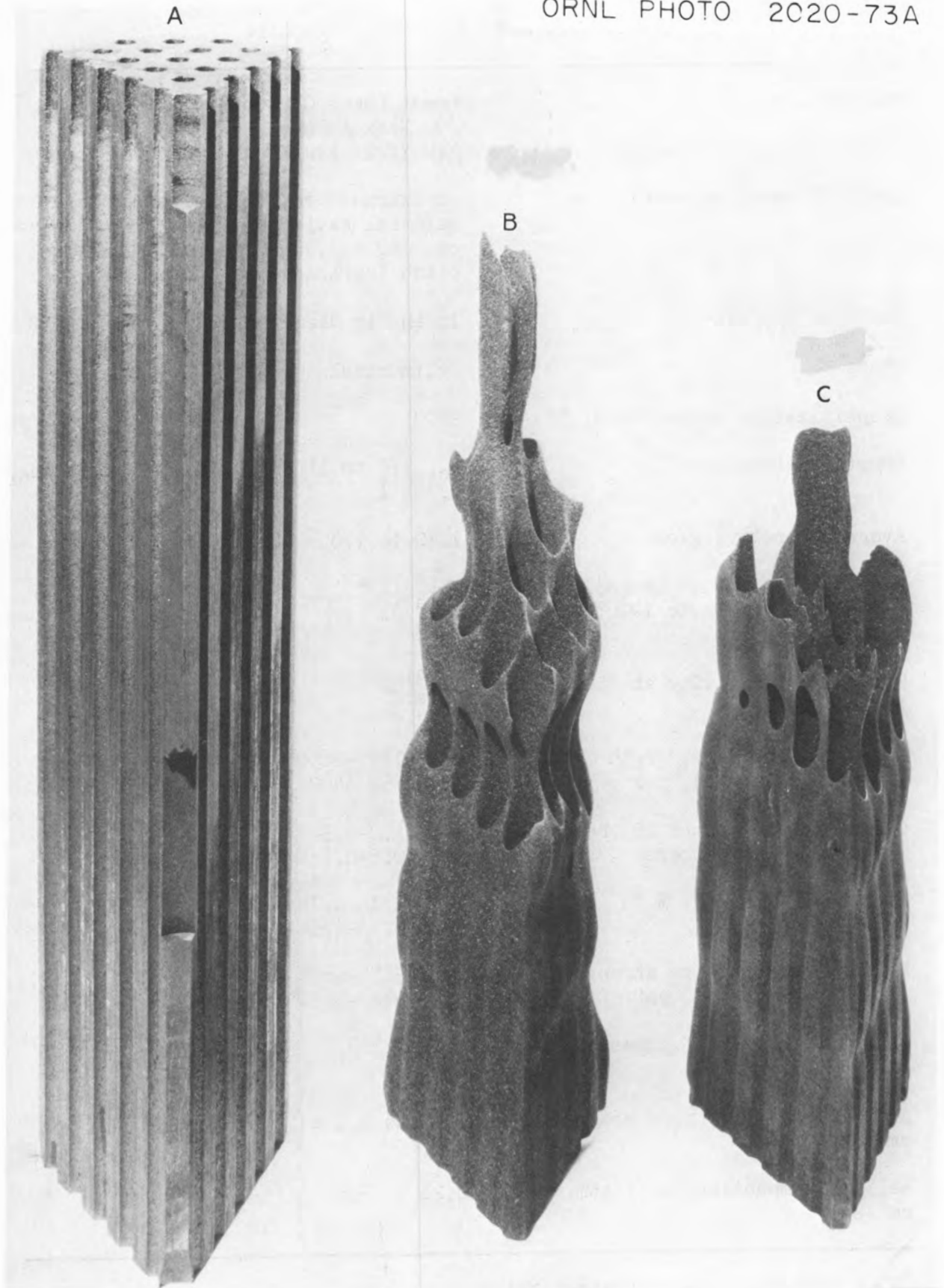


Fig. A.5. One-sixth of a Fort St. Vrain fuel block before and after burning.

Table A.2. Properties of H-327 Graphite<sup>16</sup>

Manufacturer	Great Lakes Carbon Corporation 299 Park Avenue New York, New York 10017
Description of material	An extruded petrochemical needle coke material having a maximum filler size of 0.60 mil, bonded with a coal tar pitch (carbonaceous binder)
Standard log size	18 in. in diameter, 34 in. long
Shape	Cylindrical
Graphitization temperature, °C	2700
Crystal parameters	$L_c$ , 770 to 1150 Å; interlayer spacing, 3.362 Å
Average density, g/cm <sup>3</sup>	1.70 to 1.8
Mean coefficient of thermal expansion from 22 to 1000°C, 10 <sup>-6</sup> /°C	WG, <sup>a</sup> 1.58 AG, <sup>a</sup> 3.35
Thermal conductivity at 800°C, Btu/hr-ft-°F	WG, <sup>a</sup> 42 AG, <sup>a</sup> 32
Measured tensile strength (fuel block grade), psi	WG, <sup>a</sup> 1150-2650 AG, <sup>a</sup> 750-1400
Chord modulus, psi x 10 <sup>6</sup> between 250 and 500 psi stress	WG, <sup>a</sup> 1.0-2.5 AG, <sup>a</sup> 0.5-0.8
Strain at fracture, %	WG, <sup>a</sup> 0.14-0.26 AG, <sup>a</sup> 0.13-0.31
Measured compressive strength (fuel block grade), psi	WG, <sup>a</sup> 3870-4680 AG, <sup>a</sup> 4120-4630
Effective number of pores per cm <sup>2</sup>	10 <sup>4</sup> to 10 <sup>5</sup>
Average effective pore radius, cm	10 <sup>-3</sup> to 2.4 x 10 <sup>-4</sup>
Helium permeability at 1 atm, cm <sup>2</sup> /sec	0.28 to 3.6

<sup>a</sup>WG = with grain; AG = against grain.

Table A.3. Spectrochemical analysis of impurity levels in twelve logs  
of Fort St. Vrain grade H-327 graphite

Log No.	Log Position	Concentration (ppm) <sup>a</sup>								Ash <sup>b</sup>	Average density of log (g/cm <sup>3</sup> )
		Al	B	Cu	Fe	Mg	Si	Ti	V		
694	End edge	1.0	NDO.5 <sup>c</sup>			2.0	<10.0	4.0	NDO.5 <sup>c</sup>	21	1.78
705	End edge	1.0	1.0			2.0	<10.0	8.0		38	1.77
739	End edge	1.0	2.0			2.0	10.0	10.0		55	1.78
744	End edge	4.0	2.0		2.0	6.0	20.0	8.0		77	1.78
769	End edge	1.0	1.0	1.0	1.0	4.0	20.0	10.0		55	1.75
956	End edge	4.0	1.0	1.0	2.0	4.0	20.0	10.0		472	1.77
958	End edge		1.0		2.0	1.0	20.0	20.0		317	1.80
1058	End edge	1.0	1.0			4.0	20.0	10.0		72	1.78
1959	End edge	6.0		1.0	10.0	10.0	80.0	10.0		77	1.77
2479	End edge	4.0	1.0	1.0	1.0	6.0	20.0	10.0		65	1.77
2482	End edge	2.0	1.0		2.0	6.0	20.0	10.0		62	1.78
42/196	End edge	20.0	10.0	<1.0	2.0	2.0	<10.0	6.0		47	
40/997	End center	2.0			1.0	2.0	<10.0	6.0			1.77
12-1	Mid-length edge	4.0	4.0		1.0	4.0	20.0	8.0			
	Mid-length center	1.0			1.0	4.0	10.0				

<sup>a</sup>Accuracy, 50%.

<sup>b</sup>Vendor's reported chemical analysis.

<sup>c</sup>Not detectable below 0.5%.

Table A.4. Typical rare-earth and alkali-metal contents of Fort St. Vrain H-327 fuel element graphite<sup>a,b</sup>

Element	Concentration (ppm)	Element	Concentration (ppm)
Ce	0.1	Sm	<0.02
Pr	0.2	Gd	0.02
Tb	0.2	Dy	0.2
Nd	0.2	La	0.02
Ho	<0.04	Tm	0.02
Lu	0.04	Na	<5.0
Er	0.02	Rb	N2.0 <sup>c</sup>
Yb	<0.02	Li	N1.0 <sup>c</sup>
Sc	0.02	K	<1.0

<sup>a</sup>A 25-g sample was analyzed.

<sup>b</sup>Method, spectrographic analysis; accuracy,  $\pm 30\%$ .

<sup>c</sup>N = not detected at a sensitivity of 2 or 1 ppm.

particles (see Table A.5). All thorium particles were reject particles obtained from the General Atomic Company. The extent, or fraction, of breakage was not known. The uranium kernels were made by the Chemical Technology Division and coated by the Metals and Ceramics Division at ORNL. Although these kernels were not reject particles, they were not highly characterized. At the time the fuel was prepared, the Metals and Ceramics Division was concerned chiefly about developing the methods for coating particles and fabricating fuel sticks. No good techniques for determining particle breakage were available to characterize these U<sub>2</sub> particles.

Table A.5. Types of coated particles used in whole-block burner tests

Run No. (WBB-)	Coated particles
12	TRISO U <sub>2</sub> , BISO ThC <sub>2</sub>
21	BISO (3Th/U)O <sub>2</sub>
31	TRISO U <sub>2</sub> , TRISO ThO <sub>2</sub>
32	TRISO U <sub>2</sub> , TRISO ThO <sub>2</sub>
33	TRISO U <sub>2</sub> , BISO ThC <sub>2</sub>

### A.3.2 Burner and off-gas system

The WBB, sized to hold one-sixth of an HTGR fuel element, was fabricated from a 4-ft length of 10-in. sched 40 pipe (347 stainless steel) (Figs. A.6 and A.7). The vessel, which was designed for a maximum pressure of 30 psig at a wall temperature of 350°C, was flanged at both ends. Cooling air was passed through the annulus between the liner and the jacket. Provision was also made to cool the vessel heads. The outer surface between the flanges was insulated in most of the runs. Three rows of thermocouples are located on the inner wall of the burner. For the last six runs, two additional rows of thermocouples were welded to the outer jacket. The temperature of each flange was measured by thermocouples (Fig. A.7). Internal temperatures were measured by thermocouples in the cooling holes of the block; one thermocouple was located in the gas stream behind the block, while another was on the outside of the support pan (Fig. A.7).

The following pressures were measured and recorded: pressures at the top and the bottom of the burner, pressure through the burner, pressures downstream of the sintered metal filters and downstream of the absolute filter, and system off-gas pressure. The system off-gas pressure was held at a preset value by the recorder-controller instrument which controlled the opening of the two parallel off-gas valves.

Throughout the first 15 runs the block sat on a stainless steel plate which had an opening that was smaller than the block, so that the block rested on a 1/4-in.-wide rim. Thus all the cooling holes in which the burning occurred were open. The steel plate, in turn, rested on a stainless steel pan (Fig. A.8), which contained holes for inserting the internal thermocouples. In the remaining runs this pan was replaced by a cone-shaped pan which allowed the coated particles to be swept out with the off-gas. The block sat on a ceramic plate, placed on top of the pan, which had holes corresponding to the coolant holes in the block. The block was surrounded by baffles (only one initially, but later four more were added), which forced the gas through the coolant holes.

The block was heated up to burning temperature by a CO-O<sub>2</sub> torch. The two gases in stoichiometric ratio were premixed before they entered the

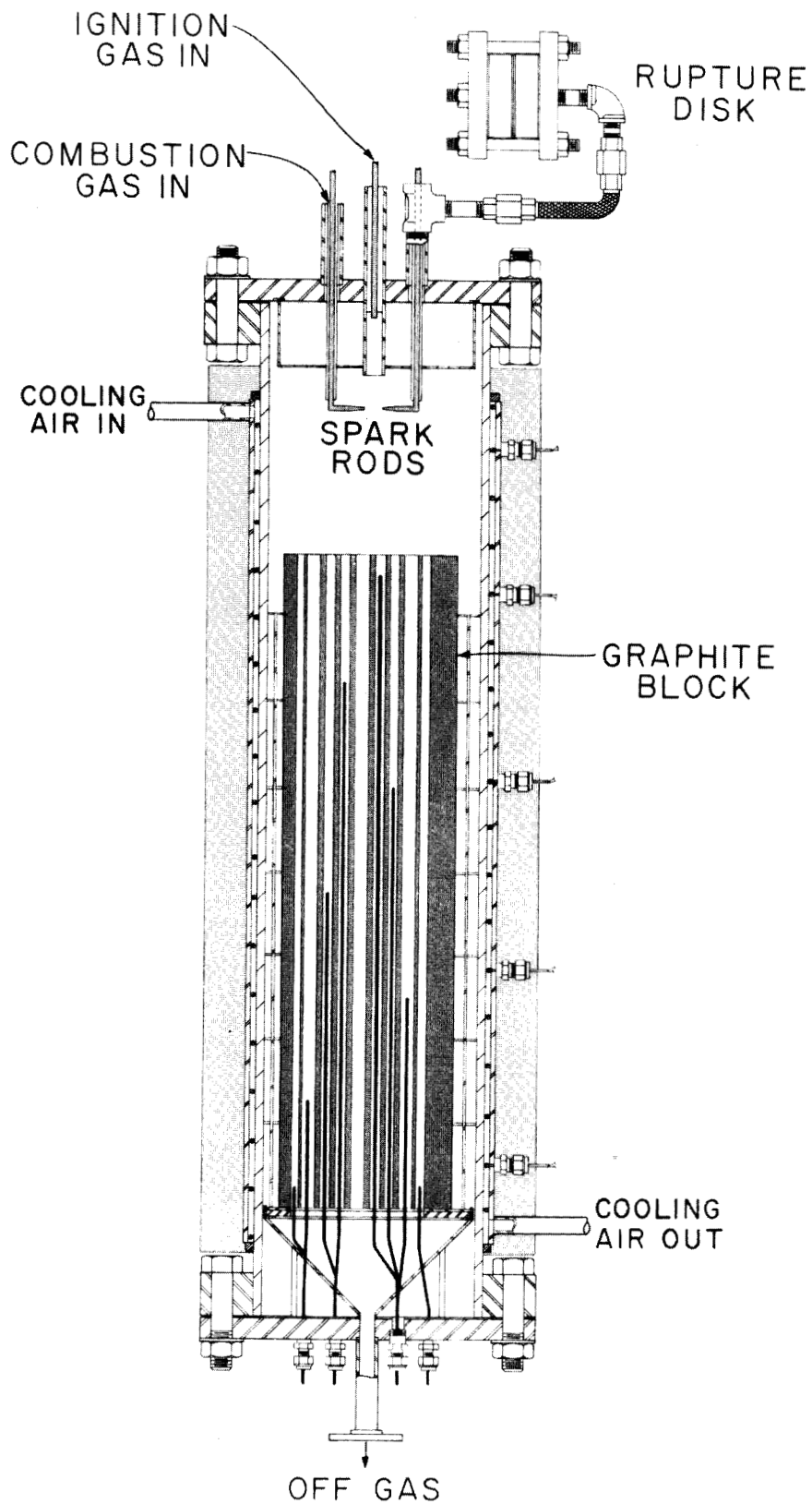


Fig. A.6. A sectional view of the experimental whole-block burner.

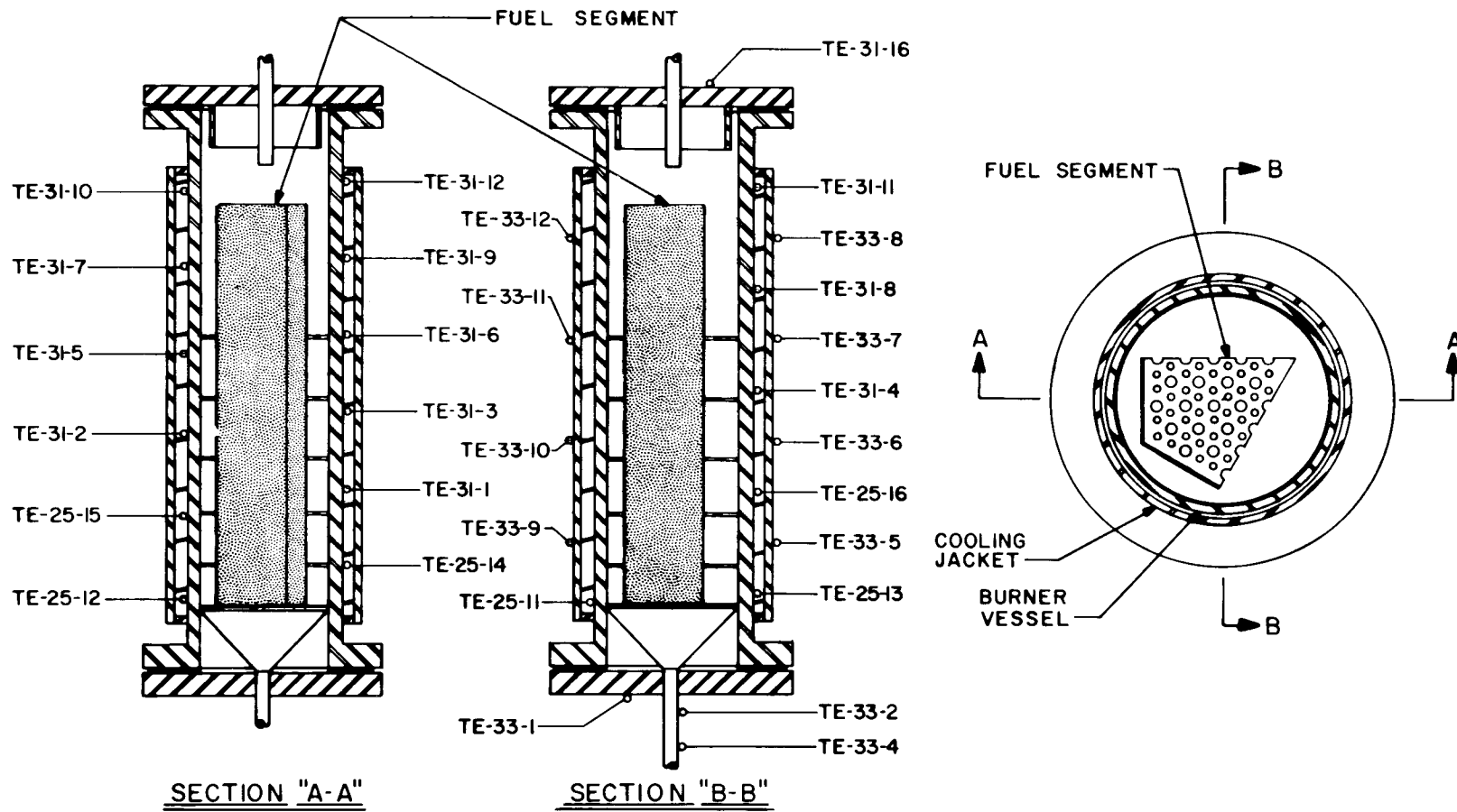


Fig. A.7. Thermocouple locations of the experimental burner.

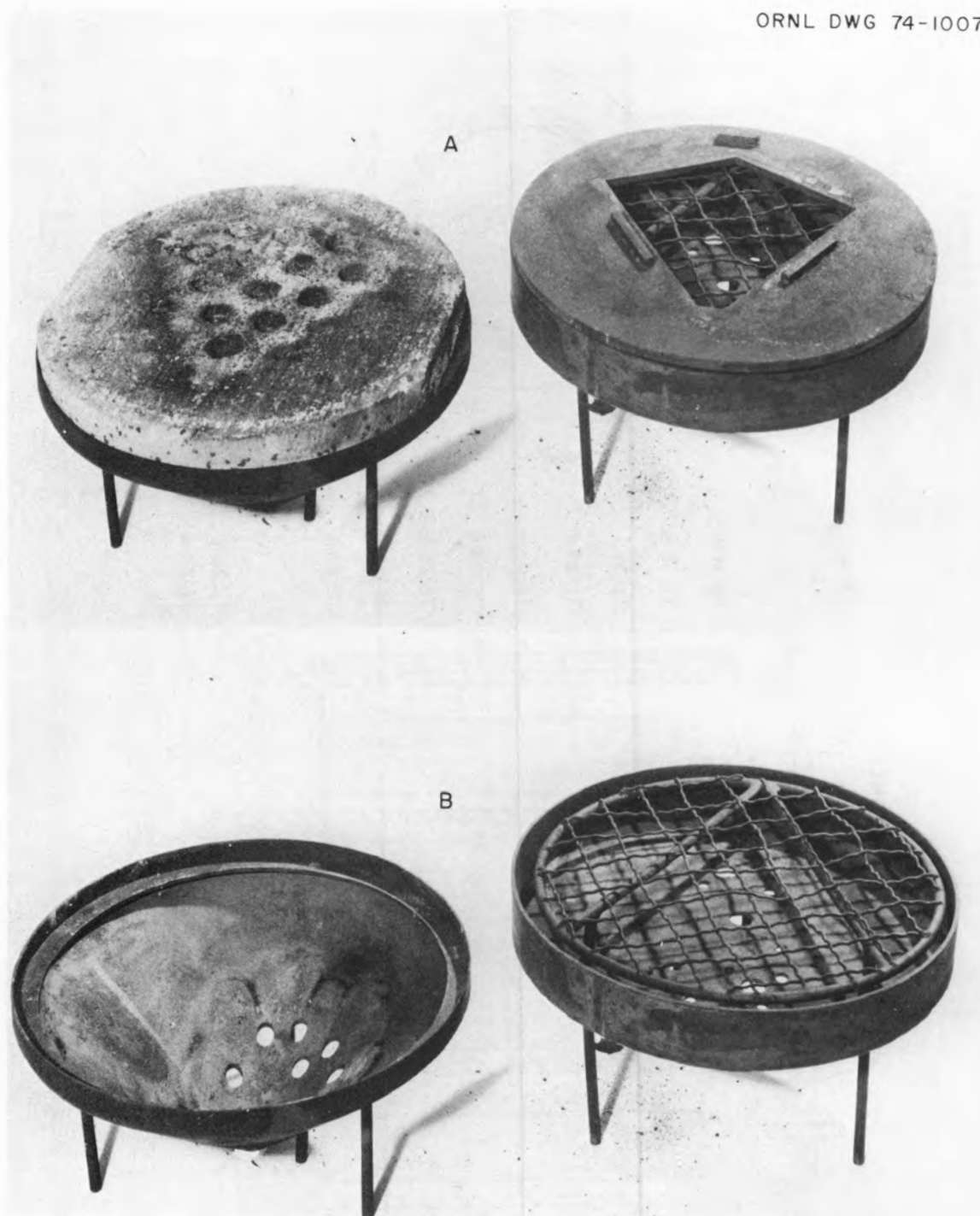


Fig. A.8. Fuel block supports for the experimental burner.

burner, where they were ignited by an electrical arc. The theoretical flame temperature is  $2468^{\circ}\text{C}$ ; the heating value,  $3033 \text{ kcal/m}^3$ ; and the flame velocity,  $1.1 \text{ m/sec}$ . The arc was on as long as the torch was on. Loss of the arc would immediately shut off the CO flow. A thermocouple at the tip of the torch measured the temperature of the flame. If the flame was lost and the torch-tip temperature dropped below a certain preset temperature, the CO flow was automatically cut off. Another safety device was a rupture disk, which would break if the pressure in the vessel exceeded  $24 \text{ psi}$ .

After the block had been heated up, the torch gas was turned off and the combustion gas, pure oxygen or an  $\text{O}_2\text{-CO}_2$  or  $\text{O}_2\text{-N}_2$  mixture, was introduced. The gas entered at the top so that the flow of gas was downward, sweeping the coated particles and graphite dust out of the burner. The off-gas system consisted of a cyclone, sintered metal filters with  $20\text{-}\mu\text{m}$  pore size, and an absolute filter. The pressure in the system was maintained by two parallel control valves in the off-gas line behind the filter system. From the off-gas pipe, a sample line branched off to the gas analyzers for CO,  $\text{CO}_2$ , and  $\text{O}_2$ .

### A.3.3 Instrumentation

All external thermocouples were Chromel-Alumel with stainless steel sheathing. This type was also used for the internal thermocouples in most of the runs; for several runs, however, Inconel-sheathed platinum/rhodium thermocouples were used to measure the temperature of the block. The accuracy of each thermocouple was  $\pm 2\%$  when new. Thermocouples that had been used for extended periods in the oxidizing atmosphere of the burner were probably less exact, due to oxidation of the wires. However, no measurements were made to confirm this since the burner would have had to be disassembled in order to reach the thermocouples. The temperatures were recorded by two 16-point recorders, three 12-point recorders, and one continuous recorder for the torch-tip temperature. Each recorder was manufactured by the Brown Instrument Division of Minneapolis-Honeywell.

All of the recorders except one were calibrated for temperatures up to  $1200^{\circ}\text{C}$ ; the recorder for the platinum/rhodium thermocouples was calibrated for temperatures up to  $1600^{\circ}\text{C}$ .

The composition of the off-gas was measured by two infrared analyzers (Lira, Model 300, Mine Safety Appliances Co.) for CO and CO<sub>2</sub>, and by one paramagnetic O<sub>2</sub>-analyzer (Model 365, The Hays Corp.). The analyzers were calibrated with gas mixtures of known composition and proved to be very accurate (< 1% error). The data are recorded by single-point recorders (Minneapolis-Honeywell, Brown Instrument Division).

All flows were controlled by rotameters which had been calibrated with air at 14.7 psig. These data were converted to the respective gases and pressures. The calibration is correct by  $\pm 3\%$ .

All instruments for measuring, transmitting, recording, and controlling of pressures and differential pressures were manufactured by Foxboro.

#### A.4 Experimental Procedures and Results

Individual procedures and results are described in this section. The overall recommendations are discussed in Sect. A.6.

##### A.4.1 Procedure of a typical run

All loading and product removal operations were carried out by disassembling the burner at room temperature. If internal thermocouples had been burned out in the previous run, the bottom flange was removed in order to replace the thermocouples. If a block with fuel had been burned, the bottom flange was also removed because a fraction of the particles was not swept out with the off-gas but remained in the burner. After the thermocouples had been replaced or the bottom had been cleaned, the flange was replaced. The test block, after weighing, was lowered from the top into the burner. The burner was then sealed and a leak check was made of the burner and off-gas system. Before the run, the off-gas analyzers were calibrated with gas samples of known composition.

At this point, the CO-O<sub>2</sub> torch was ignited and kept burning until the temperature in the middle region of the block was about 800°C. Then the torch flow was gradually decreased while the feed gas flow was increased. This procedure was usually completed in 10 min. The actual burning was always started with pure oxygen. With the torch still on and pure oxygen as the feed gas, the temperature in the block increased

rapidly with only a slight  $O_2$  peak in the off-gas. Afterward,  $CO_2$  could be introduced to control the temperature of the block if this could not be accomplished by the cooling air alone. The  $CO_2$  was chosen as a diluent of the feed gas because the proposed treatment for burner off-gases cannot handle greater amounts of inert gases.<sup>17</sup>

About two-thirds of the block could be burned before the oxygen in the off-gas started increasing. This was the result of two effects: (1) the surface of the block became too small to use up all the oxygen, and (2) part of the gas passed around the block unused. Since some burning always takes place on the outside of the block, the block shrinks, leaving a gap between the block and the baffles and exposing some of the holes in the ceramic plate.

When the temperature of the block starts dropping, the cooling air flow is reduced and, with pure oxygen as feed gas and a moderate flow rate, it is possible to burn the block completely. If the feed gas flow is too high (e.g., due to dilution) the remainder of the block is cooled down too fast and the block is not burned completely.

When the block is burned completely or the run is terminated for other reasons, the feed gas is turned off and the burner is swept with nitrogen until the temperatures are close to ambient. Meanwhile, the gas analyzers are checked with pure  $CO$ ,  $CO_2$ , and  $O_2$  to see whether any drift in zero or range setting occurred during the run.

Table A.6 lists all the experimental WBB runs (except those that had to be shut down prematurely due to equipment failure), along with the type of fuel contained in the blocks and the objectives of the runs.

#### A.4.2 Burning rate and burning behavior

In our experiments, the gas was forced through the coolant holes of the block by baffles around the block. The burning took place at the surfaces of the coolant holes. The coolant holes assumed a tapered shape in the burning zone, usually 6 to 10 in. long. The length of the burning zone was probably dependent on temperature profile, flow rate, and dilution of the combustion gas. Figure A.5 shows one-sixth of a block before burning (left) and two blocks, each of which lost 65% of

Table A.6. Summary of experimental WBB runs

Run (WBB-)	Fuel	Goal of run
4→	Extruded rods, TRISO-coated ThC <sub>2</sub>	Ignite block
7→	Extruded rods, TRISO-coated ThC <sub>2</sub>	Burn block completely
9→	Extruded rods, TRISO-coated ThC <sub>2</sub>	Burn block completely
10	Graphite only	Find out which shape the block assumes during burning
11	Graphite only	Find out which shape the block assumes during burning
12	TRISO-coated UO <sub>2</sub> , BISO-coated ThC <sub>2</sub>	Study behavior of fuel sticks and particles
13	Graphite only	Improved O <sub>2</sub> consumption by putting five baffles around block
14	Graphite only	Decrease O <sub>2</sub> with decreasing block surface
15	Graphite only	Study influence of pressure and feed gas dilution
16	Graphite only	Study changes due to new cone-shaped pan
17	Graphite only	Study changes due to new cone-shaped pan
18	Graphite only	Study off-gas composition at various gas flows
19	Graphite only	Study off-gas composition at various gas flows
20	Graphite only	Improve start-up procedure
21	BISO-coated (3Th/U) O <sub>2</sub>	Study behavior of particles
23	Graphite only	Heat transfer calculations
24	Graphite only	High dilution of feed gas
25	Graphite only	High burning rate
26	Graphite only	Minimum O <sub>2</sub> /CO <sub>2</sub> ratio in feed gas
27	Graphite only	Temperature changes due to countercurrent cooling air flow
28	Graphite only	Burning rate in burner without insulation
29	Graphite only	Keeps flows constant for heat transfer calculations
30	Graphite only	Heat transfer calculations for different dilutions of feed gas
31	TRISO-coated UO <sub>2</sub> , TRISO-coated ThO <sub>2</sub>	Determine particle breakage
32	TRISO-coated UO <sub>2</sub> , TRISO-coated ThO <sub>2</sub>	Determine particle breakage
33	TRISO-coated UO <sub>2</sub> , BISO-coated ThC <sub>2</sub>	Determine particle breakage

their weight during burning. Both blocks exhibit dents on the outside where the baffles were located. Since there was a gap between the burner wall and the plate on which the block was set, a small amount of gas always flowed around the block, burning it from the outside even if the gap was sealed with asbestos (see the block on the right in Fig. A.5). The block in the middle shows more burning on the outside. The surface is rougher, and the block has assumed an amorphous shape. The small gap was not sealed in this case, allowing additional gas to flow along the outside of the block. The more the block burned from the outside, the larger the gap between the baffles and the block became. When some of the holes in the ceramic plate were exposed, the amount of unused oxygen in the off-gas increased rapidly.

As a block is burned down, the surface area becomes small so that the oxygen is not completely used. The oxygen content of the off-gas increases when more than two-thirds of the block is burned. Nearly 100% of the feed oxygen was found in the off-gas when the last few percent of a block was burned. Decreasing the oxygen flow as the surface area decreased was not effective. Because of the lower flow velocity, the diffusion of the oxygen to the surface of the block slowed down; thus, nothing was gained.

When the surface area had decreased to the point that utilization of oxygen was not complete, the heat production decreased due to diminished combustion. Then the cooling air flow could be reduced and eventually turned off. The block slowly cooled down when more heat was removed by the combustion gas than was produced by the burning process. In order to burn a block completely, the gas flow must be sufficiently high to ensure fast diffusion of the oxygen to the graphite surface; however, it must not be so high that the block is cooled excessively by the gas.

We burned one of the one-sixth block segments completely with pure oxygen (WBB-9). The  $O_2$  flow rate in this experiment was 61.5 std liters/min, which is equivalent to a gas velocity (at standard conditions) of 0.02 m/sec in the empty burner. In a second run, a block was burned with a gas mixture of 113 std liters/min  $O_2$  and 80 std liters/min  $CO_2$ , which is equivalent to a gas velocity (for standard conditions) of 0.06 m/sec

in the empty burner. Although higher temperatures ( $> 1200^{\circ}\text{C}$ ) were reached during this run, as compared with a maximum of  $1050^{\circ}\text{C}$  in the previous run, the higher gas throughput caused the block to cool faster and 3.4% of the original block remained unburned.

Three runs were made with blocks filled with extruded fuel rods which contained TRISO-coated fertile particles. Five runs were made with blocks filled with 2-in.-long fuel sticks containing different kinds of coated particles (for particle breakage results, see Sect. A.4.4). Neither the rods nor the sticks created any problems during the burn. Their graphite matrix burned at practically the same rate as the block graphite. A few of the sticks dropped out of the block during the runs. Some fell on the bottom flange while others dropped in the off-gas line, but none caused a plug in the system. Nevertheless, future designs should have arrangements to handle unburned or partially burned fuel sticks.

The highest temperature indicated for the graphite in the burning zone was between  $1050$  and  $1350^{\circ}\text{C}$  in most runs. The temperatures were kept below  $1400^{\circ}\text{C}$ , which is the maximum the fuel blocks are expected to experience during HTGR operation. We did not want to put an additional thermal stress on the fuel during burning because the blocks may contain TRISO-coated particles, which must be kept intact.

In the temperature range  $1050$ - $1350^{\circ}\text{C}$ , the chemical reaction rate is so fast that the burning is diffusion-controlled. The diffusion coefficient increases with temperature, but the main influence is the flow rate. Provided that the flow rate is sufficiently high to ensure a fast diffusion of the oxygen (see Sect. A.4.5), all oxygen introduced was used. Since a future whole-block burner would have to be designed for a high throughput, we normally aimed for a high burning rate and the temperature in the burning zone was between  $1250$  and  $1350^{\circ}\text{C}$  in most cases. Therefore, a temperature dependence of the burning rate was not studied. A dependence of the burning rate on pressure was not observed for the range 0 to 20 psig.

For most of the runs, the burner was insulated with a fiberglass blanket. The highest carbon burning rate achieved with this insulation

was 122 g/min for one-sixth of a block (run WBB-25). The combustion gas consisted of 70%  $O_2$  and 30%  $CO_2$ . The maximum wall temperature was  $925^\circ C$  with maximum cooling air flow.

For several runs the burner was without insulation, so that more of the heat was removed by radiation of the burner walls. The highest carbon burning rate achieved in this case was 136 g/min (run WBB-33). The combustion gas consisted of undiluted  $O_2$ . The maximum wall temperature was  $950^\circ C$  at the maximum cooling air flow.

In each run the combustion gas flow and the cooling air flow were the maximum throughputs possible for the off-gas and cooling air systems. The limitation for the burning rate is the capacity to remove the reaction heat--not the chemical reaction rate, which is an order of magnitude higher than the rate we have reached. Thus, these are the possibilities for increasing the burning rates:

- (1) Increase the  $CO_2/O_2$  ratio of the feed gas, so that more heat is removed from the system by the off-gas without a further load on the cooling air system.
- (2) Enlarge the cooling air system. The cooling medium must be a gas since water is prohibited because of criticality limitations. It will probably not be feasible to leave the burner uninsulated in a hot cell, as this would add too much heat to the cell atmosphere.
- (3) Allow CO rather than  $CO_2$  to form in the combustion of the graphite. The reaction heat for the formation of CO is 27 kcal/mole, whereas that for the formation of  $CO_2$  is 94 kcal/mole.

According to theory, only CO should be produced by the burning process in the temperature range where the burning takes place; however, since the CO is probably oxidized in the gas phase, the off-gas consists mainly of  $CO_2$ . If the combustion gas flow is increased due to a higher dilution with  $CO_2$ , a greater gas velocity in the coolant holes will result, removing more of the CO before it is oxidized. The CO could be oxidized to  $CO_2$  in catalytic beds behind the burner, so that the bulk of the reaction heat is released outside the burner.

The burning rate of a whole block, based on the carbon burning rates of 122 g/min and 136 g/min, respectively, for a one-sixth segment may be estimated in two ways:

- (1) Assume that the burning rate for a whole block will be six times that for a one-sixth segment. This gives carbon burning rates of 732 g/min and 816 g/min, respectively, for a whole block. The rates per square foot of burner cross section (assuming a burner diameter of 17 in.) per hour would be 27.9 kg C and 31.1 kg C.
- (2) Since the method of dividing a whole fuel block into six pieces involves cutting through three rows of coolant holes, a one-sixth segment has only 13 intact holes. Assuming that all the burning takes place in the coolant holes, extrapolation from a one-sixth segment to a whole block would yield carbon burning rates of 38.6 kg/ft<sup>2</sup>. hr and 43 kg/ft<sup>2</sup>. hr for a 17-in.-diam burner.

The actual rate will probably lie somewhere between these values and will be determined, as mentioned before, by the capability for removing the reaction heat.

Figure A.9 shows the graphite after several hours of burning. The rough texture is the result of the graphite fabrication method; fine and coarse particles are mixed, bonded with coal tar pitch, and graphitized. During burning, the binder is oxidized faster than the particles. This leaves the particles exposed, thereby giving the surface a rough and pitted look.

#### A.4.3 Heat removal and temperature control

The whole-block burner used for these experiments has shortcomings which limit both the correlation of experimental data and the analyses by theoretical approaches. Also, the asymmetry of the one-sixth segment creates problems and uncertainties for heat-transfer calculations. In

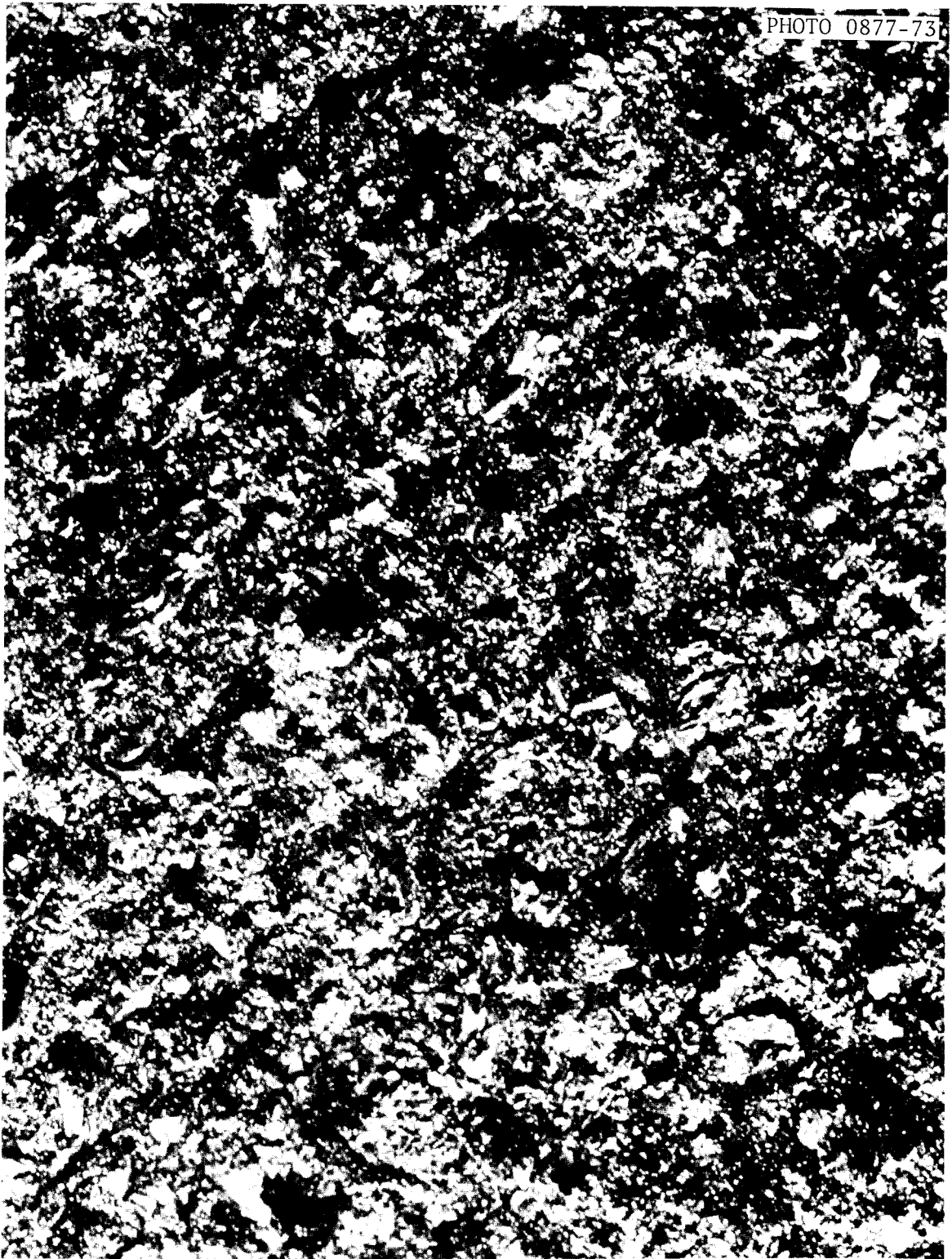


Fig. A.9. Graphite surface after 4 hr of burning. Magnification, 10X.

addition, the temperatures of greatest importance were inadequately measured; this is particularly true for graphite temperatures, since all measured values would be lower than the true maximum graphite temperature and the magnitude of the difference is uncertain. The controlling mechanism of heat transfer is radiation; therefore, it is controlled by the configuration of the system (radiation geometry) and the hot body (graphite) temperature, with the coolant flow rates and temperatures in the reactor walls contributing only small effects.

Results from two experimental runs. The most detailed analyses of experimental results for heat transfer and mass balances were those for a series of runs made as a MIT Practice School study.<sup>18</sup> The description and discussion of the results obtained in this study are reported here, with some changes. Two runs were made in an attempt to experimentally characterize the burning rate and heat transfer. In the first run, 100 std liters per minute (SLM) of pure  $O_2$  was fed to the burner to support combustion. In the second run, 110 SLM of  $O_2$  was fed to the burner, with various amounts (30 to 60%) of  $CO_2$  being added to the feed as a diluent to reduce combustion temperature. During each run, ~1200 SLM of cooling air was flowing in the cooling annulus. Temperature profiles and off-gas composition, which are the only measurable quantities, are presented.

The sample temperature profile presented in Fig. A.10 shows the temperature distribution in the graphite block, walls, and outside the insulation. At the time these readings were made, the temperature of the outer wall was higher than that of the inner wall. This was caused by the gross asymmetry of the burning zone which, in fact, results from the original shape of the block and the subsequent unequal burning (see Fig. A.5). As a result, at some fixed axial position, it is possible for heat to be removed from the burner in one direction by the spiral air flow and then returned into the burner on another side. This hypothesis could not be tested because only one side of the burner has thermocouples on both the internal and external walls. Since the thermocouples touching the inner wall are being cooled by the annular air stream, the inner wall temperatures were measured incorrectly.

ORNL DWG 74-10101

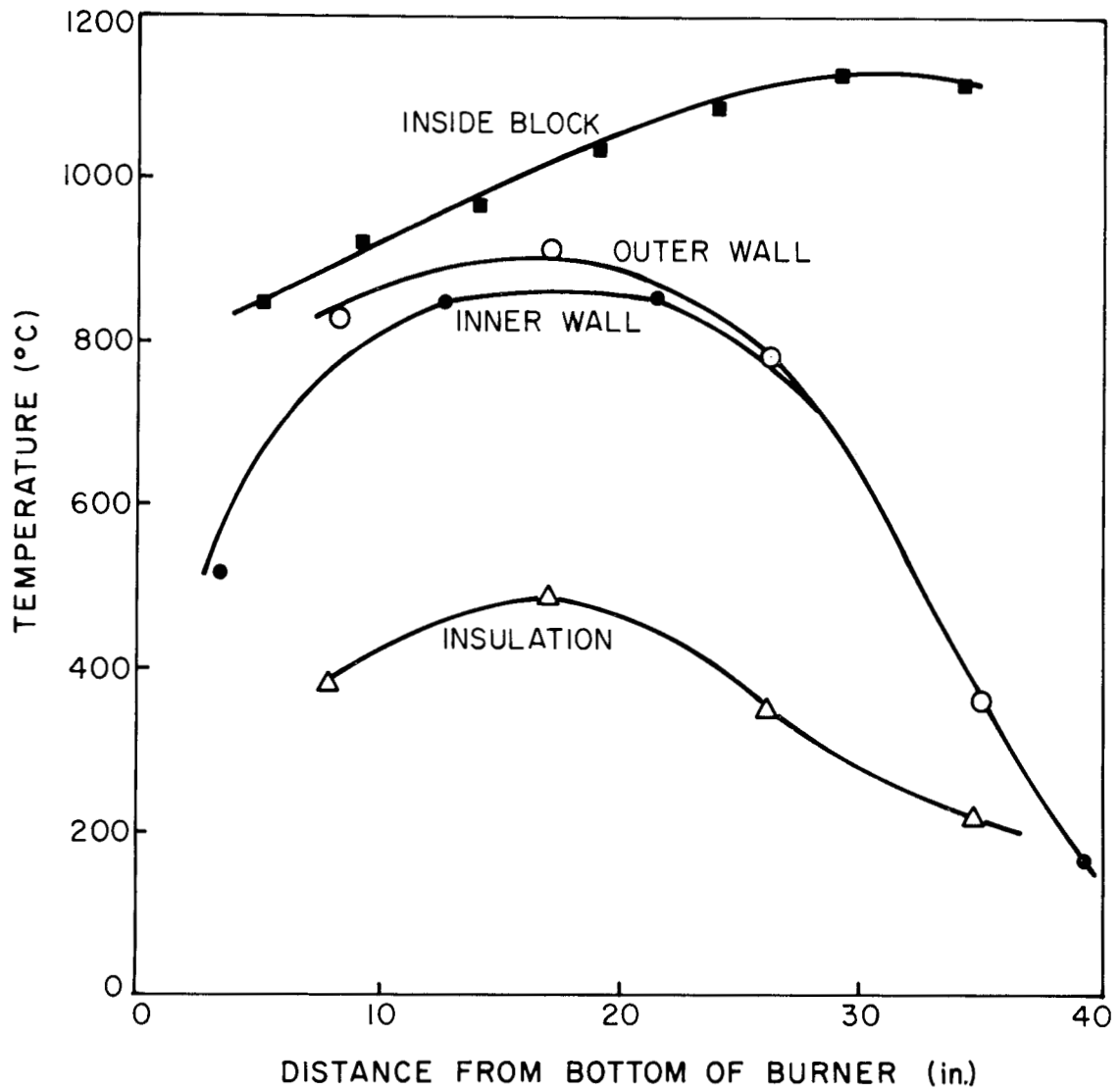


Fig. A.10. Temperature profile after 0.5 hr of burning (Run C).

The existing theory on graphite combustion (see Sect. A.2) predicts that, at a burning temperature of 1100°C, the major off-gas product would be CO. Figure A.11 shows that the CO<sub>2</sub> concentration did not fall below 85%. The flow rate in the combustion tube is laminar, with a Reynolds number of about 500. A possible explanation is that the oxidation of graphite to CO is O<sub>2</sub> mass-transfer-controlled through the boundary layer and slow as compared with the gas-phase oxidation of CO.

In these experiments, the tube-shape nature of the holes slowly gives way to an amorphous structure (see Fig. A.8). With the resulting large increase in surface area, the surface reaction to produce CO is enhanced and an increase in CO concentration is observed toward the end of the run. Also, by this time, the burning zone is closer to the burner bottom where off-gas temperatures are quickly lowered by heat transfer through flanges, thus quenching the oxidation of CO. Therefore, the increase in the CO and O<sub>2</sub> contents of the off-gas during a 2- to 3.5-hr run is due to an increased surface area and is further enhanced during the last hour or so by rapid thermal quenching of the off-gases as they leave the burner. Channeling of the gas stream would also affect the off-gas composition.

These results indicate that the existing block geometry is inadequate for determining the nature of the burning zone, and consequently the actual off-gas compositions for a uniform burning zone. Calculation of the carbon burning rate based on off-gas composition showed values of 50 g/min for Run 1 and 59 g/min for Run 2. (In other runs, burning rates three times as great as this were achieved, but no attempt was made to attain maximum rates.)

Table A.7 shows a carbon mass balance for each run at various times based on equating the mass lost from the block during burning with the net carbon in the off-gas stream. Initial poor results led to an investigation of the flow-meter calibrations; the table shows results for improved calibrations. It is believed that, with accurately calibrated flowmeters, the mass balance closes to within an acceptable error limit.

The overall heat balance on the burner is presented in Table A.8. The cooling air is responsible for removing approximately 70% of the heat generated in the burner. In addition, radiation is responsible for

ORNL DWG 74-10102

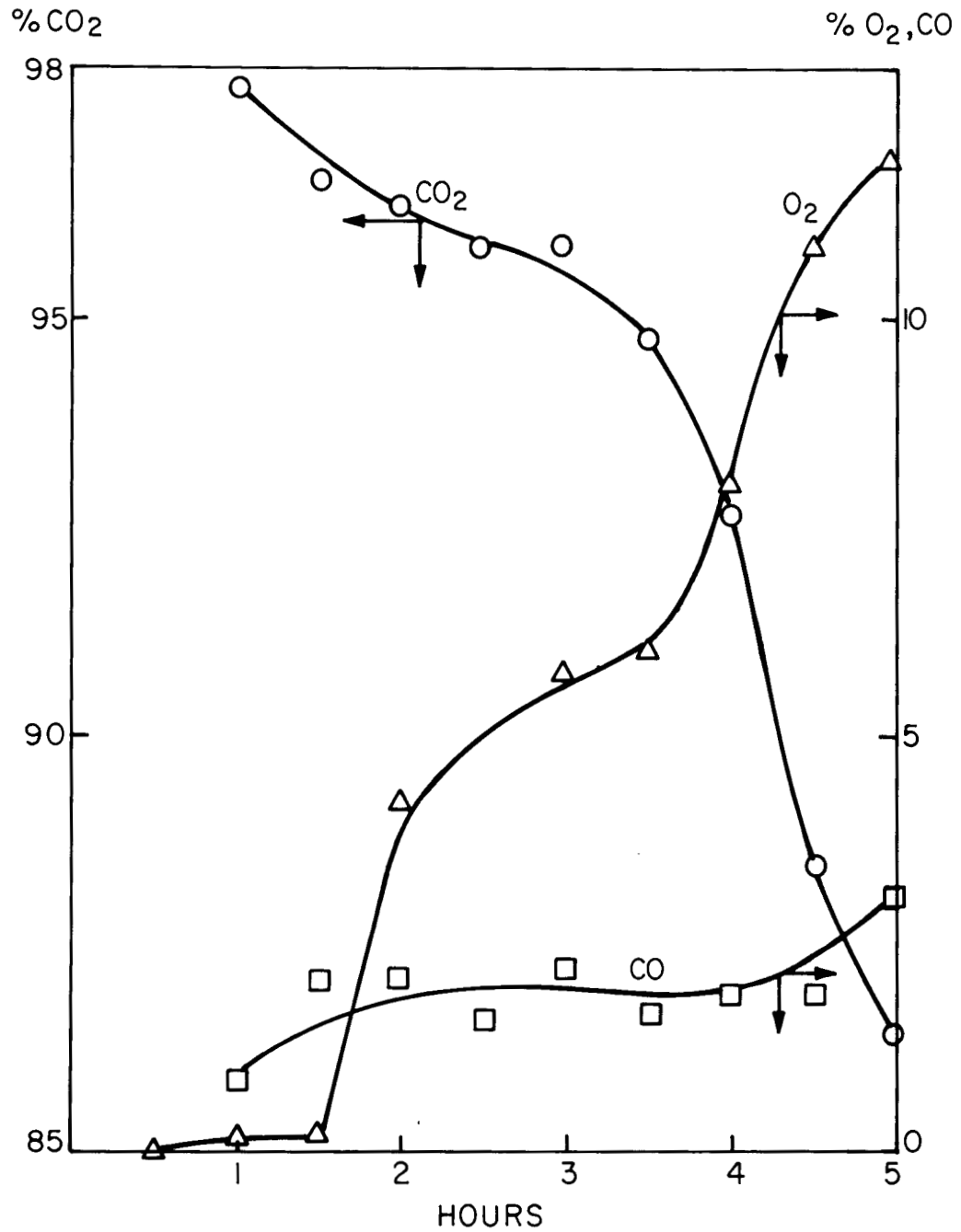


Fig. A.11. Variations in off-gas composition with time.

Table A.7. Mass Balance on Carbon

## Conditions:

Run 1: Pure O<sub>2</sub> feed at 100 SLM.  
Cooling air at 1200 SLM.

Run 2: O<sub>2</sub> (65/50%) feed at 110 SLM flow rate; kept constant.  
CO<sub>2</sub> (35/50%) feed at appropriate flow rate.  
Cooling air at 1200 SLM.  
CO<sub>2</sub>/O<sub>2</sub> feed composition was varied at prespecified times.

Time (min)		Quantity of Carbon (g)	
		Run 1	Run 2
120	In	5,346 ± 3	6,780 ± 180
	Out	4,820 ± 440	6,298 ± 575
195	In		13,433 ± 345
	Out		12,420 ± 1130
255	In		16,243 ± 345
	Out		14,902 ± 1370
300	In	13,367 ± 6	
	Out	11,535 ± 1060	

Table A.8. Overall Heat Balance for the Experimental WBB  
 Prototype Fixed-Bed Combustion

$$[q_1 + q_2 - q_3 = q_4 + q_5 + q_6 + q_7]$$

Description	Heat Balance (kcal/min) in Run 1 <sup>a</sup> After Burning Time of:		Heat Balance (kcal/min) in Run 2 After Burning Time of:	
	2 hr	5 hr	2 hr <sup>b</sup>	3.25 hr <sup>c</sup>
Enthalpy inlet gas ( $q_1$ )	~0	~0	~0	~0
Heat internally generated via chemical reaction ( $q_2$ )	290	269.4	342.2	304.2
Internal depletion ( $-q_3$ ) <sup>d</sup>	<u>43.0</u>	<u>~43.0<sup>e</sup></u>	<u>43.0</u>	<u>~43.0<sup>e</sup></u>
$q_1 + q_2 - q_3$	333.3	312.4	385.2	347.2
<hr/>				
Heat transferred to cooling air ( $q_4$ )	276.9	281.9	290.3	288.2
Heat transferred to off-gas ( $q_5$ )	17.0	18.6	36.4	52.7
Heat transferred to insulation:				
Conduction through insulation ( $q_6'$ ) <sup>f</sup>	34.0	31.7	38.0	29.4
Convection and radiation from surface ( $q_6'' + q_6'''$ ) <sup>g</sup>	(68.1)	(31.1)	(36.4)	(23.8)
Heat transferred through flanges:				
Convection ( $q_7'$ )	0.9	0.8	1.0	0.9
Radiation ( $q_7''$ )	<u>7.0</u>	<u>6.8</u>	<u>8.9</u>	<u>9.2</u>
$q_4 + q_5 + q_6' + q_7' + q_7''$	335.8	339.8	374.6	380.4

<sup>a</sup>Feed, pure O<sub>2</sub>.

<sup>b</sup>Feed, 35% CO<sub>2</sub>/65% O<sub>2</sub>.

<sup>c</sup>Feed, 50% CO<sub>2</sub>/50% O<sub>2</sub>.

<sup>d</sup>Sensible heat of graphite.

<sup>e</sup>Approximated from values at 2 hr.

<sup>f</sup>Heat transferred to insulation approximated by conduction through insulation,  $q_6'$ , only.

<sup>g</sup>Heat transferred to insulation approximated by convection/radiation from outside surface,  $q_6'' + q_6'''$ , not used in the calculation for total heat transferred.

transferring heat from the burner to the atmosphere and surroundings. By varying the  $\text{CO}_2$  concentration of the feed gas of Run 2 from 35% to 50%, there was a subsequent increase in heat removal by off-gas by about 45%. This implies that adding a diluent to the feed stream would be an effective way to control the surface burning temperature.

Summary of heat transfer results and mass transfer calculations. As part of the MIT Practice School study, 16 simultaneous equations were suggested from models for reaction rates and heat transfer.<sup>18</sup> Even this approach required a number of simplifying assumptions, including a cylindrical graphite shell, negligible effects from pore diffusion, no radial temperature profile, and reaction rate constants which are known and are independent of catalysis or other uncorrelated variations. The conclusion was that a computer program could be prepared to make calculations but that the models would have to be confirmed by comparing results with experimental data.<sup>18</sup>

Calculations were made to give values of heat transfer coefficients for comparison with the heat fluxes and temperatures observed experimentally.<sup>19</sup> The following were conditions and heat balances for a selected run:

Feed gas: 140 SLM of  $\text{O}_2$  and 80 SLM of  $\text{CO}_2$

Heat removal: 60% to cooling air; 17% in burner exit gases;  
23% losses to surroundings

The calculated results included:

- (1) Burner gas Reynolds number, 639
- (2) Cooling air Reynolds number, 16,400
- (3) Burner gas heat-transfer coefficients, 0.4 to 1.2 Btu/hr-ft<sup>2</sup>-°F
- (4) Cooling air heat-transfer coefficients, 70 Btu/hr-ft<sup>2</sup>-°F
- (5) Reactor-wall-to-surroundings heat transfer coefficient;  
1.8 Btu/hr-ft<sup>2</sup>-°F
- (6) Total reaction heat, 141,000 Btu/hr.

These results show that the principal mechanism for removal of heat from the block must be radiation. As a result of the complex radiation and mass transfer configuration, the uncertainties in the calculations of

radiation are larger than the contributions of convection and conduction (for heat transfer from the block to the burner wall). Therefore, the initially planned calculations were not completed.

Calculations were also made for a highly simplified model in which the heat is either radiated from the graphite to the burner walls or is removed as sensible heat in the burner gas. These calculations are described briefly in Sect. A.6. The results are:

- (1) Mass transfer calculations for pure  $O_2$  indicate carbon burning rates of 40 g/min, which is in reasonable agreement with the experimentally observed rates for the one-sixth-scale block burner.
- (2) The calculated graphite temperature for the maximum experimental burning rates is 2210°K, or 1940°C. Therefore, high graphite temperatures appear almost certain if an entire block is burned with pure  $O_2$  at the rate of 1 kg of carbon per minute.
- (3) The steady-state graphite temperature decreases as the  $O_2$  is diluted with  $CO_2$  and becomes too low (< 1100°C) to allow continued burning for some  $O_2$  concentration between 33 and 25%.

The selection of assumptions for these calculations was influenced by the experimental results; hence the calculations are partly empirical. The surface area for burning was for coolant channels tapered over a 6- to 10-in. length.

#### A.4.4 Particle breakage

Fuel blocks containing fuel sticks made by extruding a mixture of graphite binder and TRISO-coated  $ThC_2$  particles were used in three runs. The temperatures in these runs ranged between 1000°C and 1200°C. The burning released the particles from the fuel stick matrix and destroyed most of the outer carbon coating. The extent of breakage of the SiC coatings was determined by leaching tests; overall particle breakage was 5%.\*

---

\*These particles were reject particles obtained from GAC. The particles had been leached before fabrication, but the fraction of breakage during fabrication was not known.

Five runs were made with blocks filled with three types of fuel particles. In the two last runs, WBB-32 and -33 (see Table A.9), the goal was to reach temperatures higher than 1400°C to see whether temperatures in this range increase particle breakage. It was formerly thought necessary to keep the burning temperature for TRISO-coated particles below the maximum particle temperature in the reactor. However, earlier studies with unirradiated particles<sup>20</sup> and recent experiments with irradiated particles<sup>21</sup> indicate that "popping" does not occur below 2000°C. Temperatures in this burner are limited since the burner walls have to be kept below 950°C and are not protected by a temperature-resistant liner (such as ceramic).

For run WBB-33, one W-Re thermocouple in an Al<sub>2</sub>O<sub>3</sub> thermowell was introduced into the burner from the top flange. Because there was no space to install several thermocouples of this type, no temperature profile of the block during the burn could be recorded. This W-Re thermocouple extended 6 in. into the block and read 1460°C as the highest temperature while the burning zone was passing it. The internal temperature for run WBB-32 can only be estimated because several thermocouples failed. It is believed that the graphite temperature in this run was comparable to that in run WBB-33. The maximum temperature indicated in runs WBB-31 and WBB-21 was 1300°C; in run WBB-12 it was 1200°C.

After each run the particles were removed from the burner and cyclone vessel and, except in one case (WBB-33), were combined. A sample of about 100 g was then taken, and a screen analysis was made. The +20 mesh fraction, which contains no fuel but consists of pieces of graphite and iron oxide flakes from the baffles and the pan, was discarded; the -20 mesh fraction was burned for 7 hr or more in a furnace in an oxygen-containing atmosphere to remove graphite dust and the remainder of the outer coating of the TRISO particles and the two carbon coatings of the BISO particles.

After the burning step the sample was leached for 4 hr in boiling 2 M HNO<sub>3</sub>. Samples containing only TRISO particles were also leached subsequently in boiling acid Thorex dissolver solution for 7 hr. The mixed oxide and the ThC<sub>2</sub> (the ThC<sub>2</sub> is converted to ThO<sub>2</sub> during the burn) dissolved very slowly and were leached up to 21 hr.

Table A.9. Leaching results from the five runs with fueled blocks

Table A.9. Leaching results from the five runs with fueled blocks

Run No. (WBB-)	Leach solution	Wt. loss of sample (g)	Solution volume (ml)	Concentration (mg/ml)			Weight (g)				Percent Recovered	Percent of sample lost to leach	
				Th	U	Fe	ThO <sub>2</sub>	UO <sub>2</sub>	Fe <sub>2</sub> O <sub>3</sub>	Total		Th	U
12	HNO <sub>3</sub>	1.0329	525	0.75	0.064	a	0.448	0.0384	a	0.4865	47.10	0.63	0.37
	Thorex	72.9687	510	115.6	0.065	a	67.087	0.0378	a	67.1248	91.99	86.10	0.34
21	HNO <sub>3</sub>	0.4909	320	0.59	0.46	0.013	0.2148	0.1669	0.0059	0.3876	78.96	0.35	0.79
	Thorex	82.2151	480	106.3	37.0	0.028	58.0600	20.1469	0.0192	78.2261	95.15	94.17	95.71
31	HNO <sub>3</sub>	0.4040	285	0.061	0.75	0.028	0.0197	0.2424	0.0195	0.2816	69.71	0.052	2.35
	Thorex	1.6793	500	2.05	0.045	0.427	1.1662	0.0255	0.3052	1.4969	89.14	3.05	0.25
32	HNO <sub>3</sub>	0.3962	280	0.022	0.63	0.028	0.0070	0.2000	0.0112	0.2182	55.07	0.017	0.297
	Thorex	1.2432	475	1.72	0.087	0.403	0.9296	0.0468	0.2736	1.2500	100.55	2.27	0.39
33 (burner)	HNO <sub>3</sub>	1.0046	330	0.106	1.43	0.134	0.0398	0.5352	0.0631	0.6381	63.52	0.053	7.18
	Thorex	65.0722	860	58.28	0.13	1.14	57.0269	0.1267	1.4016	58.5552	89.98	76.69	1.70
33 (cyclone)	HNO <sub>3</sub>	0.6372	300	0.125	0.79	0.091	0.0426	0.2688	0.0390	0.3504	54.99	0.070	4.42
	Thorex	57.6856	865	56.19	0.046	0.126	55.3021	0.0450	0.1557	55.5028	96.22	91.09	0.74

<sup>a</sup>Not determined.

After each leach, the insoluble residue was rinsed with distilled water, dried, and weighed. The wash and leach solutions were combined, and a sample of each solution was then analyzed for thorium and uranium. Since the iron (from iron oxide flakes from the baffles and the pan) in several samples disturbed the analytical procedure, it was separated and the amount determined (see Table A.9).

Leaching results for run WBB-12 are not directly comparable to those for the other runs. The sample was leached only 1 hr in  $\text{HNO}_3$  and 2 hr in acid Thorex solution. Later studies showed that only about 90 to 95% of the leachable heavy metals will dissolve in such a short time.

Table A.9 contains the leaching results obtained from the five runs with fueled blocks. It gives the weight loss of each sample to the leach solution and the fraction of this loss that was recovered. The last two columns show the thorium and uranium losses as related to the thorium and uranium in the original sample (not the weight loss of the sample during leaching).

The particles collected from the burner and the cyclone in run WBB-33 were kept separate instead of being combined as in the other runs. The leaching data show nearly twice as much particle breakage for the sample from the burner as for that from the cyclone. The reason for this difference is supposedly that the particles in the burner were confined in a hot zone ( $\sim 800\text{-}1000^\circ\text{C}$ ) for several hours during which the thorium reacted with the silicon of the TRISO particles to form a low-melting compound. The particles in the cyclone, on the other hand, were at ambient temperature where no such reaction could take place.

Table A.10 shows that the recoveries of thorium, uranium, and iron for the  $\text{HNO}_3$  leaches are lower than those for the Thorex leaches. The reason for this is twofold:

- (1) The concentration of heavy metals in the nitric acid leachates is low as compared with the Thorex leachates. The analytical methods are less exact at the low concentrations.
- (2) The nitric acid leach precedes the Thorex leach; therefore, the impurities are dissolved in the nitric acid. Analyses

Table A.10. Percent recoveries of thorium, uranium, and iron from HNO<sub>3</sub> and acid Thorex solutions as a function of concentration

Average recovery for HNO<sub>3</sub>: 61.56%

Average recovery for Thorex: 93.84%

Run No. (WBB-)	Leach solution	Weight loss (g)	Concentration in solution (mg/ml)			Percent recovery
			Th	U	Fe	
12	HNO <sub>3</sub>	1.0239	0.75	0.064	a	47.10
21	HNO <sub>3</sub>	0.4909	0.59	0.46	0.013	78.96
31	HNO <sub>3</sub>	0.4040	0.061	0.75	0.028	69.71
32	HNO <sub>3</sub>	0.3962	0.022	0.63	0.028	55.07
33 (cyclone)	HNO <sub>3</sub>	0.6372	0.125	0.79	0.091	54.99
33 (burner)	HNO <sub>3</sub>	1.0046	0.106	1.43	0.134	63.52
12	Thorex	72.9687	115.6	0.065	a	91.99
21	Thorex	82.2151	106.3	37.0	0.028	95.15
31	Thorex	1.6793	2.05	0.045	0.427	89.14
32	Thorex	1.2432	1.72	0.087	0.403	100.55
33 (burner)	Thorex	65.0722	58.28	0.13	1.14	89.98
33 (cyclone)	Thorex	57.6856	56.19	0.046	0.126	96.22

<sup>a</sup>Not determined.

were made for only thorium, uranium, and iron; thus other constituents may have dissolved also, but are not accounted for.

#### A.4.5 Off-gas composition

The off-gas from the burner consists of CO, CO<sub>2</sub>, and O<sub>2</sub>. The oxygen consumption was 99% during steady-state burning. When the block had been burned from the outside so that the gap between the baffles and the block had increased, the oxygen content in the off-gas started increasing, usually after two-thirds of the block had been burned. At gas velocities of less than 1 m/sec in the coolant holes, the burning rate was low, the oxygen was not consumed, and the off-gas contained considerable O<sub>2</sub> (up to 20%). The burning rate at high temperatures depends on the O<sub>2</sub> diffusion rate, and the low flow rates result in a thick film and a low O<sub>2</sub> diffusion rate. The gas flow in a coolant hole is laminar without radial mixing from convection.

We assume that both the main stream and the boundary layers are laminar at very low flow rates. If the gas velocity is higher than 1 m/sec, the boundary layer becomes turbulent even though the main stream is still laminar. One would expect an even higher burning rate when the main stream also becomes turbulent. Due to the limited flow capacities of our burner system, turbulent flow of the main stream could not be attained.

Both CO and CO<sub>2</sub> are formed in the combustion of carbon--the former in the presence of excess carbon, the latter in an excess of oxygen. Since the experimental burner operates with an excess of graphite, the off-gas should contain practically no CO<sub>2</sub>. Experimentally, we find that there is no CO in the off-gas until the indicated temperatures reach 1200°C. The results are in reasonable agreement with those reported for burning of early graphite-uranium fuels.<sup>5</sup> For temperatures between 1300 and 1400°C, the CO concentration ranges from 15 to 25%. We assume that, at the low flow rates used for the experiments, the CO is partially oxidized in the gas phase before leaving the burner. This assumption has not been verified because the gas flow capacity of the burner used in our studies is limited. The flow was laminar in each run with a

Reynolds number below 1500. When we removed the first block support pan [see Fig. A.8(b)] and installed the cone-shaped pan in the bottom of the burner,  $O_2$  and CO were sometimes present in the off-gas at the same time in considerable amounts (up to 43% CO and 21%  $O_2$ ). It is assumed that the layers of unused oxygen and the CO from the reaction are not mixed since the cone-shaped pan is favorable for laminar flow. The first pan had no holes except those through which the thermocouples (1/8 in. diam) extended into the block. Therefore, the gas was thoroughly mixed while passing through these holes and the CO and  $O_2$  reacted, leaving only  $CO_2$  and the excess  $O_2$  or CO in the exit stream to the analyzers.

#### A.4.6 Formation of graphite fines

The amount of graphite dust that is carried with the off-gas stream to the filters generally increases with increased combustion feed gas flow (Table A.11). Variations with the  $CO_2$  content of the feed were small and inconsistent. The highest value of 1.7% dust was for run WBB-26, where dilution of the  $O_2$  with  $CO_2$  was high and the block cooled slowly so that no steady-state burning occurred. Consequently, the off-gas temperature was several hundred degrees lower than normal and the dust, which was usually burned in the hot gas stream before leaving the burner, reached the filter in this run.

Table A.11. Unburned graphite dust

Run (WBB-)	Time (min)	Feed Gas		Dust in cyclone (% of weight loss of block)
		Average gas flow rate (SLM)	$CO_2$ content in gas (%)	
23	268	170	19	0.23
24 } 25 }	350	216	43	0.42
26	180	211	65	1.71
27	207	176	28	0.26
28	112	193	0	0.5
29	294	100	0	0.18
30	240	155	22	0.35

Table A.12 shows the size distribution of the dust for several runs in which graphite blocks without fuel were burned. A dependence of the size distribution on temperature or flow rate could not be established. Practically all of the graphite dust was found in the filter-cyclone vessel. The packed fiberglass filter contained only negligible amounts of graphite at the point where the inlet gas impinged directly onto the fiberglass bed.

### A.5 Whole-Block Burner Calculations

Some detailed calculations of significance to discussions in the body of the report are briefly presented here.

#### A.5.1 Burning rates and temperatures for radiation-controlled heat transfer\*

The one-sixth-scale burner experiments were made with high  $O_2$  concentrations in the feed gas and with well-cooled metal burner walls. For these conditions, the burning rate is controlled by mass transfer of  $O_2$  through the gas boundary layer. The graphite temperature is controlled by the radiation of heat to the cooled metal walls; however, the heat capacity of the burner gas is also significant. The maximum burning rate occurs for the maximum (that is, inlet)  $O_2$  concentration, although the graphite temperatures may be higher inside the block where the coolant channel walls have a small view factor for radiation.

In these experiments with high feed  $O_2$  concentrations, the coolant holes developed a tapered shape which commonly indicated high rates of burning over 6- to 10-in. lengths. The total surface area,  $A$ , involved in burning is then on the order of  $2000 \text{ cm}^2$ . The heat to be transferred to the burner walls,  $Q$ , can be estimated from:

$$Q = 94,030A \frac{D \Delta C}{\Delta x} - (C_p \Delta t), \quad (\text{A.5-1})$$

---

\*Unpublished calculations by P. A. Haas, ORNL, 1973.

Table A.12. Sieve analyses of dust found in cyclone for several runs with unfueled graphite

Sieve mesh	Amount of dust (wt %) in Run No.:					
	WBB-24 + WBB-25	WBB-26	WBB-27	WBB-28	WBB-29	WBB-30
+35	25.7	16.2	6.5	7.8	35.0	25.6
-35 +40	7.2	6.3	2.2	1.4	9.3	10.6
-40 +45	7.2	5.4	3.5	1.7	10.5	8.6
-45 +50	5.8	3.9	2.5	1.4	7.6	5.4
-50 +80	14.8	11.4	8.9	3.7	13.5	11.3
-80 +100	6.1	6.1	5.5	2.1	3.8	4.4
-100	33.1	50.6	70.9	81.8	20.2	34.0

where

$D$  is a diffusion coefficient for  $O_2$ - $CO_2$ ,  
 $\Delta C$  is a concentration gradient for  $O_2$ ,  
 $\Delta x$  is an equivalent thickness of boundary layers,  
 $C_p$  is heat capacity,  
 $\Delta t$  is temperature change.

The  $(C_p \Delta t)$  term allows for the removal of heat as sensible heat of the burner gas, and  $C_p$  is approximately 13 cal/g-mole for  $CO_2$ . For a Schmidt number of 0.94 for  $O_2$ - $CO_2$ ,

$$D = \frac{\mu}{0.94p} = \frac{\mu V}{0.94M}, \quad (A.5-2)$$

where

$\mu$  is gas viscosity,  
 $V$  is molal volume,  
 $M$  is molecular weight.

An average value of  $\Delta C$  for a feed mole fraction  $O_2$  of  $y_0$  might be  $y_0/2V$ . For pure  $O_2$ ,  $AD \Delta C/\Delta x$  then gives a calculated carbon burning rate of 40 g/min, which is a reasonable check of the experimentally observed burning rates. The increased turbulence at the entrance end from natural convection probably gives thinner boundary layers and higher rates than those calculated. Also, the reaction of  $CO_2$  with graphite becomes important at temperatures above 1200°C and can make important contributions to the burning. The maximum carbon burning rates that have been experimentally observed, 120 to 140 g/min, would be equivalent to 0.06 or 0.07 g/min·cm<sup>2</sup>. The value of  $Q/A$  from these maximum burning rates would be 28,000 cal/cm<sup>2</sup>·hr for pure  $O_2$  feed.

Transfer of heat to the burner walls by radiation can be used to calculate a graphite temperature from

$$Q = F_{\sigma} (T_c^4 - T_{wall}^4)A, \quad (A.5-3)$$

where

$T_c$  is the graphite temperature,  
 $\sigma$  is the Stefan-Boltzmann constant.

The view factor,  $F$ , would average less than the value of 0.5 for a hemisphere; hence a value of 0.25 will be used for calculations. While the leading edges of the graphite will have a higher  $F$ , they are also exposed to the highest  $O_2$  concentration and receive radiation from hotter graphite along the coolant channel. The exact wall temperature,  $T_{\text{wall}}$ , has little effect since the term  $T_{\text{wall}}^4$  is small compared with  $T_c^4$ ; therefore, a value of  $723^\circ\text{C}$  or  $1000^\circ\text{K}$  will be assumed. The calculated value of  $T_c$  is then  $2210^\circ\text{K}$ , or  $1940^\circ\text{C}$ . At one-third this maximum rate of burning [or the rate calculated from Eq. (A.5-1)], the calculated values of  $T_c$  are still  $1675^\circ\text{K}$ , or  $1400^\circ\text{C}$ . The view factor becomes small down the coolant channels toward the interior of the block, and higher temperatures are likely. From these calculations, excessive graphite temperatures appear almost certain for pure  $O_2$  at the desired burning rates. Calculations using the thermal conductivity of graphite show that axial conduction in the graphite contributes little to heat removal.

The same type of heat balance can be used to estimate the allowable dilution of the feed  $O_2$  with  $CO_2$ . For a specified  $O_2$  flow rate and carbon burning rate, the addition of  $CO_2$  to the feed gas provides additional cooling [the  $C_p \Delta t$  term in Eq. (A.5-1)] and changes both the  $\Delta C$  and  $\Delta x$  values for mass transfer of  $O_2$ . The minimum graphite temperatures for practical steady-state burning rates are higher than  $1100^\circ\text{C}$ , or about  $1400^\circ\text{K}$ . Using these values in Eq. (A.5-3) gives a  $Q/A$  of  $3500 \text{ cal/cm}^2\text{-hr}$ . Substitution in Eq. (A.5-1) indicates that  $1/3 O_2$ - $2/3 CO_2$  would give the required value of  $Q/A$  (that is,  $T_c > 1100^\circ\text{C}$  and steady-state burning would continue), while  $1/4 O_2$ - $3/4 CO_2$  would give  $T_c < 1100^\circ\text{C}$  (and the block would cool down and stop burning). This conclusion is dependent on the assumptions made, but the assumptions are consistent with the observed temperature for higher  $O_2$  concentrations.

#### A.6 Recommendations

The whole-block burner that was used for the experiments described in this report has several shortcomings which prevented us from investigating some of the problems:

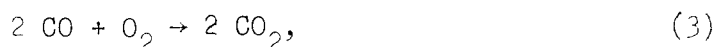
- (1) The off-gas system is too small to attain turbulent flow in the coolant holes of the block. Either a larger gas system or fewer coolant holes would eliminate this limitation.
- (2) The asymmetry of the test block creates problems and uncertainties for the heat transfer calculations.
- (3) The method for measuring the graphite and gas temperatures needs to be improved. A larger quartz window for an optical pyrometer should be installed in the top flange so that the surface temperature of the graphite in the burning zone can be measured. Thermocouples should be inserted horizontally into the graphite block to measure the temperature distribution in the block. In the present configuration, all internal thermocouples are located in the coolant holes where they may or may not be touching the block. There are an insufficient number of thermocouples on the burner walls. Thermocouples should be placed on both the inner and outer walls in each quadrant and should not be spaced more than 5 in. apart.
- (4) Heat removal appears to be the controlling factor for operating the burner at high burning rates. It will be more important when a whole block instead of one-sixth segment is burned, because the segment has a much higher surface area/volume ratio and thus more heat can be transferred from its surfaces.

There are four means of increasing the heat removal:

- (a) increasing the cooling air flow,
- (b) saturating the cooling air with water,
- (c) increasing the dilution of the combustion feed gas, and
- (d) preventing the secondary reaction of the CO with O<sub>2</sub> to form CO<sub>2</sub> and oxidizing the CO to CO<sub>2</sub> outside the burner in a catalyst bed. At high flow rates it may be possible

to remove the CO from the hot zone before it has time to react. A higher burning rate would be possible if the problem of heat removal were solved. The reaction rates given in the literature are at least an order of magnitude higher for a given temperature than those we achieved. An adiabatic flow reactor concept has now been proposed which includes recycle of cooled gas to provide temperature control and heat removal.<sup>3</sup>

- (5) It is necessary to find out where (in or behind the block) and at what rates the following four reactions occur:



and



According to equilibrium considerations, only CO should be present in the off-gas in the temperature range in which the burner is operated. It appears that the CO is oxidized in a secondary reaction away from the surface of the block. A reaction of the CO<sub>2</sub> with the graphite beneath the burning zone is also feasible. Checking on these reactions would require an internal probe, preferably in a block with only one hole.

- (6) The off-gas line must be sized and arranged so that pieces of graphite and partially burned fuel sticks cannot block the outlet. Also, there is some indication of bridge building by the graphite; however, it has not been possible to establish to what extent it occurs because these bridges always collapse by the time the bottom flange is removed.

- (7) If a CO-O<sub>2</sub> torch is used as a heat source, the design of the system must be improved. The arc rods burn away, the ceramic insulators break, and it is impossible to relight the torch while the furnace is warm.
- (8) In the event that the experimental burner is used to obtain additional preliminary data, at least three things should be done: (a) round or hexagonal pieces of graphite should be used as test blocks, (b) two more vertical rows of thermocouples should be welded to the outer burner wall, and (c) since the cooling coils on the top flange are never used, a bigger quartz window should be mounted in the top flange and a continuously reading pyrometer should be installed.

Many of the problems could be investigated in a proposed small burner (miniburner), where a round piece of graphite with one center hole would be burned. This burner would have a movable probe for gas sampling along the length of the block. A pyrometer would read the temperature of the block surface. The block could be heated by induction to a uniform temperature, or the bottom and top halves of the block could be heated separately.

The main points to investigate with the miniburner would be:

- (1) occurrence of the four oxidation reactions, depending on flow characteristics, feed gas dilution, temperature, and catalysts (H<sub>2</sub>O);
- (2) distribution of the reaction heat, conduction in the block, transfer through the walls, removal with the off-gas, and heating of the lower part of the block by the off-gas;
- (3) determination of the length of the burning zone, depending on flow rate, feed gas composition, and temperature;
- (4) optimization of the start-up procedure;
- (5) determination of the amount of unburned graphite dust carried out with the off-gas, depending on flow rate and feed gas composition;
- (6) heat removal studies, which could be performed initially with a ceramic tube around the block in the miniburner (since a commercial burner would probably contain a ceramic liner to protect the steel wall); and
- (7) maximum burning rates at high gas velocities.

The data from the miniburner and the modeling program will allow the concept of a whole-block burner to be detailed and revised, if necessary. A full-scale burner should then be built to evaluate this concept.

One proposed concept for a whole-block burner calls for a burner in which several blocks are placed behind each other and which contains a ceramic liner to protect the burner wall. A burner should be capable of burning a whole block under conditions similar to the proposed concept and thus permit the data from the miniburner and the modeling program to be checked.

•

•

•

•

•

•

APPENDIX B: A SUMMARY OF TECHNICAL CONSIDERATIONS FOR  
THE WHOLE-BLOCK AND FLUIDIZED-BED BURNERS

In order to determine hot-cell space requirements and relative equipment complexity, it is necessary to describe each of the two primary burner concepts explicitly. The concepts are specified in terms of six major considerations as follows:

- (1) Burner feed preparation
- (2) Feeding the burners
- (3) Burning the graphite
- (4) Heat removal
- (5) Burner product withdrawal
- (6) Off-gas handling

B.1 Burner Feed Preparation

This is a consideration for fluidized-bed burning only; whole-block burning has no counterpart. The feed required for fluidized-bed burning is presently specified to consist of particles that are less than  $3/16$  in. Thus, the spent HTGR fuel element must be reduced from a solid with a bulk volume of about  $3 \text{ ft}^3$  to particles of less than  $2 \times 10^{-6} \text{ ft}^3$ .

The system presently being used to accomplish this size reduction consists of three crushers, referred to as the primary, secondary, and tertiary crushers. Figure 10 is a schematic of the crusher system. Jaw crushers that have an included angle of about  $20^\circ$  are being evaluated at GAC for use as the primary and secondary crushers. These units are handling unirradiated fuel elements satisfactorily. At least one manufacturer of jaw crushers, Gruendler\*, has recommended an included angle of about  $10^\circ$ . At present, it is not known whether irradiation alters the physical properties of the graphite sufficiently to require an included angle less than  $20^\circ$ . However, for the purposes of this evaluation, it is assumed that the  $20^\circ$  included angle is satisfactory. If a smaller value of the

---

\*Gruendler Crusher & Pulverizer Co., St. Louis, Mo.

angle is required, it will increase the height of the primary crusher system as presently conceived.

The theoretical throughput of the primary crusher is about two orders of magnitude greater than that required for a 1.5-MTHM/day\* fuel reprocessing plant. Whether the jaw crushers are allowed to run continuously and are fed at short time intervals or whether they are stopped and started several times per day has not been considered for this study. Also, the bearings, lubrication, gas sealing, dust-handling, inventory, and holdup are considered only in that estimated hot-cell space is allotted for these requirements. Some of these are expected to require significant developmental testing.

The tertiary crusher shown in Fig. 10 is a centerroll type. Double-roll crushers are being evaluated at GAC for suitability as the tertiary crusher. However, the centerroll crusher was used for layout purposes in this study at the suggestion of GAC. The arrangement shown implies that no feeders or hoppers are located between the three crushers. Since the throughputs of the crushers are in the order primary  $\geq$  secondary  $\geq$  tertiary, bridging is a distinct possibility. Thus, provisions for removing the crusher system must be allowed. In addition, other maintenance requirements dictate that the design include provisions for removing the crushing system.

For the purposes of this study, it is assumed that both maintenance and bridge breaking (very stable bridging) would be accomplished by removing the crusher system from the crushing cell into a decontamination and maintenance area. If feeders and/or hoppers are required between the various crushers, the cell volume required to contain the crushing equipment will be larger than that considered here.

The last piece of equipment required for the feed preparation is some type of classifier to return the oversize,  $> 3/16$ -in., particles to the tertiary crusher. A pneumatic separator was chosen for this study (see Fig. 10). A mechanical screen would be expected to require

---

\*A reprocessing plant sized for about 50,000 MW(e) of installed HTGR electrical capacity.

frequent (relative) maintenance and is thus not shown; also, it would probably occupy more cell area than a pneumatic separator.

Another aspect of feed preparation involves transfer of the  $< 3/16$ -in. material to the FBBs. The method selected consists of pneumatic transfer to a primary hopper loading station where the batch of crushed blocks is loaded into the appropriate number of primary hoppers. An inventory is made by weighing each of the loaded primary hoppers. The loaded and tared primary hoppers are moved mechanically to the proper burner location and positioned for feeding into the FBB. After being emptied, these primary hoppers are weighed and either sent to a storage area or returned to the primary hopper loading station. Two crushing trains and two primary hopper loading stations are assumed (recommended by GAC) for a 1.5-MTHM/day HTGR reprocessing plant. The need for two crushing trains is based on reliability, not on throughput.

An alternative method for transferring the  $< 3/16$ -in. material to the primary hoppers was considered but not utilized. This method consisted of pneumatically transferring the crushed material to the appropriate primary hopper which was in a fixed location. Consideration of the following aspects of this method led to its discard:

- (1) The piping and valving of such a system in a manner suitable to ensure that the material was being transferred from the crushing system to the selected primary hopper was complex, usually requiring double valving and a testing procedure to guarantee that the valves were positioned properly. (Note: the number of primary hoppers is assumed to be ~40 in a reprocessing plant of this size.)
- (2) Accountability in such a system appeared to be difficult; the simplest method consisted of weighing the loaded primary hoppers. (This is the method adopted for accountability in the method chosen.)
- (3) The simplest arrangement of the primary hoppers was a circular plan consisting of at least two primary hopper islands. However, this appeared to lead to an inefficient usage of cell space when considered in conjunction with the arrangement

of the other items (e.g., burners, crushers, dissolvers, etc.). A linear arrangement of the primary hoppers, although allowing more efficient usage of the cell areas when considered in conjunction with the arrangement of other items, required a more complex piping and valving system. Part of this complexity is due to the requirement that both crusher systems be able to supply each primary hopper.

The method selected for operating the feed preparation equipment is envisioned as follows (see Fig. B.1 for a schematic representation). A single fuel element at a time is fed into the primary crusher through a gas lock (see Fig. B.2), and is allowed to pass through the secondary and tertiary crushers and the pneumatic separator before another fuel element is fed into the primary crusher. The crushed product,  $< 3/16$  in., is pneumatically conveyed continuously to the primary burner hoppers. This procedure is repeated until the entire daily batch of fuel elements to be crushed is completed.

The primary burner hoppers are weighed and moved to the appropriate burner and positioned for feeding the FBB. If a discrepancy between the weight of the batch fed into the primary crusher and the weight collected in the primary burner hoppers is detected, an inventory of the crushing system must be made. Such an inventory could entail tasks ranging from simply checking the equipment, by inspection through ports, to removing the crushing system to another cell and dismantling for inspection.

The average batch for crushing is considered to be 24 fuel elements--one day's feed for a FBB. The number of primary burner hoppers required per batch could vary from two to six. Four primary burner hoppers, with six crushed fuel elements per hopper, are assumed for this study.

Each of the two crushing systems required for a 1.5-MTHM/day HTGR fuel reprocessing plant would occupy a cell volume 8 x 24 x 40 ft high. The total cell volume required for the feed preparation system is found by adding the volume needed for these two crushing systems to that associated with the primary burner hoppers and their storage and moving cell volumes.

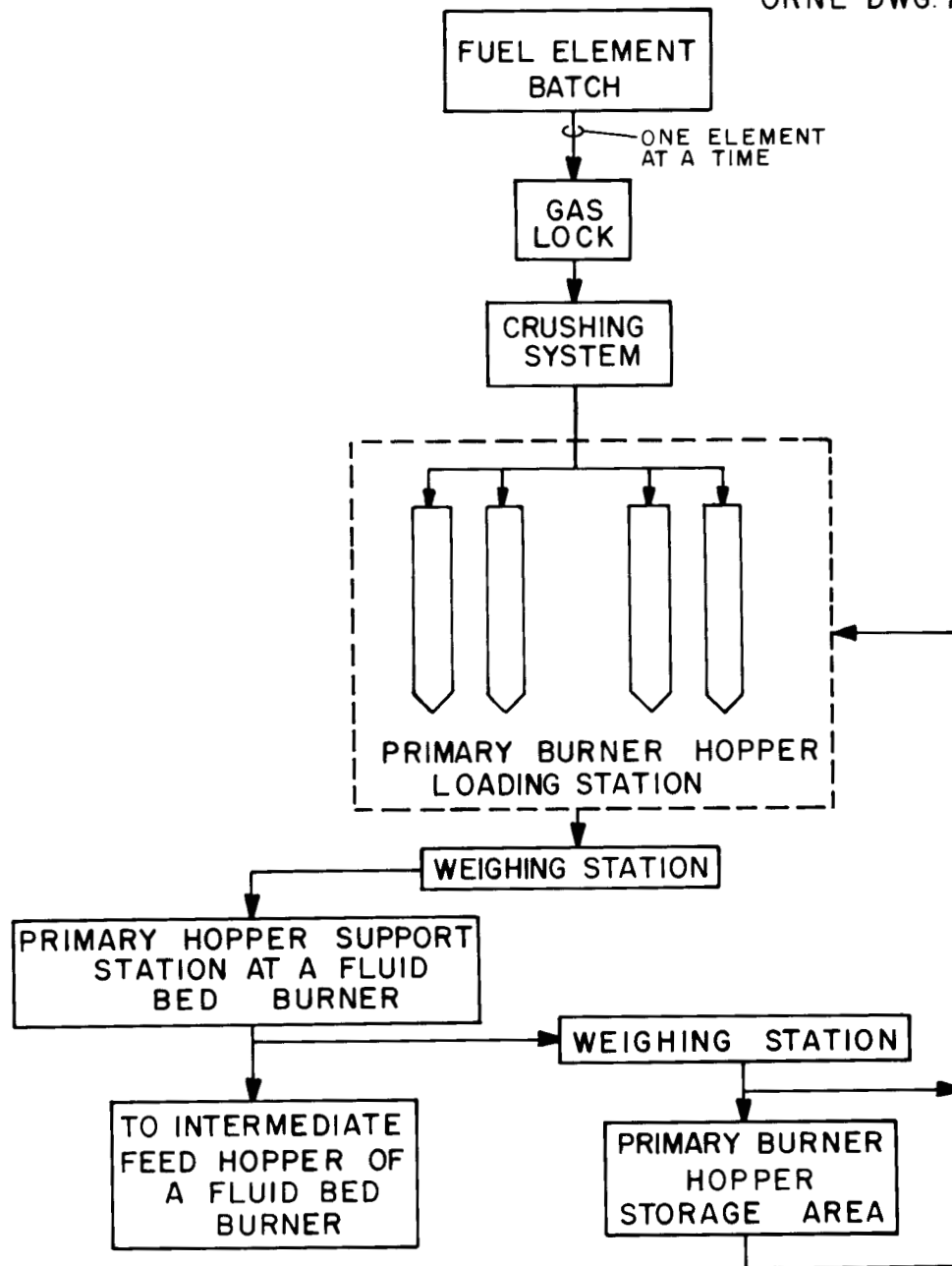


Fig. B.1. Schematic representation of the feed preparation equipment.

ORNL DWG. 73-11880RI

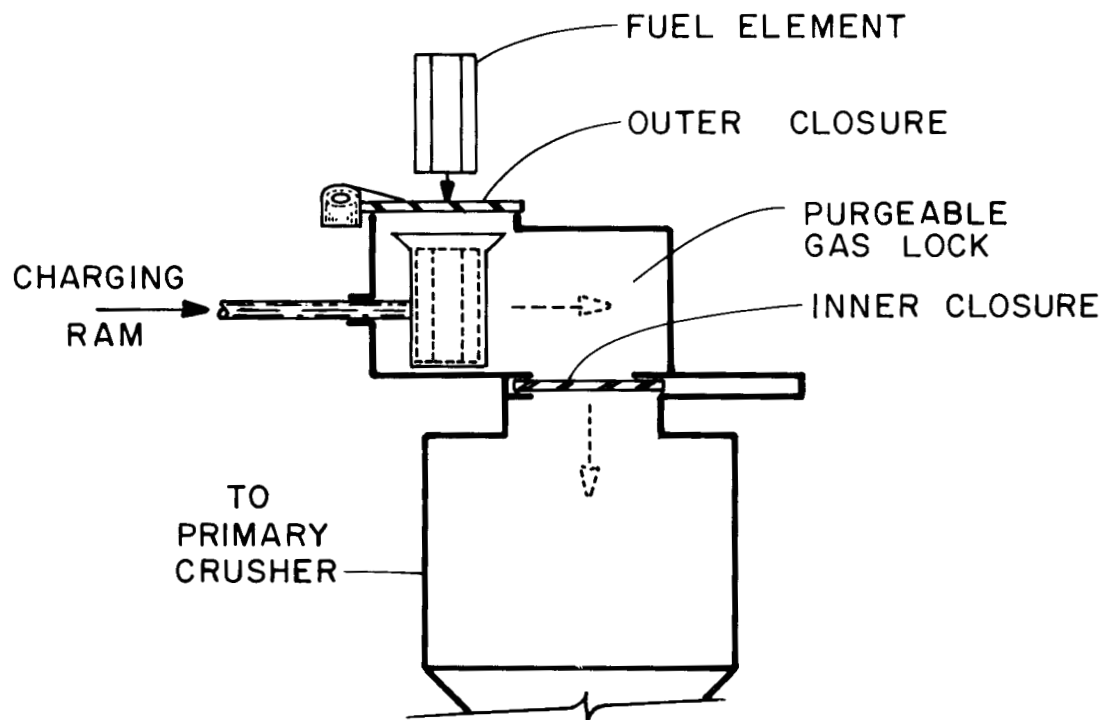


Fig. B.2. Schematic representation of the crusher charging system.

The use of one crushing system per FBB was considered as an alternative to the primary hopper moving system but was abandoned because it would be too expensive.

## B.2 Feeding the Burners

Whole-block burner feeding. One spent fuel element at a time is loaded into the WBB by being passed through a gas lock consisting of two closures. The inner closure, which is normally open, is closed during fuel element loading, while the outer closure, which is normally closed, is opened during this operation. This technique is commonly used for continuously operated reduction furnaces. A schematic representation of the charging system is shown on Fig. 5. The effect of heat on this mechanism is considered in Sect. B.4.

During normal operation, the column of fuel elements is advanced at the rate of about 1/3 in./min either mechanically or by gravity, depending on the orientation of the burner. HTGR fuel elements have not been fed continuously in any WBB tests made to date. In one test of whole-block burning at ORNL, a fuel element was partially burned using gravity feed (see Sect. B.3). Several HTGR fuel element segments (i.e., one-sixth of a fuel element) have been burned in a stationary configuration. This was accomplished by placing the fuel element on a support plate and burning downward as discussed in Appendix A. Determination of the optimum feed direction--vertical, horizontal, or somewhere between--for a WBB must await further developmental studies. In this study, horizontal feeding was selected to maximize the cell area required for the WBB. This represents the least favorable case for whole-block burning as related to cell area.

Fluidized-bed burner feeding. Crushed fuel, < 3/16 in., is fed from the primary burner hoppers into the FBB at the average rate of one spent element per hour. Both pneumatic transfer and augering, with top or bottom feeding, have been studied for this purpose (see Figs. B.3 and B.4). Continuous feeding of the FBB and bottom feeding of the FBB have been judged to be impractical by GAC personnel, who recommended that a batch feeding procedure (i.e., feeding a batch into the FBB, burning, dumping, and

ORNL DWG 73-11877

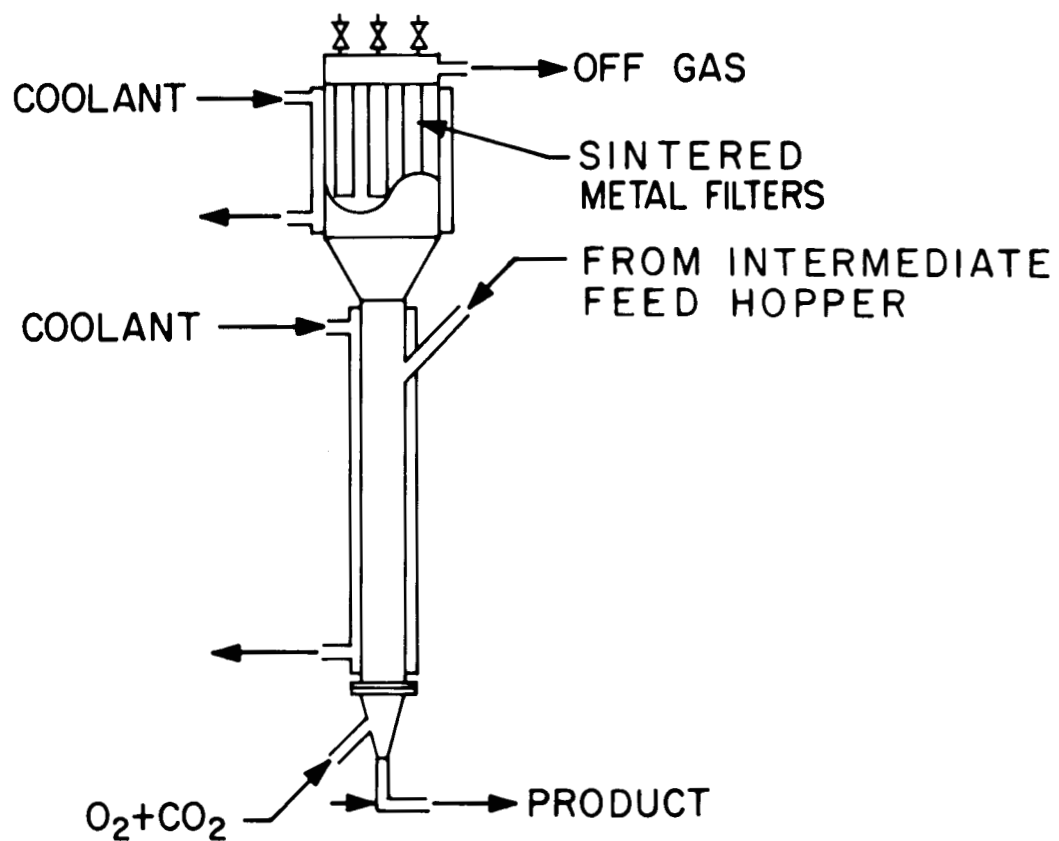


Fig. B.3. Fluidized-bed burner with top feeding.

ORNL DWG 73-11876

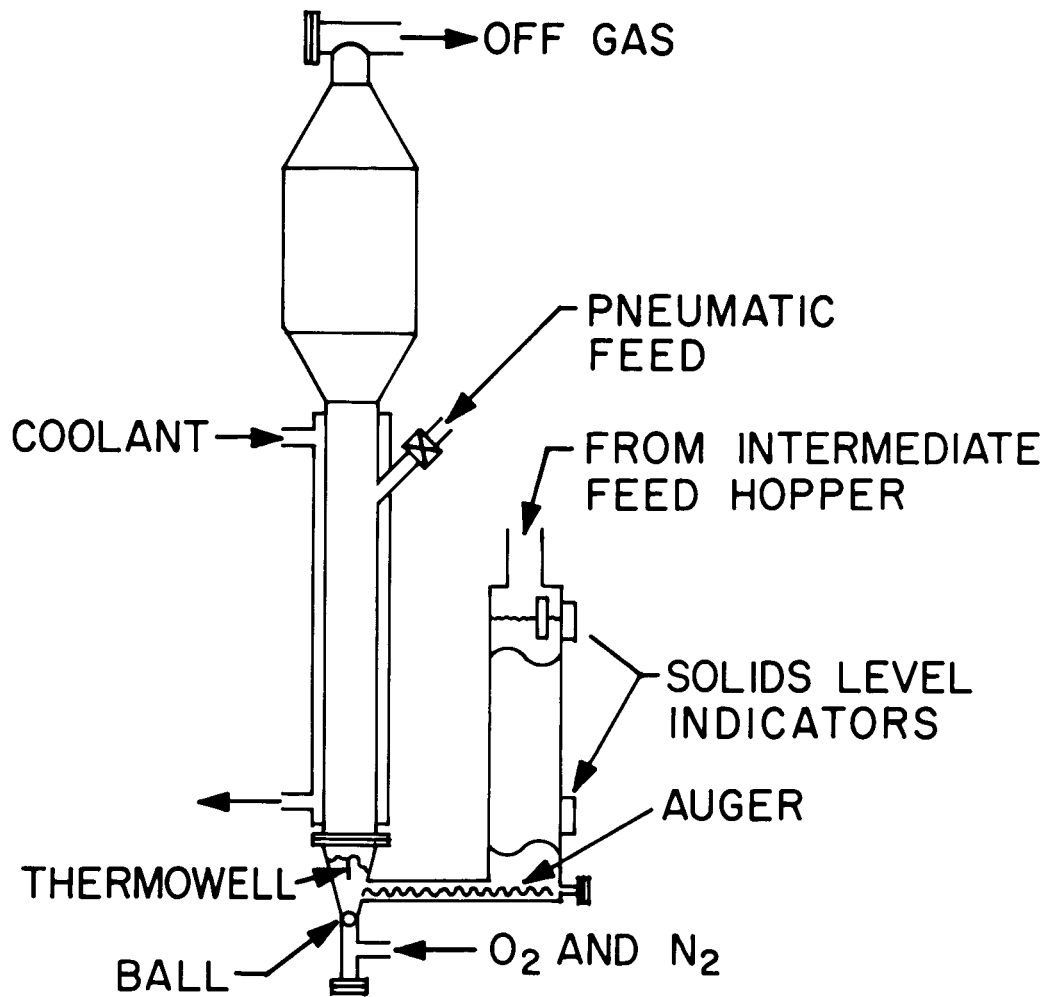


Fig. B.4. Fluidized-bed burner with pneumatic feeding at the top and auger feeding at the bottom.

refeeding) be considered for this study. An alternative method utilizing incremental feeding has also been considered.

Pneumatic top feeding has been selected as the reference feeding method for FBB because it reduces the amount of cell area required. (An auger would occupy additional space.) The procedure envisioned to feed a FBB is as follows: Sufficient crushed fuel to fill an intermediate feed hopper (approximately one fuel element) is transferred from the primary burner hopper into an intermediate feed hopper which feeds the FBB. The crushed fuel is incrementally transferred by pneumatic means from the intermediate feed hopper into the FBB. The number of feed increments required to empty the intermediate feed hopper may vary from 1 to about 20, depending on the mode in which the FBB is operated. This procedure is repeated until the primary burner hopper is empty, at which time the empty primary hopper is moved to the weighing station and another primary hopper is valved into service.

A procedure for following the level or weight of the bed of crushed fuel in the intermediate hopper needs to be incorporated into the design. A mechanical foot which follows the bed elevation was assumed for this study.<sup>22</sup> Such a provision is required to allow the operator to follow the flow of material into the FBB. On completion of a batch, the intermediate hopper is inventoried to ensure that it is empty.

### B.3 Burning the Graphite

Graphite burning in the whole-block burner. The WBB burns the fuel elements over one face of a column of fuel elements, with the combustion products passing, for the most part, through the coolant holes of the elements. The column of fuel elements will probably have a length equivalent to at least three fuel elements.<sup>3</sup> Thus, the combustion products will be in contact with excess graphite, not unlike the FBB. Consequently, the composition of the off-gas with regard to  $O_2$ ,  $CO_2$ , and  $CO$  should vary according to the temperature of the fuel element column. In ORNL experiments using one-sixth of an HTGR fuel element, no  $CO$  was detected in the off-gas whenever the temperature of the fuel element segment (in this case, one fuel element long) was below  $1200^\circ C$ . As the temperature of the fuel element was increased above  $1200^\circ C$ , however,  $CO$  appeared in the off-gas.

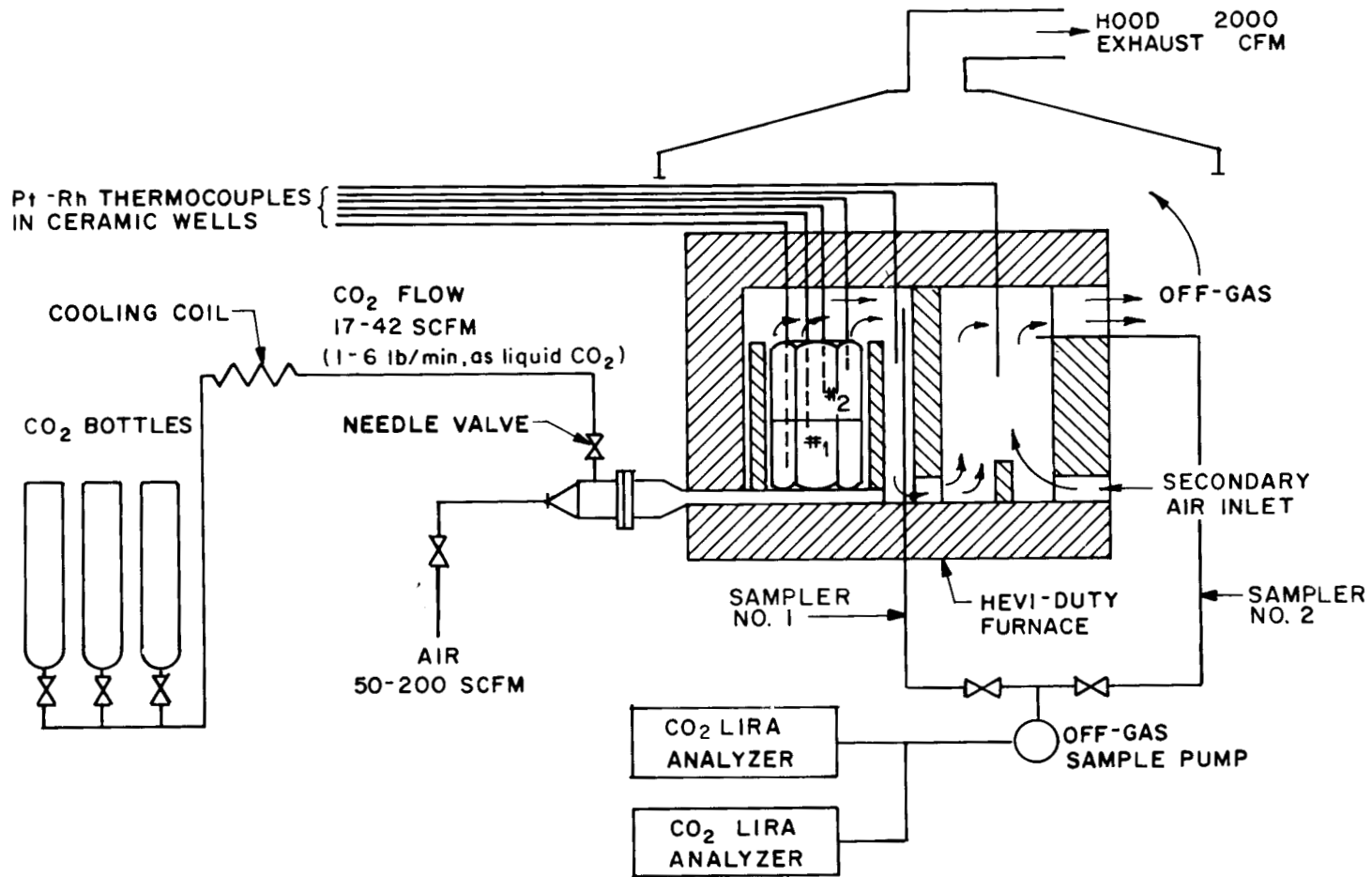
It is anticipated that the rate of burning in the WBB will be controlled by feed gas composition and flow rate, combined with the removal of combustion heat in the gas leaving the burner. This heat will then be removed in a separate heat exchanger.

The off-gas from the WBB is cooled, partially recycled, and mixed with  $O_2$  to form the burning atmosphere. For a given  $O_2$  feed rate, the quantity of off-gas recycled is adjusted to control the temperature of the burning zone. In this manner, the heat capacity of the recycled off-gas and  $O_2$  is controlled to absorb the heat liberated from the oxidation of the graphite, taking into account heat losses from the WBB. Calculations indicate that the volume of recycled off-gas required may be as much as seven times the volume of  $O_2$ .<sup>3</sup> This total flow for a burning rate of 16 spent fuel elements per day would yield a Reynolds number of about 30,000 (gas at STP) through the coolant holes. The high velocity of the gas through the coolant holes would carry any free fuel particles along with the off-gas stream. Thus, the fuel particles would exit at the fuel element charging end of the WBB. This problem is considered in Sect. B.5. For the purpose of this study, it is assumed that the burning rate per unit cross section for the WBB is comparable to that of the FBB, namely, 30 to 40  $kg\ hr^{-1}\ ft^{-2}$ .

Ignition of the WBB is achieved with a  $CO-O_2$  torch which impinges on the face of the fuel column to be burned. The fuel column is heated to the desired temperature, at which time the  $CO$  flow is reduced and the  $O_2$  flow is increased in order to achieve ignition. The exact procedure to be used for increasing the recycled gas flow must await developmental experiments.

In two experiments at ORNL, a whole block was burned in air in an upward direction while resting on a grate;  $CO_2$  was used as the diluent gas.<sup>23</sup> A schematic drawing of the burning system is shown in Fig. B.5.

The flow of air and  $CO_2$  was not restricted to the coolant holes by the use of baffles around the fuel block. Thus, the burning gas mixture bypassed the block to a large extent in these two experiments. The fuel block burned at a reasonably uniform rate across its entire face. The block, which had been cut into halves prior to burning, is shown on



0/11

Fig. B.5. Flow diagram for fixed-bed graphite burning test.

completion of burning in Fig. B.6. Uniformity of the burning on the face of the fuel block is shown more effectively in Fig. B.7.

Graphite burning in the fluidized-bed burner. The FBB burns the crushed fuel ( $< 3/6$  in.) in a fluidized bed where combustion occurs primarily within a small vertical height of the bed. The velocity of the gas required to maintain fluidization is on the order of 1 to 2 fps. There is a natural tendency for the fluidized bed to segregate according to particle size and density. Thus, the fuel particles tend to locate themselves near the lower portion of the fluidized bed, while the smaller particles, particularly soot, tend to locate themselves high in the upper portion of the fluidized bed. Operation of the bed in a fully fluidized condition produces considerable mixing within the bed; even so, segregation is prone to occur. Such behavior must be recognized in the design of a fluidized-bed system. The following paragraphs enumerate some of the effects of segregation and discuss their consequences.

1. Large graphite particles concentrate near the bottom of the fluidized bed where the  $O_2$  concentration is highest. In the event that these large fuel particles do not fluidize into an area of low  $O_2$  concentration, they oxidize rapidly and become very hot. In some instances, particles (or groups of particles) have burned holes in the burner walls so rapidly that a thermocouple located nearby ( $< 1/2$  in.) did not have time to respond. The criterion that all fuel particles be less than  $3/16$  in. arose from a consideration of this problem.<sup>24</sup>
2. Large fissile and fertile particles gravitate toward the bottom of the fluidized bed. The violent motion experienced within a fluidized bed leads to numerous collisions between the large, hot graphite particles and the fissile and fertile particles. Small quantities of sodium are known to promote sintering of uranium and thorium oxides. Also, silicon and thoria sinter at temperatures below that at which thoria sinters. On various occasions, workers at GAC have experienced sintering in the lower portions of the

PHOTO 94790

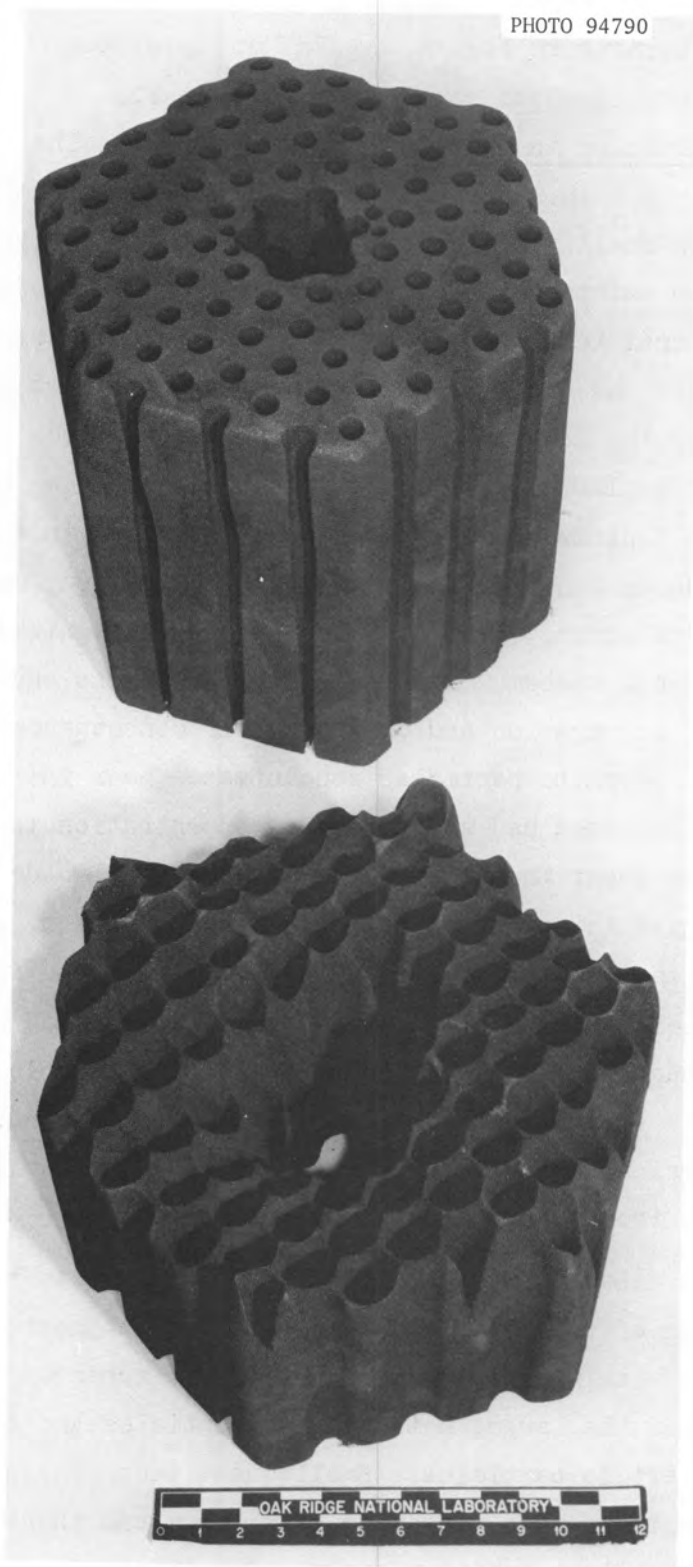


Fig. B.6. Photograph of top and bottom portions (inverted) of the element used in the test.

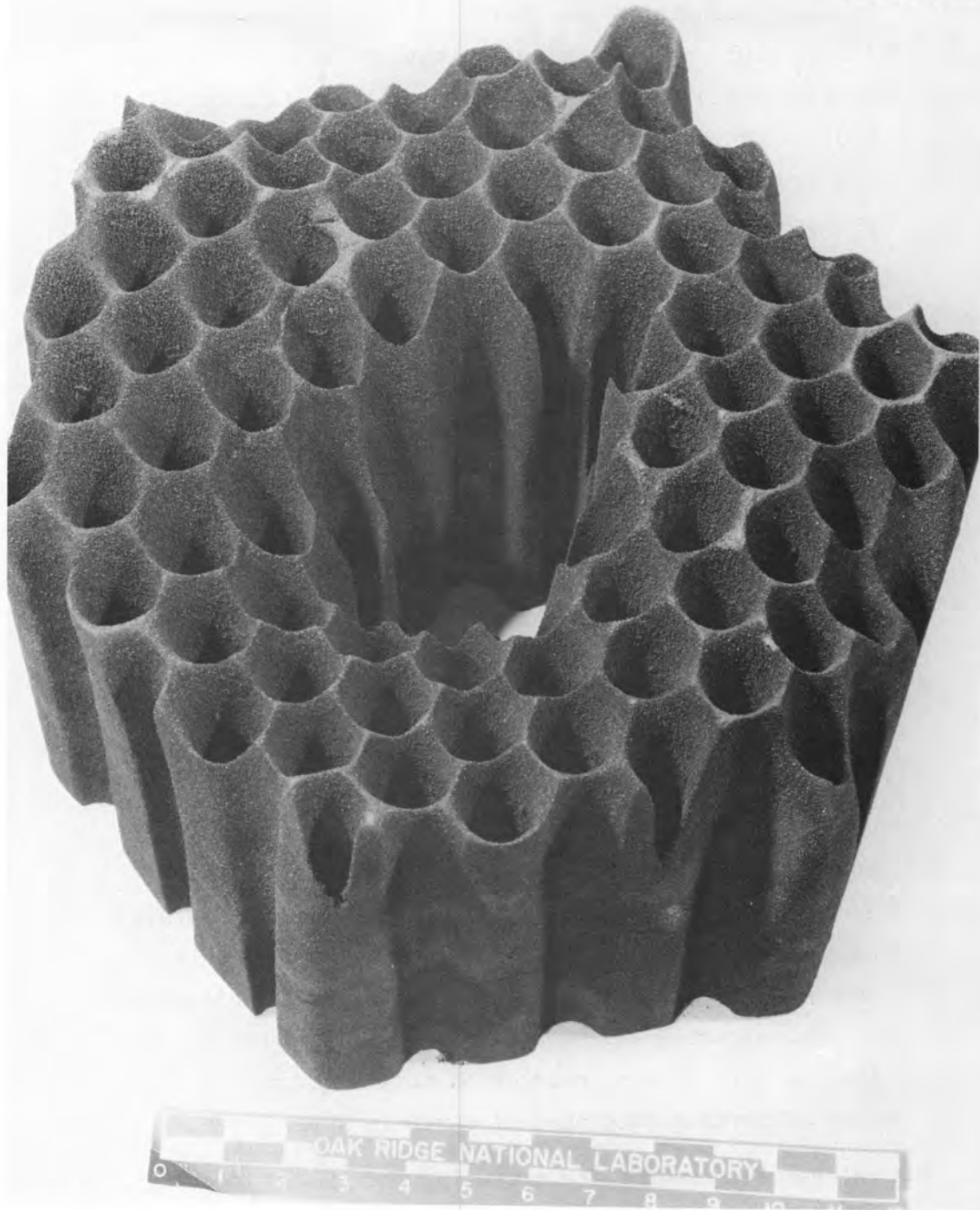


Fig. B.7. Photograph of the bottom (supporting) face of the fuel column (consisting of one block).

FBB. The consequences have varied from the formation of small nodules to the growth of stalagmites several inches high on the lower distribution plate. (The distribution plate is a requirement of large fluidized beds.) GAC has reported that the formation of these stalagmites, once initiated, appears to be self-propagating. These stalagmites usually have formed whenever the CO torch, used for start-up, was operating. However, there is evidence that on at least two occasions the stalagmite formation was initiated after the fluidized bed had been operating for some period of time.

3. The small graphite particles, or those with the largest surface area per unit weight, are found near the top of the fluidized bed where the concentration of  $O_2$  is very low. GAC has reported that about 55 to 60% of the weight of crushed material fed to the FBB appears as soot. The bulk density of this soot ranges from 0.1 to 0.25 g/cc.<sup>25</sup> In the fluidized-bed burning work performed at KFA, a feed of one particle size was used and less than 10% of the feed appeared as soot. It is not anticipated that a monoparticle diameter can be obtained from a crushed HTGR fuel element. However, results of studies on the oxidation of graphite<sup>8-10</sup> have provided evidence that soot formation is a very strong function of  $O_2$  concentration and temperature. It is suspected that the low rate of soot production at KFA was more a function of burning rate than of particle size.

The reference procedure for operating the FBB is to charge the contents of a hopper into the FBB prior to withdrawing any product. Thus, there is a limitation on the quantity of soot a FBB can contain and still remain operable.

In several instances, at both ACC and GAC, soot that had accumulated on surfaces in the top position of the FBB fell into it and, in turn, extinguished it.

#### B.4 Heat Removal

About  $3 \times 10^6$  Btu of heat is liberated for each fuel element burned to form  $\text{CO}_2$ . It has been estimated that the TRISO coatings will break at temperatures above  $2000^\circ\text{C}$ .<sup>20,21</sup> Earlier, it was stated that at temperatures above  $1200^\circ\text{C}$  the concentration of carbon monoxide increased in the off-gas from the one-sixth-scale WBB at ORNL. At temperatures below about  $800^\circ\text{C}$  the burning rate is intolerably low. Thus, it would appear that  $800$  to  $1200^\circ\text{C}$  is the optimum temperature range for a burner.

Heat removal in the whole-block burner. For a given burning rate, the fraction of heat removed by the off-gas stream in a WBB can be varied by varying the ratio of diluent gas to oxygen. When this ratio is zero, most of the heat must be removed via the WBB walls; as the ratio is increased, a proportionally large fraction of the heat is removed by the off-gas stream until, finally, all of it is removed by this means. The latter removal mode will be referred to as the adiabatic mode of heat removal.<sup>3</sup>

Heat balances made with the one-sixth-scale WBB indicated that, at a constant burning rate, the fraction of heat removed by the off-gas stream increased from 10% to 14% as the diluent gas/oxygen ratio was increased from 0.54 to 1.0. The design of the off-gas system of the one-sixth-scale WBB limited tests to ratios of less than about 1. Calculations indicate that the diluent gas/oxygen ratio will be about 7 for adiabatic mode burning.<sup>3</sup> These calculations also indicate that the off-gas temperature for a three-fuel-element column will be between  $1000$  and  $1100^\circ\text{C}$  for all ratios from 0 to about 7. The kinetics, heats of reaction, and equilibria among  $\text{O}_2$ ,  $\text{CO}$ , and  $\text{CO}_2$  adjust the exit temperature to this value.

For a WBB consuming 16 fuel elements per day, a  $\text{CO}_2$  flow rate of about 600 scfm will remove the heat with a gas temperature rise of  $900^\circ\text{C}$ . The burner off-gas stream can be used as the diluent gas. However, since this gas stream will be contaminated, one must bear a penalty either for filtration or for recirculating a contaminated gas stream. It has been assumed that filtration of the recirculated diluent gas is more costly than recirculation of the contaminated off-gas stream.

The proposed method (adiabatic) for limiting the temperature within the WBB is shown in Fig. 9. A separate gas recycle system is shown for the WBB external surface cooling. The quantity of heat removed by this circuit will be small along the burner length, yet quite large at the fuel element charging end where the metal surfaces are in direct contact with the burner off-gas stream (1000-1100°C). The ram that advances the fuel elements about 1/3 in./min will require cooling since it is in contact with the fuel element and burner off-gas. Although its detailed design is not considered in this study, the ram is an important item for design of a horizontally mounted WBB. It has been assumed that a successful design, test, and operating procedure for this ram would be accomplished during developmental research. In this comparative FBB-WBB study, sufficient hot-cell space is allowed to accommodate the required ram system.

Volatile elements will tend to plate out on the cooled metal surfaces at the fuel element charging end of the WBB. Hot-cell tests have suggested that one might expect Ce, Ru, Cs, Zr, Se, and Nb to collect on the ram as well as on the metal surfaces at the charging end of the WBB. Thus, any maintenance performed on these mechanisms must take into account high radiation levels due to the presence of these elements.

Heat removal in the fluidized-bed burner. The heat of combustion is removed from the FBB by heat transfer through the walls of the burner, by the heat capacity of the off-gas, and by the use of a heat exchanger located within the upper portion of the FBB. This latter means has been judged to be impracticable by GAC and thus will not be considered further. Hence, the heat must either be removed through the FBB walls or by the burner off-gas stream. The quantity of off-gas must be sufficient to produce fluidization of the FBB but not high enough to carry excessive material from the burner. Consequently, one has limited control over the amount of heat removed via the off-gas stream. In practice, GAC has found that about 1% of the heat is removed via the off-gas stream; the remaining heat is lost through the burner walls.

As was indicated previously, the major portion of the heat is liberated near the bottom of the fluidized bed. Thus, a fully fluidized-bed condition with heat transfer particles is required to transfer the heat

to the FBB walls and to prevent excessive temperatures. Experimentally it has been found by GAC that the burned-TRISO fissile particles or the burned-BISO\* (oxide only) fertile particles suffice as heat transfer media. If the bed contained both fissile and fertile particles consisting of carbide kernels with BISO coatings, an inert heat transfer medium would be required. However, since the Fort St. Vrain Reactor\*\* has TRISO-coated carbide kernels and the reference fuel for the large HTGRs is comprised of TRISO-coated uranium carbide kernels (for all  $^{235}\text{U}$  streams) and BISO-coated thorium oxide kernels, the use of an inert heat transfer medium is not considered as a primary requirement in this study.

GAC recommended that the FBBs to be considered in this study have a diameter of 24 in. According to their evaluation, a FBB of this size will not require additional internal heat transfer surfaces. It is felt that a 2-FBB system consisting of a primary FBB and a separate soot burner merits attention. Therefore, such a system is also evaluated in this study.

The recommendation by GAC that a burning rate of 24 fuel elements per day be considered for a single 24-in.-diam FBB was adhered to in this study. In the 2-FBB system, an 18-in.-diam FBB was used for the crushed fuel burner and a 24-in.-diam FBB was used for the soot burner. Further, it was assumed that about 40% of the graphite is burned in the crushed fuel burner and about 60% is burned in the soot burner.

Figure 17 is a schematic diagram of the 24-in.-diam FBB system showing filters, heat exchangers, and blowers. The largest gas flow rate required for this case is that associated with external cooling of the burner. While this flow rate is large, 8000 to 16,000 cfm, the gas does not require filtration. Figure 18, which is included for completeness, is a similar schematic of the 2-FBB system. (The only significant difference between these two systems is the extra FBB, which is required for the 2-FBB system.) Off-gas filters, heat exchangers, blowers, and pumps could be shared between the crushed fuel and the soot burners; however, operating flexibility may dictate separate components.

---

\*Burned-BISO particles consist of bare oxide kernels.

\*\*Platteville, Colorado.

The formation of hot spots on metal walls in a hot carbon system may lead to a type of intergranular action in which the carbon attacks the surface grains of iron-base alloys. In such instances, the grain is simply spalled off the metal surface and removed by the fast flowing gas. During certain maloperations with FBBs, holes have appeared in the burner wall with no evidence of melting. Some of these burnthroughs may have been due to metal "dusting" in a manner similar to that described above.

GAC has successfully operated FBBs for long periods of time without any evidence of such attack. Avoidance of this and other problems lies in understanding the important parameters of burning and, in turn, prevention of burner maloperation.

As in the case with WBB, some of the problems associated with burning in the FBB require additional development work. Two important areas involve the development of (1) a satisfactory ignition process, and (2) a satisfactory distributor plate to give an adequately uniform velocity distribution in the fluidized bed. While these items require further study, it is assumed that satisfactory solutions will be found.

#### B.5 Burner Product Withdrawal

Product withdrawal in the whole-block burner. Virtually nothing is known about product withdrawal problems associated with the WBB. During one run in the one-sixth-scale WBB using a fuel block that contained BISO-coated fertile and TRISO-coated fissile particles, a difference in particle breakage of about a factor of 2 was noted between particles retained in the burner promptly upon release from the graphite block. It was speculated that, in the case of the retained particles, the thoria (present as  $\text{ThC}_2$  prior to burning) reacted with the SiC coatings to form a low-melting thoria-silica compound which failed.

Behavior of the fuel particles in a WBB will depend on several factors (e.g., off-gas velocity through the coolant holes of the fuel element column and orientation of the WBB). The velocity of the off-gas through the coolant holes might vary by a factor of 10, depending on whether pure  $\text{O}_2$  or an  $\text{O}_2$ -CO mixture is used in burning. In the latter case (the

adiabatic mode), the fuel particles would tend to be entrained irrespective of WBB orientation, whereas in the former case the particles would not move if the block were burned horizontally. The velocity varies from about 4 to 40 fps (STP) for these two cases. For this study, it is assumed that fuel particles will be both discharged from the WBB by gravity at the burning end and entrained in the off-gas stream (horizontally mounted WBB).

Product withdrawal in the fluidized-bed burner. Several methods of removing fuel particles from the FBB have been studied at GAC. It is GAC's recommendation that the procedure considered for this study consist of accumulating as large a batch of fuel particles in the FBB as permissible, stopping the feeding, burning off as much carbon as possible, dumping the FBB, recharging, and igniting. If the next process step should require continuous feed, an intermediate hopper and feeder system would be needed.

In the 2-FBB system it may be possible to continuously feed all the elements of a certain type (from one HTGR) to the burner prior to discharging the product heel. This method of burning will require the development of a reliable continuous product withdrawal procedure. The minimizing of thermal cycles on the burner is a desirable goal for the development program.

#### B.6 Off-Gas Handling

Off-gas handling as defined for the purposes of this study consists of cooling and removing particulate matter from gaseous streams. In a sense, this is a pretreatment step for the removal of  $^3\text{H}$ ,  $\text{I}_2$ ,  $\text{Rn}$ , and  $^{85}\text{Kr}$ . It has been assumed that this step applies to both the burner off-gas stream and the burner coolant gas stream. The former stream will always be highly contaminated, while the latter may not be contaminated at all. In any event, it must be assumed that the coolant gas is contaminated because of the possibility that a hole will burn through the inner burner wall.

It has been assumed that an HTGR spent fuel reprocessing plant will be designed and operated in such a manner that an overall plant confinement

factor (radioactive material introduced/radioactive material released) of  $> 10^{10}$  will be obtained for particulate matter. Three equivalent stages of HEPA filtration will be required in order to achieve this large overall plant confinement factor for particulates. This criterion can be met by the use of three stages of HEPA filtration or two stages of HEPA filtration plus one stage of sand filtration. Considerations of the effect of a tornado causes one to favor using two HEPA filters and a sand filter.

If the soot contains long-lived alpha contaminants, a 1.5-MTHM/day HTGR fuel reprocessing plant would be allowed to release only about 2 mg of soot per day to the atmosphere. (This assumes a burner confinement factor of  $10^{10}$ .) While this may at first appear to be a very stringent requirement, it is one that may be feasible to meet in practice. In a recent hot-cell burning experiment at ORNL,<sup>26</sup> a confinement factor of  $> 10^{10}$  was observed. The filtration system in this experiment was comprised of two 20- $\mu$  sintered metal filters (at 500°C), two 0.2- $\mu$  silver filters (one at 500°C and one at ambient temperature), and one fiberglass filter (HEPA equivalent) at ambient temperature.

It has been assumed that an HTGR fuel reprocessing plant will have an off-gas decontamination system for  $^3\text{H}$ ,  $\text{I}_2$ , Rn, and  $^{85}\text{Kr}$ . Since  $\text{CO}_2$  is compatible with the KALC\* process,<sup>27</sup> it has been assumed to be the coolant gas for the burners and the sweep gas for the FBB crushing equipment. Therefore, wherever large flows of  $\text{CO}_2$  are required for heat removal, a closed recirculating loop of  $\text{CO}_2$  has been considered.

Currently, it is not known how much particulate decontamination can be expected to take place in the  $^3\text{H}$ ,  $\text{I}_2$ , Rn, and  $^{85}\text{Kr}$  decontamination process(es). The off-gas decontamination development program currently under way at ORNL and at ACC will determine these DFs.

Two types of off-gas heat exchangers have been considered: gas-to-gas, and gas-to-liquid. The latter type is most economical; however, criticality considerations of burners preclude them from certain applications in which a failure of the heat exchanger could transfer water

---

\*Krypton Absorption in Liquid C $\text{O}_2$  process.

into an equipment item containing fissile materials, thereby leading to a critically unsafe situation.

Various other assumptions which have been made for this study are as follows:

- (1) The temperature of the off-gas at the HEPA filter is less than 200°C.
- (2) The cross-sectional areas of the HEPA filters are sized such that the maximum velocity, normal to the filter face, does not exceed 4.2 fps.<sup>28</sup>
- (3) The filter housings are designed for a single-stage HEPA filter system efficiency of 99.97% for 0.3- $\mu$  particles.

Two potentially hazardous conditions are associated with burner off-gas handling. These are the reaction of CO and O<sub>2</sub> in the burner off-gas and the reaction of O<sub>2</sub> and dust in the crushing operations. Carbon monoxide explosions can be prevented by prohibiting explosive mixtures from accumulating. The upper and lower explosive limits of CO in the tertiary system CO-O<sub>2</sub>-CO<sub>2</sub> are shown in Fig. B.8. Thus, procedures for burning should limit the CO concentration to less than 15 mole %. A potentially hazardous condition could also result from improper operation of the CO torch used for ignition. However, CO burns easily, and the technology for its burning has been developed. While other methods have been considered for ignition, the CO-O<sub>2</sub> torch has been assumed for this study. It is not to be implied that a CO explosion is a more severe problem with the FBB than with the WBB; in fact, since the off-gas temperature of the WBB is higher than that for the FBB, the reverse is probably true.

Although explosions with carbon dust have been reported, the Bureau of Mines has been unsuccessful in producing graphite dust explosions.<sup>29</sup> As a safety precaution, all equipment containing graphite dust, soot, etc., should be maintained under an oxygen-free atmosphere. For the purpose of this study, it is assumed that CO<sub>2</sub> is used as the blanket gas. (Thus, all off-gas streams are compatible with the KALC process.)

ORNL DWG 73-11885

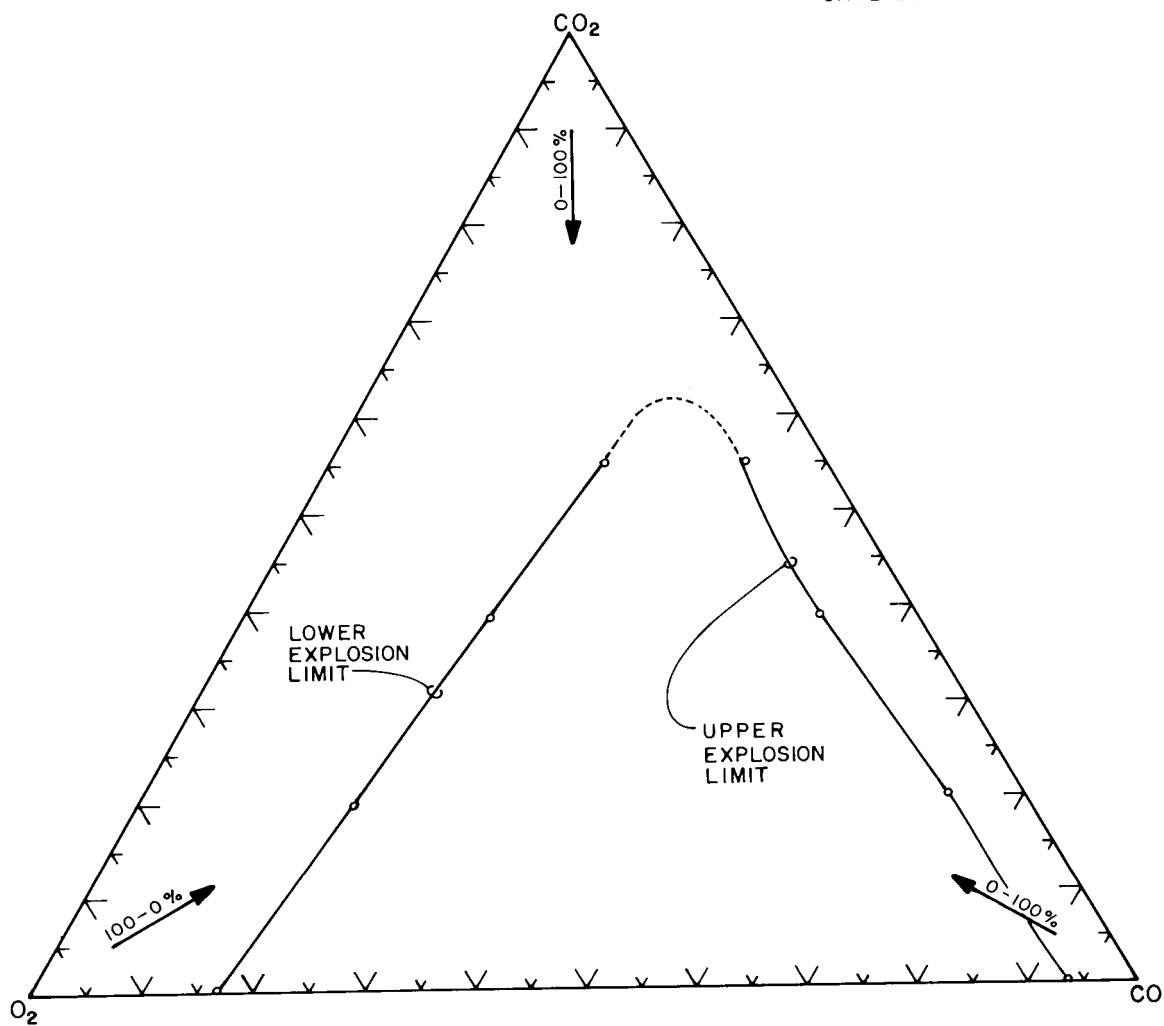


Fig. B.8. Explosive limits of carbon monoxide in mixtures of oxygen and carbon dioxide.

APPENDIX C: HTGR FUEL ELEMENT AND FUEL PARTICLE NOMENCLATURE  
AT THE REPROCESSING PLANT

The following discussion is presented in an attempt to avoid confusion concerning the identification of HTGR fuel elements and HTGR fuel particles at reprocessing time.

The three types of fuel elements entering the HTGR are: (1) the IM fuel elements, which contain virgin uranium (~93% enriched in  $^{235}\text{U}$ ) plus thorium; (2) the 25R fuel elements which contain recycle uranium (~30% enriched in  $^{235}\text{U}$ ) plus thorium; and (3) the 23R fuel elements, which contain  $^{233}\text{U}$  plus thorium. These fuel elements contain three fissile materials, which must be handled separately in the HTGR fuel reprocessing plant, and a single fertile material. The fissile particles in the elements which entered the reactor enriched to about 93% in  $^{235}\text{U}$  are discharged at an enrichment of about 30% in  $^{235}\text{U}$ ; those in the elements which entered the reactor enriched to about 30% in  $^{235}\text{U}$  are discharged at an enrichment of about 10% in  $^{235}\text{U}$ . Additionally, a portion of the thorium entering the reactor is discharged as  $^{233}\text{U}$ .

The IM, 25R, and 23R nomenclature is desirable for fuel element identification at the reactor because it helps identify the various fissile fuels entering the reactor. However, at the reprocessing plant (it is assumed that the refabrication plant will be located within the same plant complex), such terminology creates confusion since the spent fuel elements entering this plant need to be identified by a system which does not change within the reprocessing and refabrication complex, and which suggests reuse or disposal of the fissile materials.

The IM fuel elements are assumed to be fabricated at the fresh fuel fabrication plant; thus, this terminology serves no useful purpose in reprocessing-refabrication. (Note that fabrication and refabrication have separate and distinct connotations.) The fuel elements that entered the reactor as IM elements should be referred to as 25R fuel elements at the reprocessing-refabrication plant since their unique feature is the fissile uranium which is enriched to about 30% in  $^{235}\text{U}$  and which will be refabricated into 25R fuel elements.

The fuel elements that entered the reactor as 25R elements should also undergo a name change upon entering the reprocessing plant. At the reprocessing-refabrication plant, they should be referred to as 25W fuel elements since their unique feature is the fissile uranium which is enriched to about 10% in  $^{235}\text{U}$  and which will leave the HTGR cycle as a waste stream.

The elements that entered the reactor as 23R fuel elements should retain their nomenclature at the reprocessing plant since the uranium is recycled in 23R fuel elements. The 23R fissile particles(s) leaving the refabrication plant is a composite of the uranium recovered from the thorium of the 23R, 25R, and 25W fuel elements which is enriched to about 90% in  $^{233}\text{U}$ , plus the 23R fissile uranium which is enriched to about 60% in  $^{233}\text{U}$ .

The spent HTGR fuel elements lose their identity during the burning (or crushing and burning) step. However, this burning must be done in such a manner that it does not jeopardize the possibility of separating the 25R and 25W streams from the thorium (and its bred  $^{233}\text{U}$ ); nor does it transfer an intolerable quantity of  $^{233}\text{U}$  into the 25W or 25R streams.

Since each of the fuel streams will be processed by a different flow-sheet following burning, it will be desirable to have a method of fuel stream identification. The magnitude of this identification problem may be realized if one reflects upon the fact that the spent fuel may arrive as oxide or carbide (both may be present within a given reactor discharge) and as BISO- or TRISO-coated fuel particles. The TRISO particles may require a secondary burning step following separation and crushing. Thus, whether a given fuel stream consists of burned BISO (BB) particles or, more importantly, burned TRISO (BT) particles is of significance in fuel stream identification; that is after separation from the 25W BB particles, the 25W BT particle (the fissile particle from the 25W fuel elements) may be disposed of without further processing or may be crushed-burned and further processed. The composition of the kernel of the 25W BT particles (i.e., carbide or oxide) could determine whether further processing is required or not. It is conceivable that 25W BT particles containing oxide kernels could be disposed of without subsequent treatment but that

carbide kernels of 25W BT particles would require further reprocessing. In other words, oxide fuel kernels may be acceptable for long-term waste disposal, whereas carbide kernels may not. There is no assurance that either one will be acceptable.

The intent of the above discussion was to emphasize the importance of having a fuel element identification system for the fabrication and refabrication plants which ensures no duplication of numbers, one that is amenable to automatic and visual verification, and one that contains certain desirable information for the reprocessing plant as well as the reactor. This fuel element identification system may be used by a centralized computer to actuate certain "go--no-go" stations beyond which the particular fuel element is nonretrievably committed. Material handling at the reprocessing plant is sufficiently complex under the best of circumstances that any system or procedure which will simplify handling warrants careful consideration.

100

1

2

3

4

5

6

ORNL-TM-4520  
UC-77 - Gas-Cooled Reactor Technology

INTERNAL DISTRIBUTION

1-2.	Central Research Library	86.	D. M. Levins
3.	Document Reference Section	87.	K. H. Lin
4-13.	Laboratory Records	88.	T. B. Lindemer
14.	ORNL Patent Office	89.	A. L. Lotts
15.	Laboratory Records, RC	90.	R. S. Lowrie
16.	H. W. R. Beaujean	91.	A. P. Malinauskas
17.	M. Bender	92.	L. E. McNeese
18.	L. L. Bennett	93.	J. P. Nichols
19.	R. E. Blanco	94.	E. L. Nicholson
20.	A. L. Boch	95-96.	K. J. Notz
21.	R. E. Brooksbank	97.	J. R. Parrott
22.	K. B. Brown	98.	R. L. Philippone (ORO-AEC)
23.	J. M. Chandler	99.	T. W. Pickel
24.	H. E. Cochran	100.	H. Postma
25.	J. H. Coobs	101.	A. D. Ryon
26.	F. L. Culler	102.	C. D. Scott
27.	F. C. Davis	103.	J. D. Sease
28.	W. Davis, Jr.	104-123.	J. W. Snider
29.	F. E. Dearing (ORO-AEC)	124.	W. E. Thomas
30.	J. P. Drago	125.	M. L. Tobias
31.	W. P. Eatherly	126.	D. B. Trauger
32.	D. E. Ferguson	127.	W. E. Unger
33.	L. M. Ferris	128.	I. J. Urza
34.	B. C. Finney	129.	J. E. van Cleve
35.	C. L. Fitzgerald	130.	V. C. A. Vaughen
36.	R. W. Glass	131.	T. N. Washburn
37.	P. A. Haas	132-141.	D. C. Watkin
38.	F. E. Harrington	142.	C. D. Watson
39.	C. C. Haws	143.	J. R. Weir, Jr.
40.	J. W. Hill, Jr.	144-145.	R. G. Wymer
41.	R. M. Hill, Jr.	146.	O. O. Yarbrow
42.	F. J. Homan	147.	J. C. Frye (consultant)
43.	A. R. Irvine	148.	C. H. Ice (consultant)
44.	J. P. Jarvis	149.	J. J. Katz (consultant)
45.	G. R. Jasny	150.	Ken Davis (consultant)
46-84.	P. R. Kasten	151.	E. A. Mason (consultant)
85.	R. E. Leuze	152.	R. B. Richards (consultant)

## EXTERNAL DISTRIBUTION

- 153. Research and Technical Support Division, USAEC Oak Ridge Operations Office, P. O. Box E, Oak Ridge, Tennessee 37830
- 154. Director, Reactor Division, AEC-ORO
- 155-156. Director, USAEC Division of Reactor Research and Development, Washington, D.C. 20545
- 157-299. For distribution as shown in TID-4500 under UC-77, Gas-Cooled Reactor Technology.